DISCOVERY OF IKBKE AND CD24 SIRNAS FOR THE TREATMENT OF TRIPLE-NEGATIVE BREAST CANCER

A DISSERTATION IN

Pharmaceutical Sciences

and

Cell Biology and Biophysics

Presented to the Faculty of the University
of Missouri-Kansas City in partial fulfillment of
the requirements for the degree

DOCTOR OF PHILOSOPHY

by

YANLI LIU

M.S., East China University of Science and Technology, 2015

B.S., Yantai University, 2012

Kansas City, Missouri

2023

DISCOVERY OF IKBKE AND CD24 SIRNAS FOR THE TREATMENT OF TRIPLE-NEGATIVE BREAST CANCER

Yanli Liu, Candidate for the Doctor of Philosophy Degree

University of Missouri-Kansas City, 2023

ABSTRACT

Triple-negative breast cancer (TNBC) represents approximately 10-20% of all newly diagnosed breast cancers and is classified as a subtype with the absence of ER, PR, and HER2 expression. TNBC displays high aggressiveness, a tendency to metastasize, a poor prognosis, and a low survival rate. Unlike other breast cancer subtypes, TNBC has limited treatment options due to the lack of targeted therapies. Therefore, there is a significant need to develop new therapies for TNBC. IKBKE, also known as IKKε or IKKi, is a member of the IKK (IκB kinase) family and exhibits high expression levels in various cancers. IKBKE functions as an oncogene in breast cancer and is overexpressed in approximately 30% of breast carcinomas. IKBKE is shown to be aberrantly amplified in TNBC and associated with proliferation, migration, and survival in TNBC cells. Breast cancer also expresses high levels of CD24, which is a heavily glycosylated glycosylphosphatidylinositol (GPI)-anchored surface protein and plays an important role in tumor growth, invasion, and metastasis. Moreover, overexpression of CD24 in tumors is associated with resistance to therapies.

Small interfering RNA (siRNA) can specifically knockdown the expression of target genes. It represents a promising tool for cancer therapy as it can silence aberrant genes that are essential for the progression of cancer cells. However, successful siRNA cancer therapy relies

on the development of safe and effective RNA delivery systems because naked siRNA is unstable and has limited cellular uptake. Numerous delivery carriers have been investigated to increase the stability and improve the cellular uptake of siRNAs. This dissertation focuses on two primary research objectives. The first objective centered on discovering siRNAs targeting IKBKE and CD24 for the treatment of TNBC. The second research objective aims to utilize a recently discovered anti-PD-L1 human domain antibody as an immune checkpoint inhibitor for cancer immunotherapy.

In Chapter 1, we briefly introduced the background of the research, the statement of the problems, and research objectives.

In Chapter 2, we reviewed potential treatment options for TNBC and provided a concise introduction to cancer immunotherapy, specifically focusing on PD-1/PD-L1 immune checkpoint inhibitors.

In Chapter 3, we utilized a cholesterol peptide-based delivery system to condense IKBKE siRNA to form nanocomplexes for the treatment of TNBC. The stability, cellular uptake, and penetration capability of the cholesterol peptide/siRNA (CCP/siRNA) nanocomplex was significantly increased. Importantly, the CCP/siRNA nanocomplex significantly inhibited tumor growth in an orthotopic TNBC mouse model. These data suggest that IKBKE siRNA could be a promising therapeutic strategy for TNBC.

In Chapter 4, we designed four CD24 siRNAs for the treatment of TNBC by targeting different regions of human CD24 mRNA. The results showed the pre-designed siRNA reduced the CD24 expression at both mRNA and protein levels in TNBC cells. CD24 siRNA efficiently inhibited the proliferation, migration, and invasion of TNBC cells. Moreover, silencing of CD24 induced tumor cell apoptosis and cell cycle arrest. Further, we evaluated the association

of CD24 expression with doxorubicin resistance. We found that both CD24 mRNA and protein levels were upregulated in doxorubicin-treated MDA-MB-231 cells and CD24 siRNA sensitized MDA-MB-231 cells to doxorubicin which was reflected by a decreased IC50 value. Overall, targeting CD24 with siRNAs may be a promising therapeutic target for TNBC or other cancers with overexpressed CD24.

In Chapter 5, we presented the work on the discovery of anti-PD-L1 human domain antibodies (dAbs) using the phage display technique for cancer immunotherapy. In this study, seven anti-PD-L1 domain antibodies were discovered. Among them, the CLV3 dAb showed the highest binding affinity to human and mouse PD-L1 proteins with KD values of 137.5 nM and 266.8 nM, respectively. The CLV3 dAb also exhibited potent binding affinity to PD-L1 overexpressing DU145 cells. CLV3 inhibited PBMC apoptosis in a co-culture system and showed better tumor penetration compared to antibody. The CLV3 dAb significantly inhibited tumor growth and increased the survival of CT26 tumor-bearing mice. The CLV3 dAb is therefore a promising PD-L1 inhibitor that can be used for cancer immunotherapy.

APPROVAL PAGE

The faculty listed below, appointed by the Dean of the School of Graduate Studies, have examined the dissertation titled "Discovery of IKBKE and CD24 siRNAs for the Treatment of Triple-Negative Breast Cancer", presented by Yanli Liu, candidate for the Doctor of Philosophy Degree, and certify that in their opinion it is worthy of acceptance.

Supervisory Committee

Kun Cheng, Ph.D., Committee Chair
Division of Pharmacology and Pharmaceutical Sciences

Gerald Wyckoff, Ph.D.
Division of Pharmacology and Pharmaceutical Sciences

Hari K. Bhat, Ph.D.
Division of Pharmacology and Pharmaceutical Sciences

Ryan Mohan, Ph.D.
School of Science and Engineering

Xiaolan Yao, Ph.D.
School of Science and Engineering

TABLE OF CONTENTS

LIST OF ILLUSTRATIONS

LIST OF TABLES

ACKNOWLEDGEMENTS

I would like to express my greatest gratitude and deep appreciation to my advisor, Dr. Kun Cheng for his excellent, patient guidance and mentorship, persistent encouragement, and continuous support throughout my Ph.D. study and research.

I would like to thank Dr. Gerald Wyckoff and Dr. Hari K. Bhat of the Division of Pharmacology & Pharmaceutical Sciences, Dr. Xiaolan Yao and Dr. Ryan Mohan of the School of Science and Engineering, for their valuable guidance and insightful suggestions for my research and the dissertation, and for kindly serving on my supervisory committee.

I would like to express thanks to all my colleagues, Yuhan Guo, Chien-Yu Lin, Maryam Nakhjiri, Reaid Hasan, John Fetse, Pratikkumar Patel, Bahaa Mustafa, Mohammed Alahmari, Sashi Kandel, Umar-Farouk Mamani, Sushil Koirala, Nurudeen Ibrahim, Yongren Li, Sherin Sajhi, Yu Ting Liu, Dr. Zhen Zhao, Dr. Hao Liu, and Dr. Yuanke Li for their time, support, and friendship during my research and study in UMKC. They make our lab a wonderful place to grow and learn.

In addition, I am grateful to other professors, staff members, and fellow students in the Division of Pharmacology & Pharmaceutical Sciences for their help and friendship.

Finally, I would like to express my deepest thanks to my parents for their love and support.

CHAPTER 1

INTRODUCTION

1.1 Overview

Worldwide, female breast cancer is the fifth leading cause of death. In the United States, Breast cancer is the most diagnosed cancer and the second most common cause of death among women. About 1 in 8 women in the U.S. will be diagnosed with breast cancer in their lifetime. [1] According to the expression of molecular receptors namely estrogen receptor (ER), progesterone receptor (PR), and human epidermal growth factor receptor-2 (HER2), breast cancer typically can be divided into four subtypes: luminal A, luminal B, HER2-positive, and triple-negative subtypes [2, 3]. Breast cancers with the absence of ER, PR, and HER2 as assessed by immunohistochemical (IHC) staining are subtyped as triple-negative breast cancer (TNBC) accounting for approximately 15-20% of all cancer cases [4]. TNBC is more likely to metastasize to organs such as lungs, liver, and brain but less frequent bone metastasis. In addition, this tumor subtype has the poorest prognosis among all breast cancer subtypes, especially those with advanced-stage diseases [5].

Cancer immunotherapy has been developed to improve the survival and quality of life of patients with cancers and tremendous studies have demonstrated that cancer immunotherapy has significantly improved the outcome of various human cancers [6]. Several negative regulators of T cell activation have been discovered to act as a "brake" role in immune functions. Immune checkpoint blockade as the immunotherapeutic approach has been developed to "release the brakes" of T cell functions [7]. PD-L1 is one of the most widely studied inhibitory checkpoint molecules. Expression of programmed cell death ligand 1 (PD-L1) has been identified in a broad range of human cancers. Ligation of PD-L1 with its receptor,

programmed cell death protein 1 (PD-1), primarily expressed on activated T cells mediates tumor immune escape [8]. Hence, the PD-1/PD-L1 axis is a potential target in cancer treatment and the blockade of PD-1/PD-L1 with checkpoint inhibitors could be a new therapeutic approach.

1.2 Statement of problem

Unlike other breast cancer subtypes, the therapeutic approaches for patients with TNBC are few due to the lack of tumor-specific therapeutic targets. Currently, chemotherapy is the primary systemic treatment option for patients with TNBC, however, it is notable that the resistance of tumor cells to chemotherapy in TNBC frequently occurs [9]. The risk of early relapse in TNBC patients within 5 years after diagnosis is nearly 3-fold higher than non-TNBC patients [10]. Moreover, compared to other breast cancer subtypes, patients with TNBC have a fourfold higher risk of developing visceral metastasis. Metastasis is the main death cause for the vast majority of TNBC patients. Therefore, more efforts need to be made to address the major challenges in the treatment of TNBC.

IKBKE has been identified to be highly expressed in various human cancers, such as glioma, ovarian cancer, breast cancer, and pancreatic cancer [11]. Overexpression of IKBKE is associated with tumorigenesis, metastasis, and chemoresistance [12, 13]. Specifically, IKBKE has been identified as a breast cancer oncogene and is overexpressed in approximately 30% of breast carcinomas [14]. In our previous work, we have demonstrated the *in vitro* antitumor activities of IKBKE siRNA in non-TNBC cell lines [15]. Recently, IKBKE has been linked to TNBC and our group reported that the IKBKE siRNA demonstrated a promising *in vivo* antitumor effect in the MDA-MB-231 tumor-bearing xenograft mouse model [16]. In this

dissertation, we aimed to explore whether IKBKE siRNA can be applied to treat TNBC and be potentially combined with other therapies in particular immunotherapy.

CD24 is overexpressed in a variety of human cancers and plays a critical role in tumor progression and metastasis [17, 18]. Recently, accumulating evidence indicated that CD24 is not only expressed on the cell surface but also exhibits a cytoplasmic accumulation, and both intracellular and surface CD24 can promote tumor progression. In addition, CD24 expression has been correlated with poor prognosis. Particularly, CD24 expression is much higher in TNBC in comparison with ER+PR+ breast cancer and healthy breast cells and CD24 overexpression is associated with poor prognosis in triple-negative breast cancer [19, 20]. Furthermore, an association of CD24 expression with resistance to chemotherapy and targeted therapies in breast cancer and other cancers has been noted [18, 21]. These findings suggest that CD24 is overexpressed across different types of tumors, and it might be a potential therapeutic target for cancer treatment.

Small interfering RNA (siRNA) can be exploited to silence specific genes for therapeutic purposes. However, the application of siRNAs remains challenging due to fast degradation and clearance in the body. Naked siRNAs are difficult to cross biological membranes due to the large molecular weight (~13 kDa) and intrinsic negative charges. siRNAs are unstable in the bloodstream, and they can be rapidly degraded by nuclease [22]. To overcome the challenges and widen the applications of siRNA as a therapeutic agent, a variety of approaches have been developed to facilitate the successful delivery of siRNA into specific sites [23, 24]. Cholesterol peptide can spontaneously form the micelle-like structure and condense the siRNA to form nanocomplexes [25]. In this dissertation, we aimed to determine whether

cholesterol peptide can protect IKBKE siRNA from degradation in serum and enhance cellular uptake and tumor penetration.

Monoclonal antibody-based cancer immunotherapy targeting PD-1/PD-L1 signaling has been widely applied to cancer treatment and demonstrated promising clinical efficacy in various therapeutic fields over the past decades. However, limitations of traditional antibodies (~150 kDa) caused by poor penetration and immunogenicity in solid tumors still need to be improved [26]. To address these limitations, smaller antibody fragments such as single domain antibody (also named VHH or nanobody, ~15 kDa) displaying similar blocking activity as the classic antibodies attract great interest [27]. Identification of anti-PD-L1 domain antibodies may potentially be used in cancer immunotherapy.

1.3 Objectives

The objectives of this dissertation are:

1. To assess the silencing and biological activities of IKBKE siRNA. RT-qPCR will be conducted to determine the silencing effect of IKBKE siRNA in EMT-6 cells. Next, we will assess tumor cell proliferation using CellTiter-Glo reagent after IKBKE siRNA transfection. Then, a transwell chamber system will be used to evaluate the migration and invasion capabilities of tumor cells after the downregulation of IKBKE. The capability of the IKBKE siRNA to induce tumor cell apoptosis and cell cycle arrest will be determined by flow cytometry.
2. To characterize the cholesterol peptide/siRNA nanocomplex (CCP/siRNA nanocomplex). First, the condensation of siRNA with cholesterol peptide will be evaluated by a gel retardation assay. Then, the particle size of the nanocomplex at different N/P ratios will be measured using a Malvern Zetasizer Nano-ZS and transmission electron microscopy. The

stability of siRNA nanocomplex will be evaluated by incubation with 50% mouse serum at different time intervals at 37℃. To evaluate the penetration of CCP/siRNA nanocomplex, a 3D spheroid model formed by EMT-6 cells will be used. To determine the cellular uptake, Cy5-labeled siRNA will be incubated with EMT-6 cells and measured using flow cytometry and fluorescent microscopy.

3. To assess the *in vivo* anti-tumor activity of the siRNA nanocomplex in an orthotopic TNBC mouse model. EMT-6 cells will be implanted into the second mammary fat pad of female Balb/c mice to establish an orthotopic mouse model. The siRNAs will be administered at 0.5 mg/kg every 3 days for a total number of five injections. The tumor size will be measured, and PD-L1 expression will be tested in collected tumors. Cytotoxic T lymphocytes demonstrate an association with the therapeutic outcome of immunotherapy. We will evaluate the density of CD3+ and CD8+ T cells in the tumor microenvironment with immunohistochemical (IHC) staining.

4. To evaluate the silencing effect and biological activities of CD24 siRNA using different assays. Here, we will design four siRNAs targeting different regions of human CD24 mRNA with online siRNA design tools. The silencing effect of designed siRNAs will be evaluated in two TNBC cells (MDA-MB-231 and MDA-MB-468) with RT-qPCR and western blotting. The proliferation of TNBC cells will be evaluated using CellTiter-Glo reagent after CD24 silencing. We will perform the transwell chamber assays to assess the migration and invasion capabilities of TNBC cells after siRNA transfection. Apoptosis and cell cycle distribution of siRNA-transfected TNBC cells will be determined by flow cytometry. The association of CD24 expression with doxorubicin resistance in MDA-MB-231 cells will be assessed with various methods.

5. To assess the purification and biological activities of discovered anti-PD-L1 domain antibody with different assays. We will run SDS-PAGE and SEC to evaluate the expression and purification of anti-PD-L1 domain antibody (CLV3). Next, we will determine the binding affinity of CLV3 against the PD-L1 protein and PD-L1 overexpressing tumor cells. The ability of the CLV3 domain antibody to reverse apoptosis of immune cells co-cultured with DU145 cancer cells will be assessed by flow cytometry. Also, cytokine secretion by T cells cocultured with DU145 cells in addition to CLV3 will be assessed using flow cytometry. Tumor penetration of CLV3 will be investigated in a 3D tumor spheroid model.

CHAPTER 2

LITERATURE REVIEW

2.1 TNBC and treatment options

2.1.1 Characteristics of TNBC

Triple-negative breast cancer (TNBC) represents approximately 10-20% of all newly diagnosed breast cancers and is classified as a subtype with the absence of ER, PR, and HER2 expression [4]. Compared with other subtypes, TNBC shows a high occurrence rate in young women under 40 and in women with African ancestry [28]. TNBC is a highly heterogeneous disease categorized into six subtypes according to the gene expression profiling in tumor samples from TNBC patients [29]. Among all TNBC subtypes, around 75% is basal-like subtype characterized by the expression of basal-associated markers such as cytokeratin, cadherin, vimentin, and epidermal-like growth factor (EGFR) [30]. Besides, mutations in breast cancer gene 1 and breast cancer gene 2 (*BRCA1/BRCA2*) are commonly associated with the basal-like subtype of TNBC. About 35% of TNBC patients carry the *BRCA1* mutation and 8% of patients have the *BRCA2* mutation [29]. TNBC is high-grade invasive ductal carcinoma and is associated with a high risk of visceral metastasis such as brain, lung, and liver, with a lower prevalence of bone metastasis. When TNBC is diagnosed, the majority of the patients are in stage T2 or T3 (T2: tumor size is 2-5cm; T3: tumor size is more than 5cm) and show locoregional metastasis such as lymph node metastasis and lymph vascular invasion [31]. A vast majority of TNBC patients die from tumor metastasis. Due to its aggressive features, TNBC has been linked to poor prognosis and low survival rates [5].

2.1.2 Risk of TNBC

Multiple potential risk factors for TNBC have been identified in studies. A median age of women diagnosed with breast cancer is 62 years old and the incidence rate increases after the age of 40 (1.5% risk at age 40, 3% at the age of 50 years, and >4% risk at age 70) [32]. By contrast, TNBC occurs more frequently in younger women under 40. Race has been linked to the recurrence of breast cancer. The incidence rate of TNBC in African American women is almost three-fold higher than in their white American counterparts [28]. Genetic mutations are reported to have a strong association with TNBC. *BRCA1/BRCA2* are tumor-suppressive genes in breast cancer and play an important role in DNA repair. Mutation of *BRCA1/BRCA2* leads to the dysfunction of the *BRCA*-mediate DNA repair mechanism. Compared with other subtypes of breast cancer, TNBC shows a prevalence of *BRCA* mutations, and the mutations have been selected as biomarkers to predict the efficacy of PARP inhibitors (PARPi) in TNBC patients[33]. Apart from *BRCA*, some common mutations in *TP53*, *PTEN*, *CDH1*, and *STK11* are also linked with breast cancer and TNBC incidence. Other potential risk factors for TNBC also have been reported including obesity, history of radiation therapy, exposure to drugs, physical activity, breast tissue density, alcohol intake, and smoking [34].

2.1.3 Diagnosis of TNBC

Classification of TNBC mainly relies on immunohistochemical (IHC) staining to assess the expression of ER, PR, and HER2. TNBC is a subgroup of breast cancer lacking the expression of these three receptors. American Society of Clinical Oncology/College of American Pathologists (ASCO/CAP) updated the guideline for ER, PR, and HER2 testing in breast cancer providing a more specific definition of TNBC [34]. For ER and PR receptors, if less than 1% of tumor cells show immunostaining in the IHC assay, the sample is considered

ER and PR negative [35]. For HER2, if the result is IHC 0 or 1+, the sample is considered as HER2 negative. If the result is IHC 2+, a fluorescence *in situ* hybridization technique needs to be applied to evaluate the gene amplification of *HER2*. HER2 is defined as negative if an average *HER2* copy number is < 4.0 signals per cell and the *HER2*/CEP17 ratio is <2.0 [36].

2.1.4 Treatment options of TNBC

2.1.4.1 Surgery

Surgery is the most conventional treatment option for locoregional breast cancer or early-stage breast cancer with sentinel lymph node metastasis. For early-stage TNBC management, a lumpectomy (surgical removal of the tumor tissue but preserving the breast) or a mastectomy (surgical removal of the entire breast or lymph dissection) can be performed according to the grade of cancer [37]. Surgery followed by radiotherapy is recommended when the tumor size is large, or regional metastasis in the lymph node is observed. Moreover, chemotherapy as a neoadjuvant or adjuvant therapy may be used with surgery for early-stage TNBC to improve the treatment efficiency or prevent the recurrence [38]. A study reveals that patients with TNBC treated by breast-conserving therapy do not have a worse prognosis than those treated by mastectomy. A recent analysis of database data demonstrates that patients with lumpectomy followed by radiotherapy show improved survival rates [39]. Patients with a family history of breast cancer or identified with gene mutations associated with TNBC such as *BRCA1* may benefit more from a mastectomy to prevent cancer recurrence. For patients with TNBC, the risk of early relapse within 3-5 years after surgery is higher in comparison with other breast cancer subtypes [32].

2.1.4.2 Radiotherapy

Radiotherapy uses high-energy radiation to destroy the remaining breast cancer cells in the cancer area and shrink tumors in the body. Radiotherapy is commonly used in the adjuvant setting in TNBC [37]. Radiotherapy after surgery reduces local recurrence in patients with TNBC. Abdulkarim et al. found that TNBC patients who received radiotherapy post-mastectomy showed a lower locoregional recurrence compared to patients treated with mastectomy alone. Moreover, radiotherapy improved overall survival rates of patients with hormone-receptor positive breast cancer [40]. However, whether radiotherapy has significant survival benefits for patients with TNBC is controversial. One study revealed the pN0 TNBC patients without radiotherapy treatment did not show worse outcomes [41]. Data from another study indicate that TNBC patients who received adjuvant radiotherapy after surgery showed improved survival than patients without radiation treatment [41]. The effect of radiotherapy in TNBC can be affected by the sequence used in the combination therapies. A study demonstrated that the sequence of radiotherapy and chemotherapy is critical for therapeutic efficacy in breast cancer patients. Compared to patients treated with radiotherapy after chemotherapy, patients who received radiotherapy between two chemotherapies (cyclophosphamide and taxane) showed lower locoregional recurrence but no difference in distant metastasis. In this study, the overall survival rate was not associated with radiotherapy sequence regardless of subtypes of breast cancer [42]. Many preclinical data reveal that there is a synergic effect between immunotherapy and radiotherapy in breast cancer. Combinations of radiotherapy and immunotherapy in early-stage and metastatic breast cancer including TNBC are currently investigated under clinical trials [43]. Radiotherapy can be affected by gene mutations in patients with TNBC. A study

revealed that TNBC patients who harbor *BRCA1* mutation are potentially radiosensitive [38]. However, radioresistance is the major challenge of radiation therapy in TNBC [44].

2.1.4.3 Chemotherapy

TNBC treatment remains challenging owing to its aggressive and heterogeneous nature. Unlike hormonal and HER2-positive breast cancers, TNBC is not sensitive to the targeted therapies due to the lack of related receptor markers. Currently, chemotherapy is still the dominant systemic treatment for patients with TNBC and many studies have demonstrated the effectiveness of chemotherapy [38]. Cytotoxic chemotherapy drugs commonly used in TNBC include anthracycline, alkylating agents (e.g., cisplatin and cyclophosphamide), taxane, and 5-fluorouracil (5-FU) [5]. Anthracycline and taxane are two standard chemotherapy regimens for TNBC and are used in neoadjuvant and adjuvant settings. Anthracycline drugs (e.g., Doxorubicin and Epirubicin) treat cancers via different mechanisms: disrupting the replication of DNA, activating immune responses, and generating oxygen-free radicals. Taxane drugs (e.g., Paclitaxel, Docetaxel, and Cabazitaxel) are known as microtubule inhibitors that inhibit tumor cell mitosis and angiogenesis [4]. Chemotherapy as a neoadjuvant can achieve higher pCR rates (30-40%) in the early stage of TNBC than non-TNBC [45]. A meta-analysis of 9 randomized trials found that the addition of platinum to neoadjuvant chemotherapy increased the pCR rate from 37% to 52.1%. In a phase III clinical trial with 634 TNBC patients, adding carboplatin to Paclitaxel-based neoadjuvant significantly improved the pCR rate of patients [46].

A large body of literature has demonstrated that TNBC patients show better chemotherapy responses than non-TNBC patients [37]. For example, in a cohort of patients with breast cancer who received taxane and cyclophosphamide as the neoadjuvant chemotherapy, the pCR rate in TNBC patients is much higher than in patients with luminal subtype breast

cancers [5]. However, increasing evidence indicates that the current chemotherapeutic drugs are more effective in patients with early-stage TNBC but less effective in patients with advanced-stage or relapsed TNBC [47]. Furthermore, even though patients with TNBC have a higher likelihood of responding to chemotherapy, many patients still suffer cancer recurrence due to the development of drug resistance [48]. Several mechanisms of chemoresistance have been identified [49]. The risk of early relapse in patients with TNBC is higher than non-TNBC patients [10]. The selection of appropriate chemotherapy or development of chemotherapy-based combination therapies is important to improve the outcomes of TNBC patients.

2.1.4.4 Targeted therapies

Many studies have focused on the identification of molecular targets that can be targeted in TNBC including surface receptors, intracellular receptors, signaling pathways, cell cycle checkpoints, and DNA damage response [50]. Different protein targets are overexpressed in TNBC such as the epidermal growth factor receptor (EGFR), vascular endothelial growth factor (VEGF), and fibroblast growth factor receptor (FGFR). Targeting these overexpressed membrane receptors provides a new therapeutic approach for TNBC. A comprehensive overview of the molecular features in the key signaling pathways associated with TNBC is critical to identify potential therapeutic targets to explore targeted therapies in TNBC. Emerging targeted therapy as a strategy to treat TNBC is being developed by targeting highly activated pathways in tumor progression including PI3K/AKT/mTOR pathway, receptor tyrosine kinases associated pathways, and Ras/MAPK pathway [48, 51].

In addition, significant aberrant alterations in gene expression or mutant genes have been noted in TNBC such as mutations in *BRCA1* or *BRCA2*. BRCA mutation is a diagnostic marker in TNBC and about 20% of TNBC harbors germline BRCA1/2 mutations. The FDA

has approved two poly ADP-ribose polymerase (PARP) inhibitors (Olaparib and Talazoparib) for the treatment of metastatic breast cancer with BRCA mutations and the potential therapeutic effect in TNBC patients is under evaluation in multiple ongoing clinical trials [52]. For example, in a phase III OLYMPIAD trial, analysis of the TNBC subgroup showed that patients with Olaparib treatment had higher response rates than those in the control group. However, no significantly improved overall survival was observed in the Olaparib treatment group [30]. Inhibitors of DAN damage checkpoint kinases (e.g., CHK1/2) and cell cycle checkpoints (e.g., CDK1/2, CDK4/6) have been explored. These inhibitors interfere with cell cycle progression or DNA repair pathways leading to cancer cell death [53].

2.1.4.5 Immunotherapy

Immunotherapy is a critically important approach to treating patients with cancers by utilizing patients' immune systems and now is widely indicated in a broad range of tumors [54]. Immune checkpoint inhibitors are a type of immunotherapies by targeting inhibitory immune checkpoints such as PD-1/PD-L1 and CTLA-4. Checkpoint inhibitors targeting these immunosuppressive receptors to augment immune activation have shown remarkable clinical efficacy and durable response in numerous human cancers [6].

A number of studies have revealed that TNBC has some unique immunogenic features such as a high level of tumor-infiltrated lymphocytes, higher PD-L1 expression in tumor cells and immune cells, and tumor mutational burden and high genomic instability which are associated with better responses to immune checkpoint inhibitors compared with other breast cancer subtypes [55]. These findings suggest that patients with TNBC may benefit more from immunotherapy. From this perspective, immune checkpoint inhibitors targeting PD-1/PD-L1 for early-stage and advanced stages of TNBC have been developed and are under clinical

evaluation [56, 57]. However, immunotherapy remains a challenge in TNBC due to the limited specific targets and complexity of the tumor microenvironment in TNBC [58]. Moreover, a vast majority of patients with TNBC treated with monotherapy show primary resistance or early progression after treatment [59]. To improve therapeutic benefits in TNBC patients treated with immunotherapies, subsequent studies shift to combination therapy with immunotherapy and other modalities such as chemotherapy. For example, a phase III IMpassion 130 clinical trial investigated the therapeutic effect of the atezolizumab (Anti-PD-L1 antibody) and nab-paclitaxel in patients with PD-L1-positive metastatic TNBC and demonstrated improved median overall survival in patients who received both treatments. However, another phase III clinical trial (IMpassion 131) failed to meet the primary endpoint (progression-free survival and overall survival) after administration of atezolizumab and paclitaxel, which has been withdrawn in the US [30].

Immune checkpoint inhibitors targeting PD-1/PD-L1 have led to a new era of immunotherapy in TNBC. Besides the immune checkpoint inhibitors targeting PD-1/PD-L1, other immunomodulators are currently in development for TNBC such as cancer vaccines, adoptive cell therapies (e.g., CAR-T), oncolytic virus therapy, and cytokine gene therapy [58]. CTLA-4 receptor is another inhibitory checkpoint highly expressed in TNBC. CTLA-4 protein binds to B7 molecules by competing with CD28 to suppress tumor immune responses. The therapeutic effect of CTLA-4 inhibitors in TNBC is under evaluation, currently, no inhibitors are approved for TNBC treatment [60].

2.2 IKBKE as a therapeutic target in cancer

IKK (IκB kinase) family consists of five members: IKKα, IKKβ, IKKγ, IKBKE, and TBK1. The IKK family is a key activator of the nuclear factor-kappa B (NF-κB) signaling

pathway and plays important roles in NF-κB-mediated biological processes such as immune cell activation, inflammatory reactions, and metabolic diseases [11]. IKBKE (also known as IKKε or IKKi) and TBK1 are referred to as non-canonical IKKs. IKBKE shares 67% homology with TBK1 in the amino acid sequence, and shares about 30% homology with IKKα, and IKKβ in the corresponding domains. Studies demonstrated that IKBKE and TBK1 are differentially regulated, and different substrates have been reported in both kinases [61]. IKBKE has been identified as an oncogene in breast cancer and is overexpressed in approximately 30% of breast carcinomas [14]. The expression of IKBKE has been linked to tumorigenesis, metastasis, and chemoresistance [62, 63]. IKBKE expression has been reported to induce aberrant activation of NF-κB signaling in breast cancers including TNBC via multiple ways. For example, IKBKE phosphorylates Ser 418 of the tumor suppressor CYLD to induce cell transformation [64]. Overexpression of IKBKE translocates NF-κB subunits (c-Rel and p65) to the nucleus in primary breast tumors. Silencing of IKBKE inhibits NF-κB activation and breast cancer cell proliferation [61]. In TNBC, tumor-associated macrophages (TAMs) upregulate IKBKE expression to activate the NF-κB pathway and subsequently enhance breast cancer cell resistance to BET inhibitors [65]. These studies indicate the important role of IKBKE in tumor progression, and the suppression of IKBKE expression may provide a novel approach to cancer treatment.

2.3 CD24 as a therapeutic target in cancer

CD24, a heavily glycosylated glycosylphosphatidylinositol (GPI)-anchored surface protein, is overexpressed in a variety of cancers, such as breast, ovarian, prostate, glioma, lung, and colorectal cancers [17, 18]. Surface CD24 has been shown to play an important role in tumorigenesis and metastasis of various cancers [66-69]. Recent studies indicated that CD24

exhibits a cytoplasmic accumulation and intracellular CD24 is also important in tumor progression. In a study, intracellular CD24 was demonstrated to promote the growth of prostate tumor cells, and silencing CD24 with shRNA reduces tumor growth and prevents functional inactivation of p53 [70]. In another study, Wei Zhang et al. reported that CD24 is co-expressed with mutant p53 in metastatic prostate tumors. Silencing CD24 enhances the restoration of mutant p53 in human PCa cells and subsequently inhibits tumor growth and metastasis [71]. More recently, a study has demonstrated that the presence of nuclear CD24 in aggressive cancer cells with the absence of surface CD24 is positively associated with reduced survival of patients [72]. In addition, an association of CD24 expression with resistance to chemotherapy and targeted therapies in breast cancer and other cancers has been noted indicating a beneficial effect of targeting CD24 with other therapies may be obtained [18, 21]. Notably, CD24 overexpression has been associated with poor prognosis in breast cancers including early invasive breast cancer and TNBC [19, 73]. For example, the authors in a study revealed that *CD24* amplification is strongly correlated with CD24 mRNA expression. Particularly, *CD24* amplification was enriched in patients with basal-like breast cancer which has a poorer prognosis [74]. These data reveal that CD24 is overexpressed across different tumor types, and it might be a potential therapeutic target for cancer treatment.

2.4 Cancer immunotherapy and PD-1/PD-L1 signaling

2.4.1 Cancer immunotherapy

The immune system can be classified into two parts: known as the innate immune system and the adaptive immune system. The innate immune system is the first fundamental line of defense to fight foreign substances already entering the body which is a nonspecific response. A collection of cells involved in the innate immune response include macrophages,

natural killer cells, dendritic cells, mast cells, basophils, eosinophils, and neutrophils [75]. Whereas the adaptive immune system defends against specific invaders. T lymphocytes (T cells) and B lymphocytes (B cells) are two major cell populations to respond to the attack of specific invaders and memorize the invaders they previously encountered [76].

In cancer progression, the tumor cells with various genetic and cellular alterations can be recognized and distinguished from their normal counterparts by the immune system leading to the eradication of cancer cells by T-cell responses. However, durable immune responses and elimination of cancers by T cells can be affected by diverse factors. To exert effective anticancer immunity, a series of events must be initiated and proceed. Daniel S. Chen and his colleague proposed a concept named cancer immunity cycle to demonstrate the process of antitumor immune response. The cycle can be divided into multiple steps: tumor cells release the antigen and are presented by APCs to T cells; after the antigen capture, T cells are activated; activated T cells traffic and infiltrate into the tumor sites; T cells recognize and kill the tumor cells [77, 78]. Besides, cancer cells can evade attacks from the immune surveillance by different mechanisms such as defective antigen presentation, low tumor immunogenicity, inhibition of T cell activation, and expression of immune checkpoints [75, 77].

Immunotherapy utilizing the patients' immune systems to augment tumor immunity and fight cancers has become a new pilar of cancer treatment. Immunotherapy was first attempted to treat cancer by harnessing the immune system in the late 19th century. In 2013, cancer immunotherapy was named "Breakthrough of the Year" by the *Science* magazine. The importance of immunotherapies was further acknowledged after James P Allison and Tasuku Honjo were awarded the Noble Prize in Physiology or Medicine in 2018 for the discovery of cancer immunotherapy by immune checkpoint blockade [6]. Now cancer immunotherapy has

been successfully applied to treat numerous human cancers and durable immune responses have been reported [79].

2.4.2 The immunosuppressive effect of PD-1/PD-L1 signaling pathway

A big breakthrough in cancer immunotherapy is the discovery of inhibitory checkpoint receptors, which act as suppressors of the immune system. The most widely studied inhibitory immune checkpoint pathways are Cytotoxic T lymphocyte antigen 4 (CTLA4), programmed cell death 1 (PD-1), and programmed cell death ligand-1 (PD-L1). Ipilimumab was the first approved anti-CTLA monoclonal antibody drug by the U.S. Food and Drug Administration (FDA) in 2011 and now has been used in a variety of malignancies [80]. PD-1, characterized as a negative regulator of both innate and adaptive immune responses, is induced in a variety of immune cells such as activated T cells, and non-T cell subsets, including B cells, natural killer cells, macrophages, and dendritic cells. It shows 20% amino acid identify to CTLA4 [81]. PD-1 has two ligands, PD-L1 and PD-L2. High expression levels of PD-L1 have been observed on tumor cells, antigen-presenting cells (APCs), and T cells. Upregulation of PD-L1 can be induced by cytokines such as interferon-γ (IFN-γ) and TNF-α. PD-L2 expression is mainly limited on activated macrophages, mast cells, and dendritic cells [8, 82]. It has been reported that the binding affinity of PD-1 to PD-L1 is three-fold higher than that of PD-1 to PD-L2. PD-L2 interacts with RGMB protein on macrophages and the function of PD-1/PD-L2 interaction may be not critical due to the rare expression of PD-L2 on tumor cells [83]. Engagement of PD-1 and PD-L1 promotes tumor immune evasion by inhibiting T cell functions, including T cell activation, proliferation, cytokine secretion, inducing apoptosis, and cytotoxic T cells cytotoxicity [81]. Recent evidence demonstrated that in addition to PD-1, another molecule CD80 (B7-1) expressed on activated T cells and APCs also interacts with PD-L1 to negatively

regulate T cell activation [8]. Therefore, PD-1/PD-L1 is emerging as a promising target for cancer treatment. Consequently, PD-1/PD-L1 blockade may be an effective cancer immunotherapy.

2.4.3 PD-1/PD-L1 inhibitors

Immune checkpoint inhibitors have been developed to block the interaction of PD-1/PD-L1 and successfully applied to the treatment of various cancers in patients. Monoclonal antibodies are a major class of drugs developed targeting PD-1/PD-L1 and have exhibited dramatic therapeutic outcomes in a variety of human malignancies [82, 83]. Currently, there are six monoclonal antibodies targeting PD-1 or PD-L1 approved by the FDA: three anti-PD-1 (Nivolumab, Pembrolizumab, and Cemiplimab) antibodies and three anti-PD-L1 (Atezolimumab, Durvalumab, and Avelumab) antibodies [84, 85]. The antibodies block the PD-1/PD-L1 interaction and subsequently restore the immune cell-killing ability [86]. Compared to conventional cytotoxic chemotherapy, monoclonal antibodies demonstrate significantly reduced toxicity and improved overall survival in patients. However, large molecular size limits the penetration capability of antibodies into solid tumors. Moreover, high immunogenicity and severe immune-related adverse events have been observed in patients after treatment with antibody drugs [7].

Compared with monoclonal antibodies, peptide-based PD-1/PD-L1 inhibitors with low molecular weight, low immunogenicity, easy synthesis, and low cost have become promising candidates. Discovery of novel peptide inhibitors such as linear peptides, macrocyclic-peptides, peptidomimetics, and D-peptides targeting PD-1/PD-L1 have been reported [87]. Most peptides are under evaluation in preclinical trials and early-stage clinical trials. For example, AUNP-12, the first reported 29-amino acid peptide inhibitor, targeted PD-1 protein and

demonstrated antitumor activities in B16F10 melanoma and 4T1 breast cancer tumor models [88]. Several macrocyclic peptides have been revealed by Bristol-Myers Squibb (BMS). Magiera-Mularz and colleagues studied the interaction of macrocyclic peptides with PD-L1 protein. They found that among the discovered peptides, two representative peptides BMS-57 and BMS-71 showed binding affinity (affinities were determined which were 566 nM and 293 nM, respectively) [89].

Non-peptide small molecule inhibitors for the blockade of PD-1/PD-L1 interaction have been developed. They are good alternatives to monoclonal antibodies due to their improved properties such as better tumor penetration and higher oral bioavailability [90]. BMS discovered and revealed multiple non-peptide small molecule inhibitors in recent years. Among the compounds, BMS-202 efficiently blocked the interaction of PD-1/PD-L1 by inducing the dimerization of PD-L1 [91]. An insight into the interaction of peptides and PD-L1 inspired the exploration of designing new peptide-based inhibitors. In a study, Tianyu Wang et al. discovered 17 small-molecule compounds, and Compound 17 was identified to promote the internalization and degradation of surface PD-L1 expression, also exert good antitumor activity in colon CT26 tumor-bearing mouse model and a melanoma B16-F10 tumor model [92].

DNA or RNA aptamer with high specific binding affinity and low immunogenicity can potentially be utilized for PD-1/PD-L1 blockade. Wei-Yun Lai and colleagues reported a DNA aptamer (aptPD-L1) and demonstrated that aptPD-L1 restored T cell functions by increasing tumor-infiltrated lymphocytes and the secretion of cytokines (e.g., IL-1, TNF-α, IFN-γ) and inhibited tumor growth in CT26 colorectal cancer and LL/2 lung cancer tumor models [93]. A major challenge in the application of aptamers is fast renal clearance in the body due to the small size. To address this problem, many studies have been conducted to prolong the

circulation time by conjugating aptamers to polyethylene glycol (PEG), dendrimers, lipid moieties, and other macromolecules. In a study, the PD-L1 aptamer was conjugated with albumin to form a larger complex which augmented the *in vitro* antitumor cytotoxicity and exhibited a better *in vivo* antitumor activity [94].

Though conventional monoclonal antibodies (mAbs) have demonstrated promising clinical efficacy in various therapeutic fields over the past decades, limitations of traditional antibodies such as poor penetration in solid tumors due to large molecular weight, high production cost, minimal flexibility in structure modification, and immunogenicity cannot be overlooked. To address these limitations, there is a growing interest in developing smaller antibody formats. Single-domain antibodies (sdAb, also named VHH or nanobody), the variable domain of heavy chain from heavy-chain antibodies (HCAbs), demonstrate a similar structure and function as the antigen-binding fragment of classic antibodies. In addition, nobodies possess several unique features over conventional antibodies such as smaller size (~15 kDa), excellent solubility, good stability, low immunogenicity, and good tumor penetration.[95, 96] Thus, sdAb represents a new type of checkpoint inhibitor for cancer immunotherapy. Many sdAbs have been reported and are currently being evaluated in pre-clinical studies. For example, Fei Zhang et al. identified an anti-PD-L1 nanobody (KN035) and demonstrated that the nanobody induced T-cell responses by elevating the levels of IFN-γ and impaired tumor growth in a xenograft tumor model [97]. Now there is one sdAb (Caplicizumab) targeting acquired thrombotic thrombocytopenic purpura (aTTP) approved by the FDA in 2019 as the first nanobody-based drug [98].

2.4.4 PD-1/PD-L1 based combination therapy

Despite the clinical success of immune checkpoint inhibitors in cancer treatment, monotherapy targeting PD-1/PD-L1 has a various response rate with an average of 15%-30% in most tumor types [6]. Therefore, combination approaches may be beneficial to improve therapeutic efficacy in a variety of cancers and meet the unmet needs of patients.

Cytotoxic chemotherapy is the most common approach applied for cancer treatment. Chemotherapy combined with other therapies may overcome the chemoresistance and improve the therapeutic efficacy. Chemotherapy in combination with PD-1/PD-L1 blockade is widely used to treat cancer patients who get less benefit from the monotherapy [99]. The rationale for the combination of PD-1/PD-L1 blockade with chemotherapy is extensively studied. Chemotherapeutic drugs induce immunogenic cell death and stimulate antitumor immunity by eliminating immune suppressive cells and activating effector cells. Chemotherapy synergizes with PD-1/PD-L1 inhibitors [100]. Like chemotherapeutic drugs, targeted therapy has immunomodulatory effects and the combination therapy of PD-1/PD-L1 blockade with targeted agents has explored. Researchers have reported that pathways such as MAPK and PI3K-AKT promote PD-L1 transcription [100]. Thus, developing combination therapies of PD-1/PD-L1 blockade with targeted therapies targeting the signaling can synergize the antitumor activity of PD-L1 treatment. The efficacy of anti-PD-1/PD-L1 drugs combined with targeted therapy is evaluated in clinical trials including EGFR inhibitors, ALK inhibitors, tyrosine kinase inhibitors, RAS inhibitors, PARP, MEK inhibitors, and AKT inhibitors [100, 101].

Radiotherapy is frequently used for cancer treatment by direct killing of cancer cells. Studies have demonstrated that radiotherapy enhances antitumor activity by increasing the release of tumor antigens, upregulating MHC class I molecules (MHC I), and inducing

immunogenic cell death. On the other side, radiotherapy can cause an immunosuppressive environment by upregulation of PD-L1 expression, and recruiting immunosuppressive cell populations (e.g., regulatory T cells, MDSCs) [102, 103]. Therefore, radiotherapy may be a good candidate for combination therapy with PD-1/PD-L1 to acquire a synergetic therapeutic effect. Data from preclinical and clinical trials is promising. For example, in a phase III clinical trial, NSCLC patients treated with durvalumab plus chemoradiotherapy showed improved progression-free survival and overall survival [100].

A combination of PD-1/PD-L1 inhibitors with other immune checkpoint inhibitors or co-stimulatory molecules has been evaluated in preclinical settings and clinical trials [104]. In a phase I/IIa trial, the efficacy of anti-LAG3 monoclonal antibody (BMS-986016) in combination with Nivolumab in the treatment of melanoma was evaluated and showed a safety profile and promising efficacy. A combination of PD-1 blockades and 4-1BB antibody shows a synergistic effect. The study has demonstrated combination treatment with anti-4-1BB monoclonal antibody and anti-PD-1 antibody elevated the level of activated effector T cells in blood [105]. As an alternative approach, developing bispecific antibodies targeting two molecules attracts great interest. These bispecific/bifunctional antibodies can simultaneously target two receptor proteins displaying advantages over the combination therapy with two antibodies. For example, M7824, a monoclonal antibody against TGF-β and PD-L1 is more effective in the suppression of tumor growth and metastasis than either antibody alone in the mouse model [106]. This bifunctional molecule is evaluated in a phase I clinical trial for the treatment of advanced solid tumors and shows a higher overall response rate [107].

Combination strategies combining PD-1/PD-L1 inhibitors with cancer vaccines have been studied. For some tumors such as pancreatic cancer and prostate cancer with the lack of

infiltration of effector immune cells, PD-1/PD-L1 inhibitors failed to demonstrate effective therapeutic effect. Cancer vaccines can activate tumor-specific T cells and increase the release of tumor antigens to further enhance antitumor responses [108]. In a study, Kevin C. Soares et al. reported that combination therapy with GM-CSF-secreting vaccine and anti-PD-1 antibody produced durable immune responses and prolonged mouse survival compared to vaccine or PD-1 blockade monotherapy [109]. An immunosuppressive environment enriched with immunosuppressive cells and dysfunctional or exhausted T cells impaired T-cell-based immune response. For example, in a study, dual blockade of CTLA-4 and PD-1 in combination with a GVAX vaccine enhanced tumor rejection. In addition, this combination therapy significantly increased tumor-infiltrated CD8+ T cells and reduced the suppressive regulatory T cells [110].

In summary, immunotherapy has shown great promising benefits in cancer treatment. The immune checkpoint inhibitors especially PD-1/PD-L1 blockade have exhibited durable and effective therapeutic effects on various cancers. Compared to conventional cytotoxic chemotherapy drugs, immunotherapy with high specificity may have a great future for cancer treatment.

CHAPTER 3

SUPPRESSION OF IKBKE WITH SIRNA INHIBITS THE GROWTH OF TRIPLE-NEGATIVE BREAST CANCER

3.1 Introduction

Triple-negative breast cancer (TNBC) is a subtype of breast cancer characterized by the absence of estrogen receptor (ER), progesterone receptor (PR), and human epidermal growth factor receptor 2 (HER2) [4]. TNBC accounts for approximately 15-20% of all breast cancer cases and is more often diagnosed in young women. It displays distinctive features, including high aggressiveness, a tendency to metastasize, a poor prognosis, and a low survival rate [5]. Unlike other breast cancer subtypes, TNBC has limited treatment options due to the lack of targeted therapies specific to the tumor. Currently, chemotherapy is the primary treatment option for TNBC patients. However, it is important to note that TNBC frequently develops resistance to chemotherapy [9, 47]. Moreover, TNBC patients face a nearly threefold higher risk of early relapse within five years of diagnosis compared to non-TNBC patients [10]. Therefore, there is a significant need to develop new therapies for the treatment of TNBC.

IKBKE, also known as IKKε or IKKi, is a member of the IKK (IκB kinase) family and plays an important role in several signaling pathways, including the non-canonical NF-κB signaling pathway, Hippo pathway, and STAT pathway [12, 13, 111]. Moreover, IKBKE exhibits high expression levels in various cancers, such as breast cancer, glioma, ovarian cancer, and pancreatic cancer [11]. The expression of IKBKE has been linked to tumorigenesis, metastasis, and chemoresistance [62, 63]. For example, Lu and colleagues revealed that IKBKE promotes glioma tumorigenesis and epithelial-mesenchymal transition (EMT) by upregulating the expressions of YAP1 and TEAD2. Silencing IKBKE with shRNA inhibits the progression of

glioblastoma [63]. In another study, the overexpression of IKBKE is associated with Cisplatin resistance in ovarian cancer, and knocking down IKBKE overcomes this resistance in ovarian cancer cells (A270CP and C13) [112]. More recently, IKBKE has been demonstrated to induce tumoral immunosuppression in mesenchymal glioblastoma [111].

In 2007, Boehm et al. identified IKBKE as an oncogene in breast cancer through integrative genomic approaches. They observed that IKBKE was overexpressed in both breast cancer cell lines and patient-derived tumors. Furthermore, they found that suppressing the expression of IKBKE could induce tumor cell death [113]. In accordance with these findings, we also demonstrated that silencing IKBKE using siRNA inhibits *in vitro* proliferation and invasiveness of breast cancer cells [15]. In recent years, accumulating evidence revealed that IKBKE plays a significant role in promoting tumorigenicity and metastasis of TNBC via different mechanisms. For example, one study reported that the overexpression of IKBKE promoted the epithelial-mesenchymal transition (EMT) and lung metastasis of TNBC cells by phosphorylating and stabilizing the EMT-related transcription factor Snail. Depletion of IKBKE could effectively inhibit breast cancer invasion and metastasis [114]. Additionally, IKBKE can promote tumorigenesis by activating IKBKE-associated cytokine signaling pathways such as NF-κB and STAT signaling. Targeting IKBKE with an inhibitor (CYT387) of TBK1/IKBKE and JAK signaling could reduce the secretion of pro-tumorigenic cytokines (CCL5 and IL-6) and subsequently inhibit tumor growth *in vitro* and *in vivo* [14]. Taken together, these studies suggest that IKBKE plays a pivotal role in tumorigenesis and metastasis, and the suppression of IKBKE expression may provide a novel approach to the treatment of TNBC.

Small interfering RNA (siRNA) has the ability to specifically knockdown the expression of target genes [115]. It represents a promising tool for therapy as it can silence

aberrant genes that are essential for the progression of diseases such as cancer [115]. However, successful siRNA therapy relies on the development of safe and effective RNA delivery systems because naked siRNA is unstable and has limited cellular uptake [116]. A number of delivery carriers have been investigated to increase the stability and facilitate cellular uptake of siRNAs [117]. Among them, non-viral delivery systems, such as siRNA conjugates and siRNA nanoparticles are gaining prominence in siRNA therapy because of their safety and ease of production [118]. In previous studies, we reported a cholesteryl peptide-based delivery system that can efficiently deliver different siRNAs into various cancer cells with negligible toxicity [25, 119]. In this study, we exploited the potential of this system in delivering IKBKE siRNA to TNBC cells. The IKBKE siRNA exhibits potent transfection efficiency, and *in vitro* studies showed its ability to effectively inhibit the proliferation, migration, and invasion of TNBC cells. Subsequently, we condensed the IKBKE siRNA with the cholesterol-peptide delivery system and assessed the stability, cellular uptake, and tumor penetration of the resulting siRNA nanoparticle. Furthermore, *in vivo* anti-tumor activity of the cholesterol peptide/siRNA nanocomplex was evaluated in an orthotopic syngeneic mouse TNBC model. These findings underscore the significance of IKBKE in tumorigenesis and metastasis, emphasizing that inhibiting IKBKE expression holds promise as a crucial therapeutic target in the treatment of TNBC.

3.2 Experimental section

3.2.1 Materials

Lipofectamine RNAiMAX reagent was ordered from Fisher Scientific (Pittsburgh, PA). Human IKBKE siRNA (Sense strand sequence: 5'-GGUCUUCAACACUACCAGCtt-3'), and mouse IKBKE siRNA (Sense strand sequence: 5'-GGUCUUCAACUCAGCCAGCtt-3') were

purchased from Invitrogen (Carlsbad, CA). Cholesterol-Cysteine-HHHKKHHHKK (CCP) was ordered from United BioSystems Inc. (Herndon, VA). CellTiter-Glo Luminescent Cell Viability Assay kit was purchased from Promega (Madison, WI). The annexin V-FITC apoptosis kit was ordered from Thermo Fisher (Pittsburgh, PA). PI/RNase was ordered from Abcam (Waltham, MA). iTaq™ Universal SYBR® Green One-Step Kit was obtained from Bio-Rad (Hercules, CA). CYTO-ID® Autophagy detection kit was ordered from Enzo Life Sciences (Farmingdale, NY).

3.2.2 Cell culture

The MCF-10A cell line was isolated from the Michigan Cancer Foundation. It is a non-tumorigenic epithelial cell line from the mammary gland of a White female with fibrocystic breasts. EMT-6 is a murine mammary carcinoma cell line derived from a transplanted hyperplastic alveolar nodule of a BALB/c mouse. The EMT-6 and MCF-10A cell lines were ordered from the American Type Culture Collection (ATCC). EMT-6 cells were cultured in Dulbecco's modified Eagle's medium (DMEM) supplemented with 10% FBS, penicillin (100 U/ml), and streptomycin (100 μg/ml). MCF-10A cells were cultured in DMEM/F12 with additives provided in a Lonza kit (1×MEGM SingleQuots Supplement Pack, Cat# CC-4136). To make a complete growth medium for MCF-10A cells, cholera toxin (100 ng/mL) and horse serum (5%) were added. Both cells were incubated at 37℃ in a humidified atmosphere with 5% CO2.

3.2.3 RNA extraction and quantitative RT-qPCR

Total RNA was extracted using TRIzol reagent (Invitrogen, Waltham, MA) following the manufacturer's protocol. The mRNA level was evaluated by reverse transcription-quantitative polymerase chain reaction (RT-qPCR) using a universal SYBR green one-step

reaction kit. The primers used for human IKBKE are 5'-GGAGATGCAGAGCACAGCCAA-3' (forward) and 5'-GCCGAAGTCTGTCAGCTTGTAG-3' (reverse). The primers for mouse IKBKE are 5'-GGAGATGCAGAGTACCACTAAC-3' (forward) and 5'-CCCGAAGTCAGACAGCTTATAG-3' (reverse). The primers for mouse 18s ribosomal RNA are 5'-GCAATTATTCCCCATGAACG-3' (forward) and 5'-GGCCTCACTAAACCATCCAA-3' (reverse). The primers for human 18s are 5'-GTCTGTGATGCCCTTAGATG-3' (forward) and 5'-AGCTTATGACCCGCACTTAC-3' (reverse).

3.2.4 Silencing activity assay

EMT-6 cells were transfected with siRNAs as we described previously [25]. In brief, 2.5×10^4 EMT-6 cells were seeded into 12-well plates and incubated at 37℃ overnight. IKBKE siRNA was condensed with Lipofectamine RNAiMAX reagent or CCP and then transfected into the cells at a final siRNA concentration of 100 nM for 24 hours. A scrambled siRNA was used as a negative control. A non-malignant human breast cell line (MCF-10A) was also used to assess the silencing specificity of the mouse IKBKE siRNA. Following transfection, total RNA was extracted with TRIzol reagent, and the mRNA level was determined by RT-qPCR.

3.2.5 Cell proliferation study

A total of 5,000 EMT-6 and MCF-10A cells were seeded in 96-well plates and incubated at 37°C overnight. Scrambled siRNA or IKBKE siRNA were then condensed with Lipofectamine RNAiMAX reagent and transfected into the cells at a final siRNA concentration of 100 nM for 6 hours. Following incubation, the Opti-MEM medium was replaced with a fresh growth medium, and the cells were further incubated at 37°C for a total duration of 72 and 96 hours. Subsequently, 100 μl of CellTiter-Glo buffer (Promega, Madison, WI) was added to the

96-well plate, and luminescence was measured using the SpectraMax iD5 Multi-mode Microplate reader (Molecular Devices, San Jose, CA).

3.2.6 Migration and invasion studies

EMT-6 cells were transfected with IKBKE siRNA using Lipofectamine RNAiMAX. After a 48-hour incubation, the transfected cells were trypsinized, resuspended in serum-free DMEM at a density of 1×10^6 cells/ml. For the invasion assay, the Transwell chamber was precoated with 50 μg of Matrigel. A volume of 100 μL of cell suspension in serum-free DMEM containing 1×10^5 cells was placed in the Transwell chamber, which was placed into a 12-well plate containing DMEM medium supplemented with 10% FBS. Following incubation for 6 and 24 hours, the cells were fixed with 10% paraformaldehyde, and stained with 0.05% crystal violet, and the counts of migrated and invaded cells were counted.

In the wound healing assay, EMT-6 cells were seeded in 12-well plates and transfected with 100 nM siRNA as described above. Once the cells reached approximately 80% confluence, a wound area was deliberately generated by gently scraping the cell monolayer using a sterile 100 μL pipette tip. Subsequently, the cells were washed with PBS to eliminate any detached cells. The cells were then incubated at 37°C, and the width of the wound area was monitored under a microscope after 24 hours.

3.2.7 Cell cycle study

Forty-eight hours after the siRNA transfection, EMT-6 cells were treated with EDTA-trypsin and washed twice with cold PBS. The cells were fixed with cold 70% ethanol at 4°C for 4 hours. After fixation, the cells were washed with PBS and incubated with PI/RNase staining buffer for 30 minutes at room temperature. Flow cytometry was employed to assess the cell

cycle, and the percentage of cells in the G0/G1, S, and G2/M phases was analyzed using ModFit LT software.

3.2.8 Apoptosis study

A total of 5×10^4 EMT-6 cells were seeded in a 6-well plate and incubated overnight at 37°C. Subsequently, they were transfected with IKBKE siRNA/Lipofectamine RNAiMAX for 48 hours. Following the incubation, the cells were stained using the Alexa Fluor 488 Annexin V/Dead Cell Apoptosis Kit (Thermo Fisher Scientific, NY) according to the manufacturer's protocol and analyzed using a FACScalibur flow cytometry (BD Biosciences, Franklin Lakes, NJ).

3.2.9 Autophagy staining assay

EMT-6 cells were seeded in 4-well chamber slides at a density of 6×10^4 cells/well and incubated for 16 h. The medium was removed, and cells were treated with 100 nM siRNA for 48 hours. Then, cells were washed twice with assay buffer and stained with CYTO-ID Green Detection Reagent and Hoechst 33342 for 30 min at 37℃. After that, cells were washed with PBS, fixed with 10% formalin for 20 min, and imaged with confocal microscopy (Leica Biosystems, Wetzlar, Germany). Chloroquine was used as a positive control.

3.2.10 Cellular uptake study

Cellular uptake was evaluated using both flow cytometry and fluorescent microscopy. For the flow cytometry analysis, 1×10^5 EMT-6 cells were seeded in 12-well plates for 16 h. The medium was then replaced with Opti-MEM containing either free Cy5-siRNA or CCP/Cy5-siRNA. After 1 h, 2 h, and 4 h of post-transfection incubation, the cells were treated with 1 mg/mL heparin to remove any siRNA that may have bound nonspecifically. The cells were collected and re-suspended in DPBS for flow cytometry analysis.

For fluorescent microscopy, 5×10^4 EMT-6 cells were seeded in a 24-well plate and cultured overnight, followed by incubation with free Cy5-siRNA or CCP/Cy5-siRNA nano-complex. After 2 h and 4 h incubation, the cells were washed with DPBS and incubated with LysoTracker Red DND-99 (Invitrogen, Carlsbad, CA), followed by fixation with 4% formalin and treatment with DAPI for nuclear staining. Images of cells from each group were captured using a fluorescent microscope (Keyence High Content Microscope, Osaka, Japan).

3.2.11 3D tumor spheroid penetration study

3D tumor spheroids were prepared using Cultrex spheroid formation ECM (R&D Systems, Minneapolis, MN) as previously reported [120]. Briefly, 3000 EMT-6 cells were suspended and mixed with 50 μL of spheroid formation ECM and added into a 96-well ultralow attachment spheroid microplate (Corning, REF# 4515), followed by centrifugation at 300 g for 5 min at 4 ℃. Subsequently, the cells were incubated at 37 ℃ for 5 days to form spheroids. After this incubation period, the spheroids were washed three times with PBS, and either free Cy5-siRNA or CCP/Cy5-siRNA was incubated with the spheroids for 6 h. After washing, penetration of the siRNA was determined using a Leica SP8 Stellaris Confocal Microscope (Leica Biosystems, Wetzlar, Germany).

3.2.12 Cellular cytotoxicity

1×10^4 EMT-6 cells were seeded in a white 96-well plate. After 24 h incubation, medium was replaced with Opti-medium containing siRNA condensed with Lipofectamine RNAiMAX reagent or CCP at final siRNA concentrations of 50, 100, and 200 nM. After 24 h incubation, cell viability was detected with a CellTiter-Glo kit. Untreated cells served as the negative control and the cells treated with 1% Triton X-100 served as the positive control.

3.2.13 Hemolysis assay

pH-sensitive endosomal disruption of nanocomplex was evaluated with an *ex vivo* pH-dependent hemolysis assay described in literature [121]. Briefly, human red blood cells (RBCs) were isolated from human whole blood (BioIVT). RBCs were washed twice with 150 mM NaCl solution and diluted in either pH 7.4 or pH 5.6 PBS to achieve a 2% (v/v) RBC solution. In a v-bottom 96-well plate, 20 μL of CCP was added to 180 μL of the RBC solution corresponding to each pH. After incubation at 37°C for 1 h, the plate was centrifuged at 1000×g for 5 min, and 100 μL of the supernatant from each well was transferred into a flat-bottom 96-well plate and the absorption was measured at 405 nm. Negative and positive controls were carried out with buffer alone and 1% Triton X-100, respectively.

3.2.14 Characterization and serum stability of CCP/siRNA nanocomplex

Cholesterol peptide was condensed with 20 μM IKBKE siRNA at different N/P ratios (1:1, 2:1, 3:1, 4:1, 5:1, 10:1, and 20:1) at room temperature for 30 min to form the siRNA nanocomplex. The formation of the nanocomplex was confirmed using a gel retardation assay as previously described [122]. Briefly, 10 μL of the nanocomplex was separated on 1% agarose gel and visualized with GelRed under UV light. Particle size of the nanocomplexes was measured in PBS (pH 7.4) using a Malvern Zetasizer Nano-ZS (Malvern Instruments, Westborough, MA). A serum stability study was performed with mouse serum. The siRNA nanocomplex was incubated with 50% mouse serum at 37°C for different time intervals. Encapsulated siRNAs were released by incubation with 40 μM of heparin for 10 min on ice and then analyzed by electrophoresis in a 1% agarose gel. siRNA was visualized by staining with GelRed.

3.2.15 *In vivo* antitumor activity study

The animal protocol was approved by the Institutional Animal Care and Use Committee (IACUC) at the University of Missouri-Kansas City. For the antitumor activity study, 2.5×10^5 EMT-6 cells were implanted into the second mammary fat pad of female Balb/c mice to establish an orthotopic TNBC mouse model as described [123]. The IKBKE siRNA or scrambled siRNA were condensed with CCP at an N/P ratio of 10:1 and administered to the mice via peritumoral injection at a dose of 0.5 mg siRNA/kg. The siRNAs were administered every three days for a total of five injections. In this study, once the tumor size reached 50-100 mm^3, the mice were randomly divided into three groups and treated with saline, IKBKE siRNA nanocomplex, and scrambled siRNA nanocomplex. Tumor volumes were monitored using the formula: 0.5 × (longest diameter) × (shortest diameter)^2. The expression of PD-L1 protein in harvested tumors was measured using ELISA kits and normalized to the total protein content in each sample.

3.2.16 Immunohistochemistry (IHC) staining

Tumor tissues were fixed in 10% formalin, embedded in paraffin, sectioned, and mounted on glass slides. The formalin-fixed paraffin-embedded tumor sections were deparaffinized and incubated in an antigen retrieval solution (10 mM citric acid, 0.05% Tween 20, pH 6) for 45 min at 95–100 ℃ to expose the epitope. The sections were stained with anti-mouse CD8 alpha antibody (Abcam, ab209775, 1:1000) and anti-mouse CD3 antibody (Cell Signaling, Cat# 99940, 1:150) overnight at 4 ℃. The slides were incubated with a biotinylated goat anti-rabbit secondary antibody, followed by the DAB chromogen reagent in the immunohistochemistry kit (Abcam, ab64261). The staining of tumor sections was visualized

with optical microscopy and quantified with ImageJ. Three regions of each section were randomly selected for imaging.

3.3 Statistical analysis

The data was presented as the mean ± SD. Statistical analysis was conducted using a one-way analysis of variance (ANOVA) with Turkey's post hoc test. A p-value less than 0.05 is considered statically significant.

3.4 Results

3.4.1 Silencing activity of IKBKE siRNA in TNBC cells

Quantitative RT-PCR was conducted to investigate whether siRNA could reduce the expression of the IKBKE gene in EMT-6 cells. The siRNA was condensed with either Lipofectamine RNAiMAX or cholesterol peptide to form nanocomplexes. The expression of the IKBKE mRNA was measured using RT-PCR 24 hours post-transfection. As depicted in Figure 1A, in contrast to the scrambled siRNA, the IKBKE siRNA silenced about 80% and 90% of the IKBKE expression in EMT-6 cells when delivered with Lipofectamine and cholesterol peptide, respectively. We then evaluated the IKBKE expression in human non-malignant MCF-10A cells after transfection with human IKBKE siRNAs. Figure 1B showed that about 70% of IKBKE mRNA was suppressed in non-malignant MCF-10A cells when transfected with human IKBKE siRNA indicating that the specificity of the human IKBKE siRNA. These findings suggest that the CCP/siRNA nanocomplex exhibited potent silencing activity with high specificity.

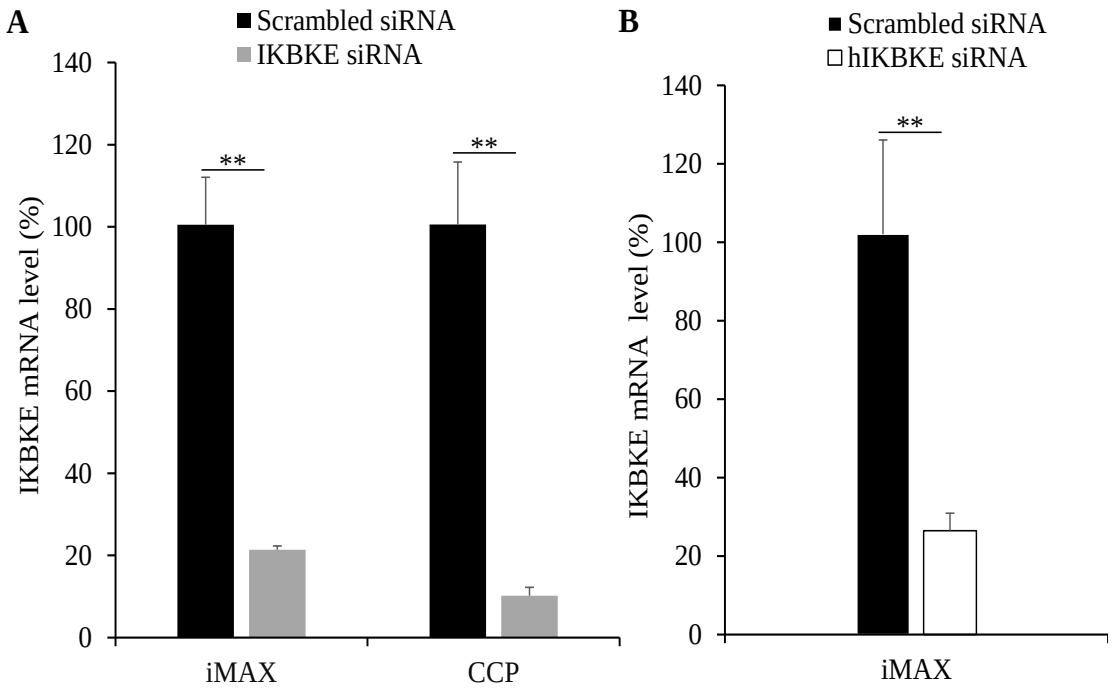

Figure 1. Silencing activity of IKBKE siRNA with Lipofectamine™ RNAiMAX reagent and cholesterol peptide (CCP) in mouse TNBC EMT-6 cells. The silencing effect of mouse IKBKE siRNA at the mRNA level was assessed in EMT-6 cells (A) and the silencing effect of human IKBKE siRNA was evaluated in non-malignant human mammary epithelial cells MCF-10A (B). All results are presented as the mean ± SD (n=3). (*$p<0.05$; **$p<0.01$)

3.4.2 Cell proliferation study

Subsequently, we assessed tumor cell proliferation using the CellTiter-Glo reagent after siRNA transfection. In a previous study, we reported that human IKBKE siRNA significantly inhibited the proliferation of human breast cancer MDA-MB-231 cells [16]. Here, we treated mouse TNBC EMT-6 cells with mouse IKBKE siRNA and measured cell proliferation at 72 and 96 h post-transfection. As shown in Figure 2A, the suppression of IKBKE by mouse siRNA was associated with a noticeable inhibition in cell proliferation in EMT-6 cells. Cells treated with mouse IKBKE siRNA exhibited a significantly lower proliferation rate than those treated with scrambled siRNA at different time points (approximately 56% at 72 h and 72% at 96 h post-transfection, respectively). In contrast, neither human nor mouse IKBKE siRNAs has an impact on the proliferation of non-malignant MCF-10A breast cells, as shown in Figure 2B. This finding revealed that IKBKE is not only overexpressed but also plays a role in the proliferation of TNBC cells [14]. Furthermore, the suppression of mouse IKBKE expression by mouse siRNA only inhibited the proliferation of mouse TNBC cells.

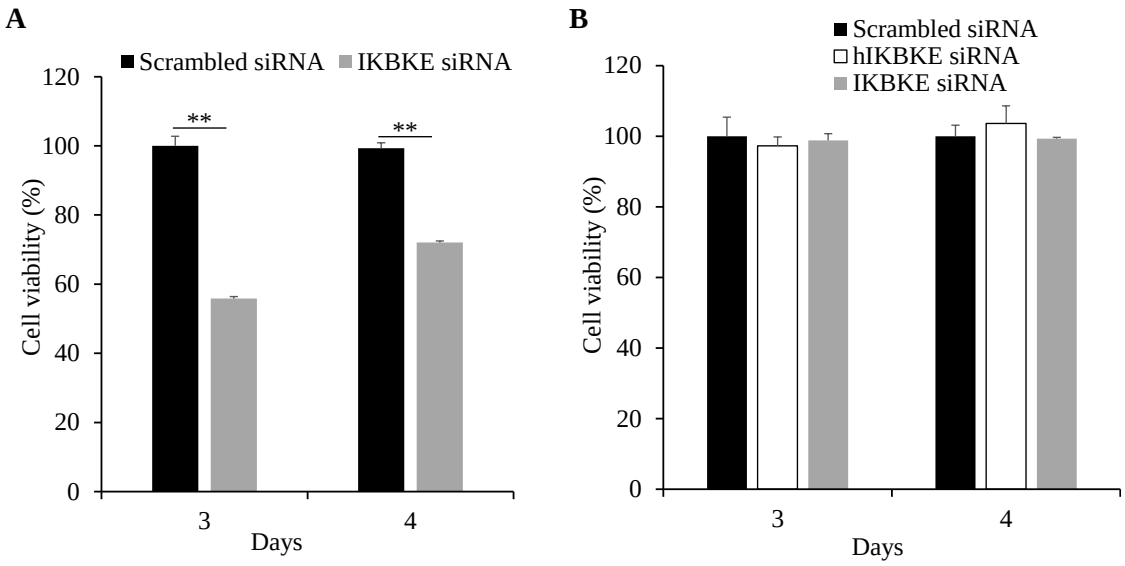

Figure 2. Silencing of IKBKE with siRNA inhibits the proliferation of TNBC cells. Silencing of IKBKE with siRNA inhibits the proliferation of EMT-6 cells (A) but not the non-malignant MCF-10A breast cells (B). Cell proliferation was determined on day 3 and day 4 after transfection using the CellTiter-Glo reagent. All results are presented as the mean ± SD (n=3). (*$p<0.05$; **$p<0.01$)

3.4.3 Cell migration and invasion studies

To assess whether the downregulation of IKBKE in EMT-6 cells impact their migration and invasion capabilities, we employed a widely accepted transwell chamber system. The results (Figure 3A) revealed that the suppression of IKBKE by siRNA reduced the number of migrated and invaded cells. As shown in Figures 3B and 3C, approximately 15% and 50% of EMT6 cells transfected with IKBKE siRNA were able to pass the transwell membrane in the migration and invasion assays, respectively, compared to the cells treated with scrambled siRNA. Furthermore, we evaluated tumor cell motility using a wound-healing assay. In this assay, a cell monolayer was scratched, and the migration of cells into the wound area was monitored 24 hours after creating the wound. Compared to the scrambled siRNA, IKBKE siRNA inhibited tumor cell migration, as shown in Figures 3D and 3E.

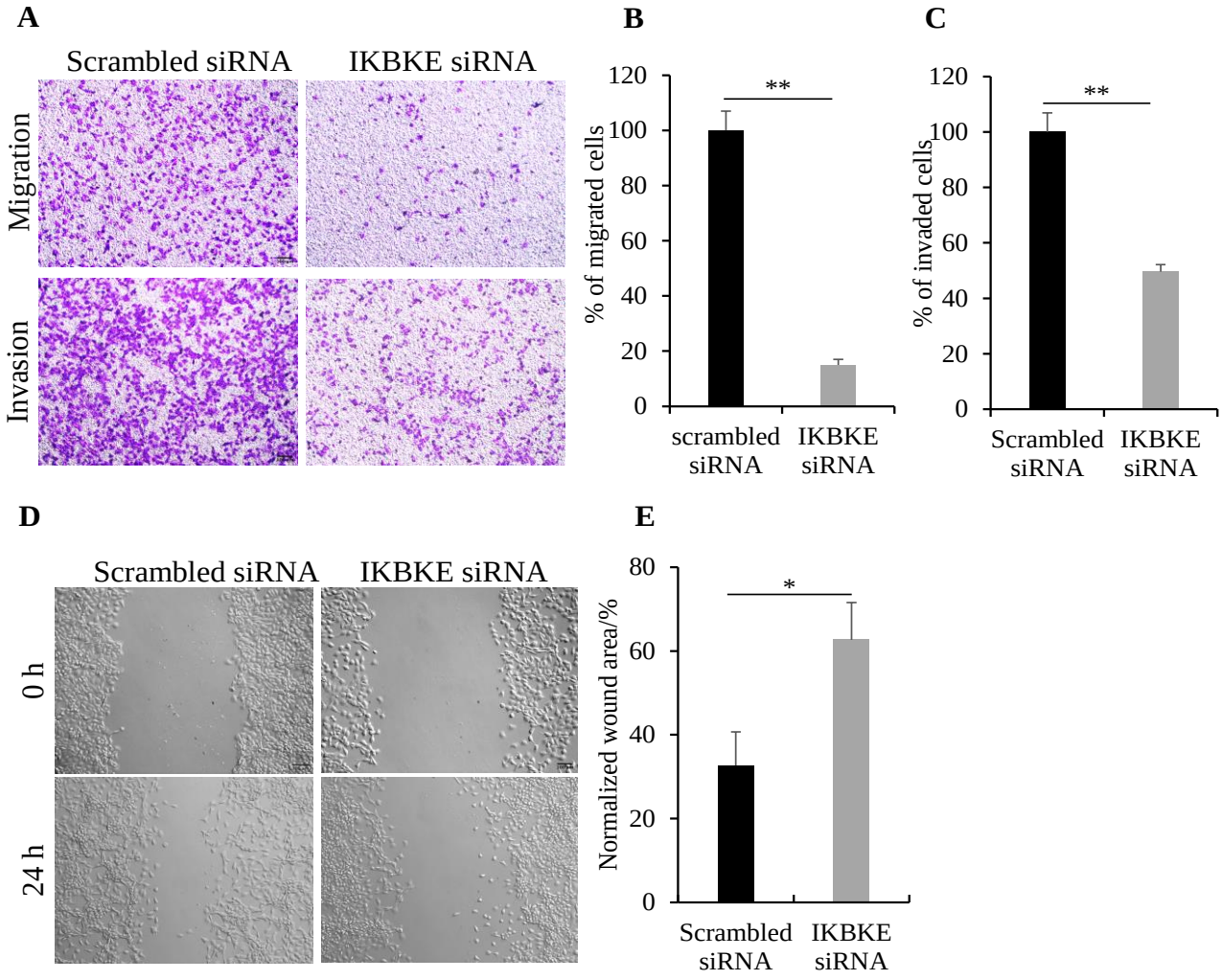

Figure 3. Silencing IKBKE inhibits the migration and invasion of EMT-6 cells. Cell migration and invasion were evaluated using a transwell assay. (A) Representative images of migrated and invaded EMT-6 cells were presented following siRNA transfection for 6 h and 24 h, respectively. (B-C) Quantitative analysis was performed by counting the number of migrated or invaded cells at the bottom of the membrane in six randomly selected microscope fields from three independent samples. A wound healing assay was employed to evaluate cell motility. The motility ability of siRNA-transfected tumor cells toward the wound area was examined 24 hours after creating the wound (D-E). The scale bar represents 100 μm. All results are presented as the mean ± SD (n=3). (*$p<0.05$; **$p<0.01$)

3.4.4 IKBKE silencing promotes tumor cell apoptosis and regulates cell cycle distribution

We determined whether IKBKE siRNA could induce apoptosis in EMT-6 cells using the Annexin Fluor 488 annexin V/Dead cell apoptosis kit. The data presented in Figures 4A and 4B demonstrated that the percentages of early apoptotic cells in the scrambled siRNA group and the IKBKE siRNA group were 2.5% and 3.9%, respectively. Similarly, the percentage of late apoptotic cells increased from 6.4% to 10.6% in the IKBKE siRNA group, indicating that silencing IKBKE induces cell apoptosis. To investigate the mechanism underlying the inhibitory effect of IKBKE siRNA on the proliferation of EMT-6 cells, we examined cell cycle distribution in EMT-6 cells transfected with scrambled or IKBKE siRNA using flow cytometry. As shown in Figures 4C and 4D, a significant increase at the S and G2 phases was observed in cells treated with IKBKE siRNA compared to the control group. There was a reduction in the proportion of cells at the G1 phase in IKBKE siRNA transfected cells (37.61%) in comparison with those treated with scrambled siRNA (42.24%). IKBKE is a positive regulator of autophagy and silencing IKBKE reduced the autophagy in EMT-6 cells (Figure 3E). These findings indicate that IKBKE siRNA can induce cell apoptosis and inhibit cell proliferation by arresting cells at the S and G2 phases.

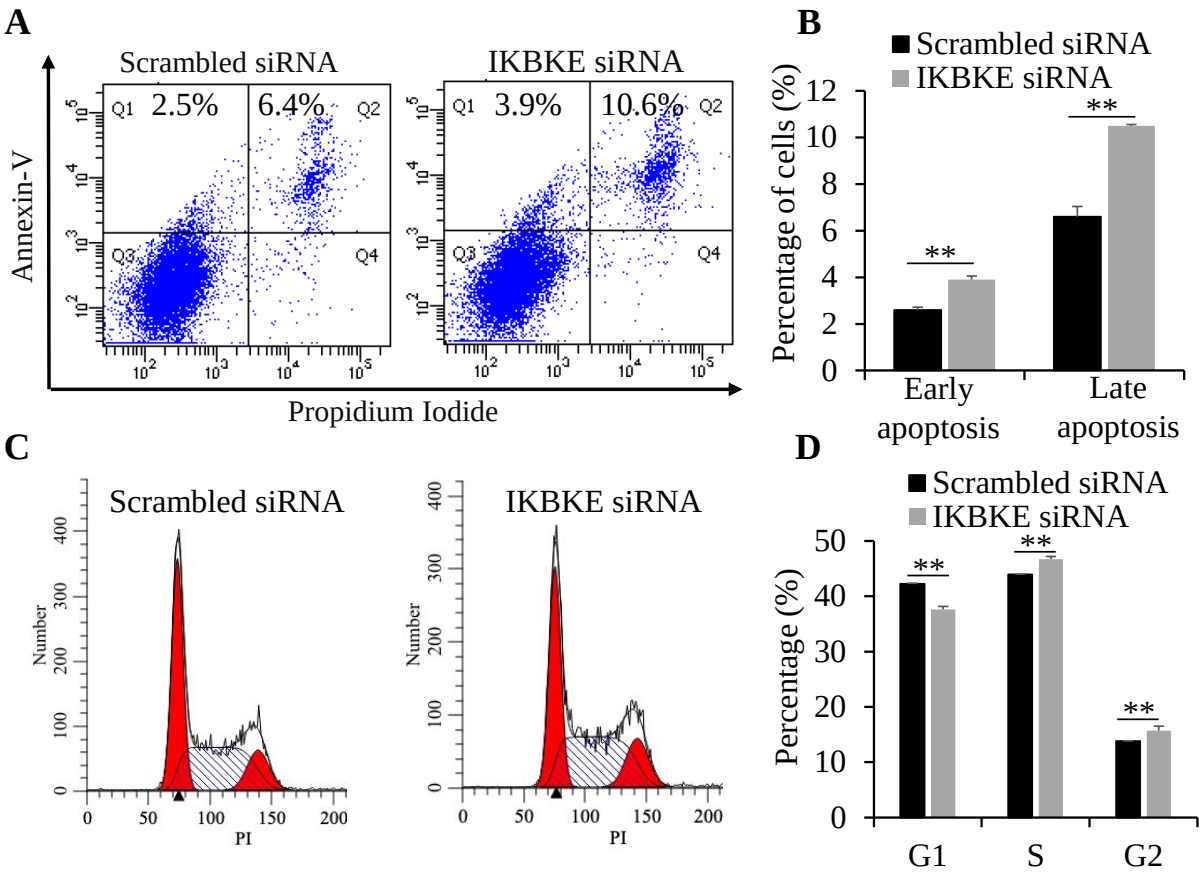

Figure 4. IKBKE siRNA induces EMT-6 cell apoptosis and cell cycle arrest at the S phase and G2 phases and inhibits autophagy. EMT-6 cells were transfected with scrambled siRNA and IKBKE siRNA at 100 nM. The cells were stained using the Alexa Fluor 488 Annexin V and propidium iodide, followed by flow cytometry analysis. Representative flow cytometry images (A) and the percentage of cells in early apoptosis (Q1) and late apoptosis/necrosis (Q2) were presented (B). The cell cycle distribution of EMT-6 cells was assessed using flow cytometry 48 hours after siRNA transfection. Representative images and quantitative analysis were presented (C-D). The cell cycle distribution of EMT-6 cells was analyzed using ModFit LT software. (*$p<0.05$; **$p<0.01$)

3.4.5 IKBKE siRNA reduces autophagy

Autophagy is a survival mechanism for all eukaryotic cells which can be triggered by nutrient deprivation and stressful conditions. After initiation, the intracellular proteins and organelle are degraded in the lysosome and recycled [124]. Many studies have demonstrated the promoting role of autophagy in cancer progression including breast cancer [125]. We, therefore, decided to use EMT-6 cells as a model to study the role of IKBKE in controlling cell autophagy. For this purpose, IKBKE was silenced with scrambled or IKBKE siRNA for 48 hours. Chloroquine can inhibit lysosomal activity by increasing the lysosomal pH which is included as a positive control. Cells were treated with Chloroquine for 24 hours. As indicated in Figure 5, the EMT-6 cells stained with CYTO-ID Green autophagy detection dye, an accumulation of green fluorescence was observed in the perinuclear region of the cells after chloroquine treatment. IKBKE silencing with IKBKE siRNA significantly reduced autophagic flux. This data indicates that IKBKE plays a positive role in controlling autophagy in breast cancer cells.

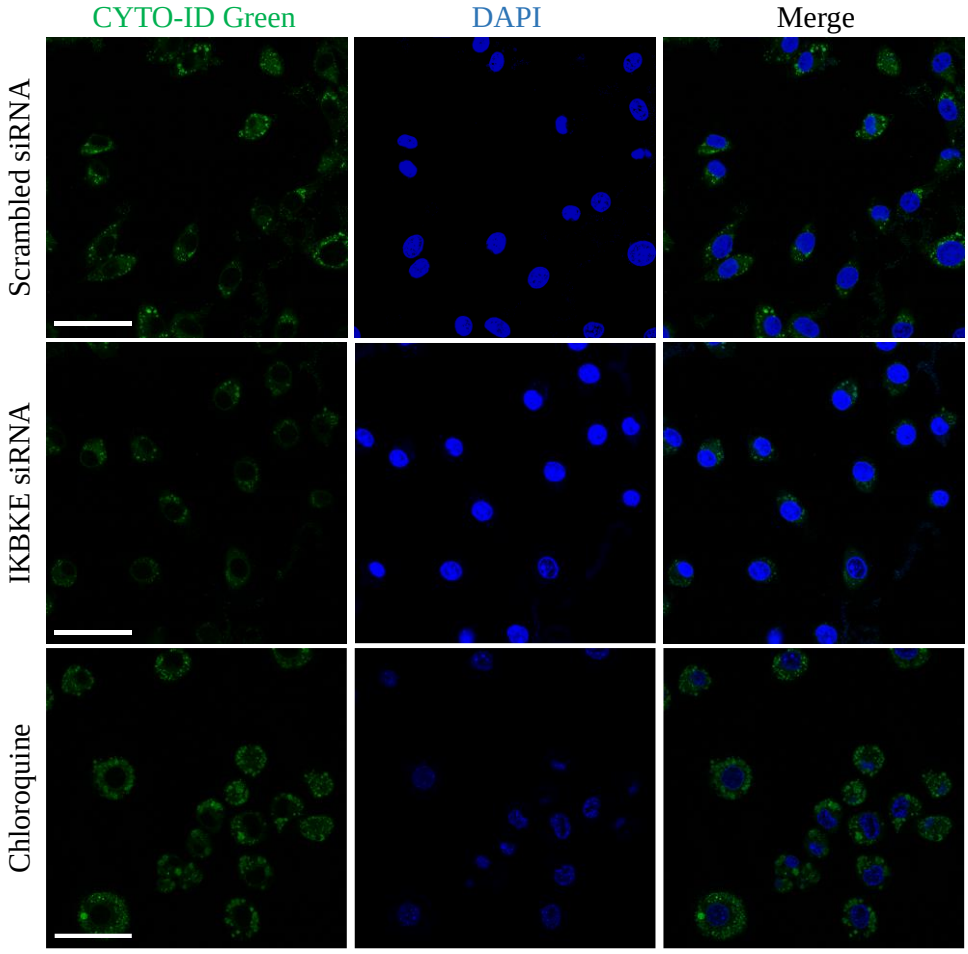

Figure 5. IKBKE siRNA reduces autophagy in EMT-6 cells. Autophagy in EMT-6 cells was evaluated with a CYTO-ID® Autophagy detection kit. CYTO-ID® Green reagent was used for the staining of autophagic vesicles in EMT-6 cells and the stained cells were analyzed with confocal microscopy 48 hours post-transfection. Chloroquine can inhibit lysosomal activity by increasing lysosomal pH which was used as a positive control. Scale bars, 50 μm.

3.4.6 Characterization and serum stability of CCP/siRNA nanocomplex

The condensation of siRNA with cholesterol peptides was evaluated using a gel retardation assay. Figure 6A illustrates that complete siRNA condensation can be achieved at high N/P ratios (3:1, 4:1, 5:1, 10:1, and 20:1). In Figure 6B, the particle size decreased as the N/P ratio increased, indicating an enhanced interaction between siRNA and cholesterol peptide at high N/P ratios. Particle size was confirmed by TEM (Fig. 6C), and these results align with the data presented in Figure 6B. Based on the findings from these experiments, we selected an N/P ratio of 10:1 for use in subsequent experiments. One of the challenges in achieving efficient siRNA delivery is the low stability of naked or unmodified siRNA. Consequently, we investigated the stability of the CCP/siRNA nanocomplex in 50% mouse serum. As depicted in Figure 6D, the nanocomplex effectively protected siRNA from degradation in the serum for up to 16 h, in contrast to free siRNA, which exhibited significant degradation after 6 h and complete degradation after 16 h.

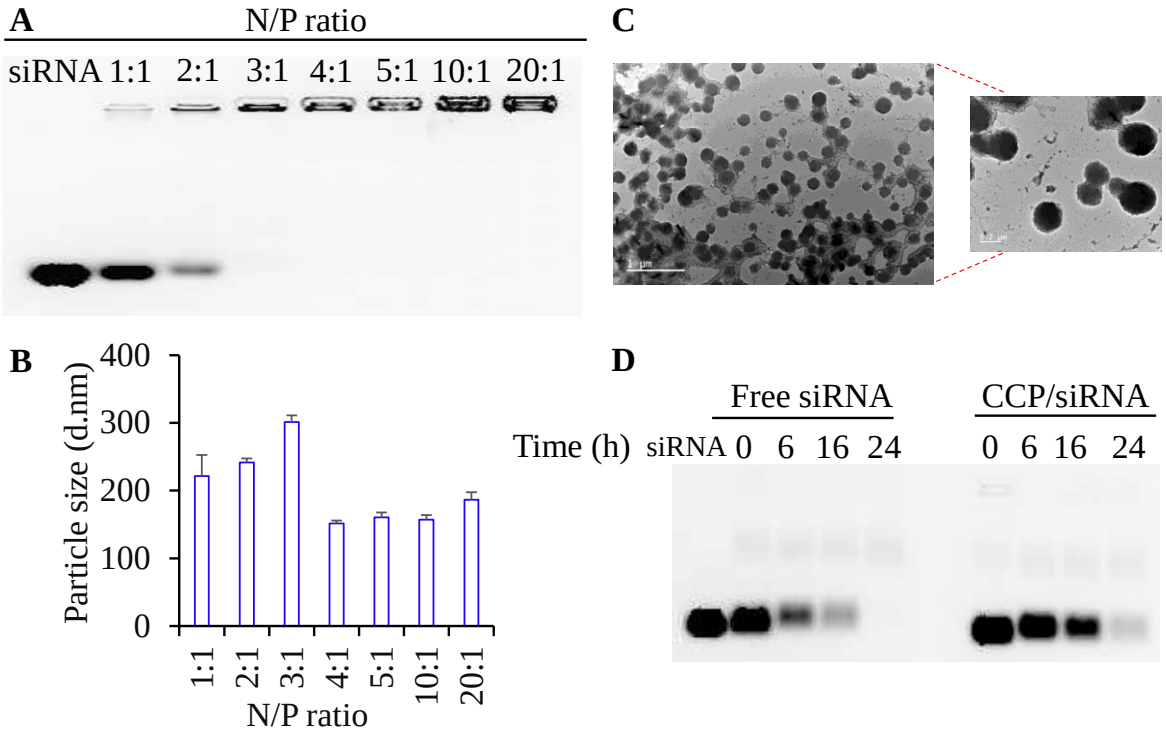

Figure 6. Characterization of the CCP/siRNA nanocomplexes. (A) Gel retardation assay of the CCP/siRNA nanocomplex at different N/P ratios. (B) Particle size of the CCP/siRNA nanocomplex at different N/P ratios. (C) Representative TEM images of the CCP/siRNA nanocomplex at an N/P ratio of 10:1. (D) Serum stability of the nanocomplex in 50% mouse serum for 0, 6, 16, and 24 hours.

3.4.7 Cytotoxicity and hemolysis of CCP/siRNA nanocomplexes

The cytotoxicity of the CCP/siRNA nanocomplexes was measured with CellTiter-Glo at various concentrations of siRNA. Compared to negative control group, no toxicity was observed in EMT-6 cells treated with CCP/siRNA nanocomplexes at the concentrations of 50 nM and 100 nM (Figure 7). The toxicity of CCP/siRNA nanocomplexes slightly increased at a higher concentration (200 nM), however, the nanocomplexes exhibited less cytotoxicity than Lipofectamine™ RNAiMAX at concentration of 200 nM. Subsequently, pH-sensitive endosomal disruption was evaluated with an *ex vivo* pH-dependent hemolysis assay. The RBC membrane serves as a substitute for the endosomal membrane. The blank nanocomplexes (0.5 μM, 1 μM, and 5 μM) corresponding to the siRNA dose of 0.25, 0.5, and 2.5 mg/kg were used in this study. Negligible hemolysis was observed at 0.5 μM and 1 μM at the physiological pH, suggesting the safety of nanocomplexes at pH 7.4 (Figure 8). At pH 5.6, nanocomplexes at 1 μM and 5 μM showed hemolysis, and the effect increased as the concentration increased, which indicates nanocomplexes disrupted the endosomal membrane to mediate endosomal escape for intracellular siRNA delivery.

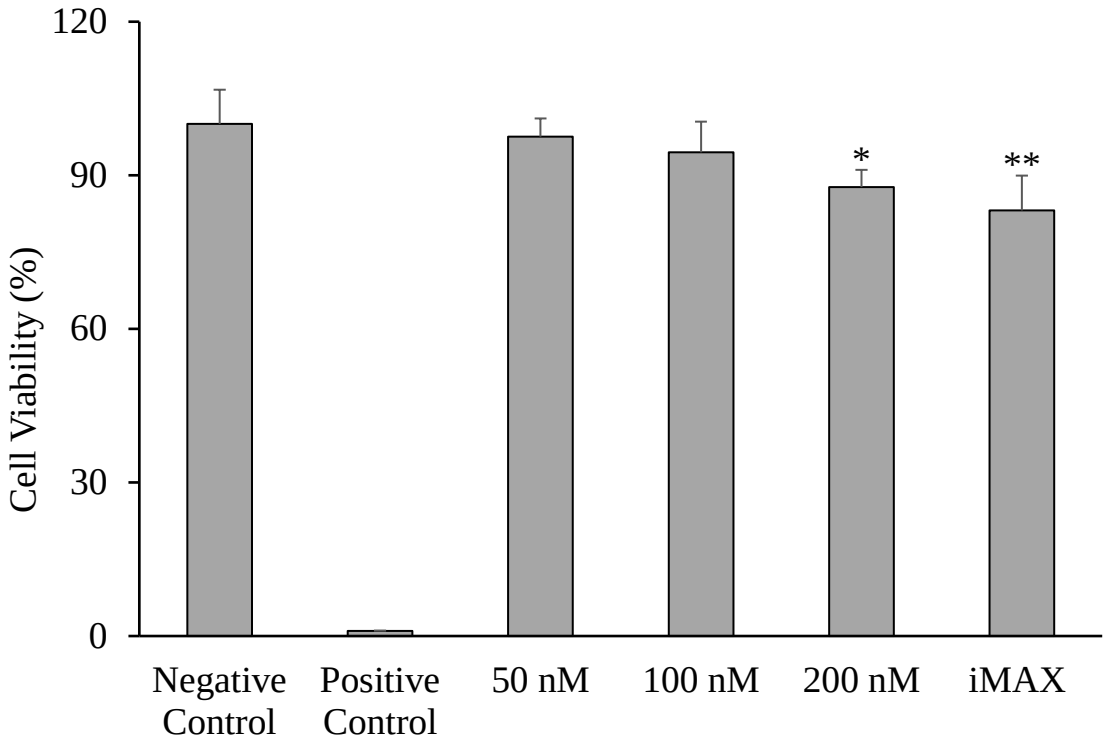

Figure 7. Cytotoxicity of CCP/siRNA nanocomplexes. Cytotoxicity of the nanocomplexes and Lipofectamine RNAiMAX at various concentrations of siRNA was evaluated 24 hours after siRNA transfection by using the CellTiter-Glo reagent. Untreated cells served as the negative control and the cells treated with 1% Triton X-100 served as the positive control. Results are presented as the mean ± SD (n = 3) (* $p < 0.05$; ** $p < 0.01$)

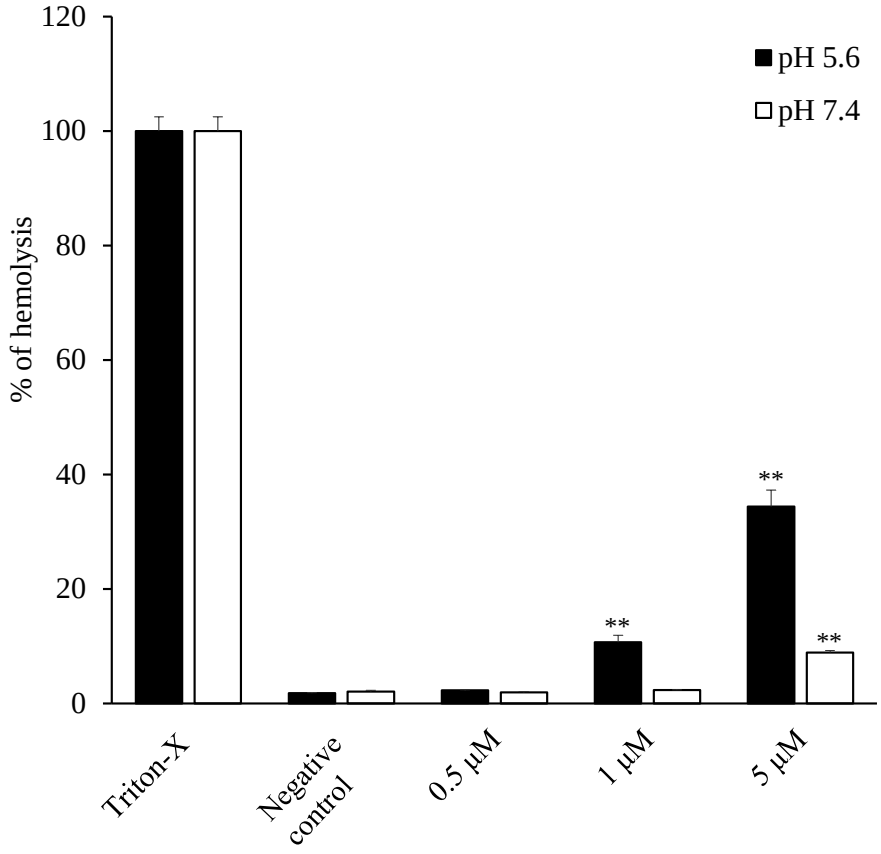

Figure 8. Hemolysis assay of nanocomplexes at pH 7.4 and pH 5.6. The blank nanocomplexes at concentrations of 0.5, 1, and 5 μM were used in this study. Negative and positive controls were carried out with buffer alone and 1% Triton X-100, respectively. The experimental samples were normalized to the A_{405} of Triton X-100-treated samples and multiplied by 100%. Results are presented as the mean ± SD (n = 3) (* $p < 0.05$; ** $p < 0.01$)

3.4.8 3D tumor spheroid penetration study

The tumor extracellular matrix is a major barrier that hinders the penetration of antitumor drugs into the tumor microenvironment. We thus evaluated the tumor penetration capability of the CCP/siRNA nanocomplex in 3D tumor spheroids formed by EMT-6 cells. The IKBKE siRNA was labeled with Cy5, and after a 4 h incubation with the tumor spheroids, the siRNA nanocomplex exhibited much deeper penetration and a higher fluorescence intensity in the central region of the tumor spheroids (Figures 9A and 9B). These results revealed that cholesterol peptide-formed nanocomplex can effectively penetrate and deliver IKBKE siRNA into the tumor.

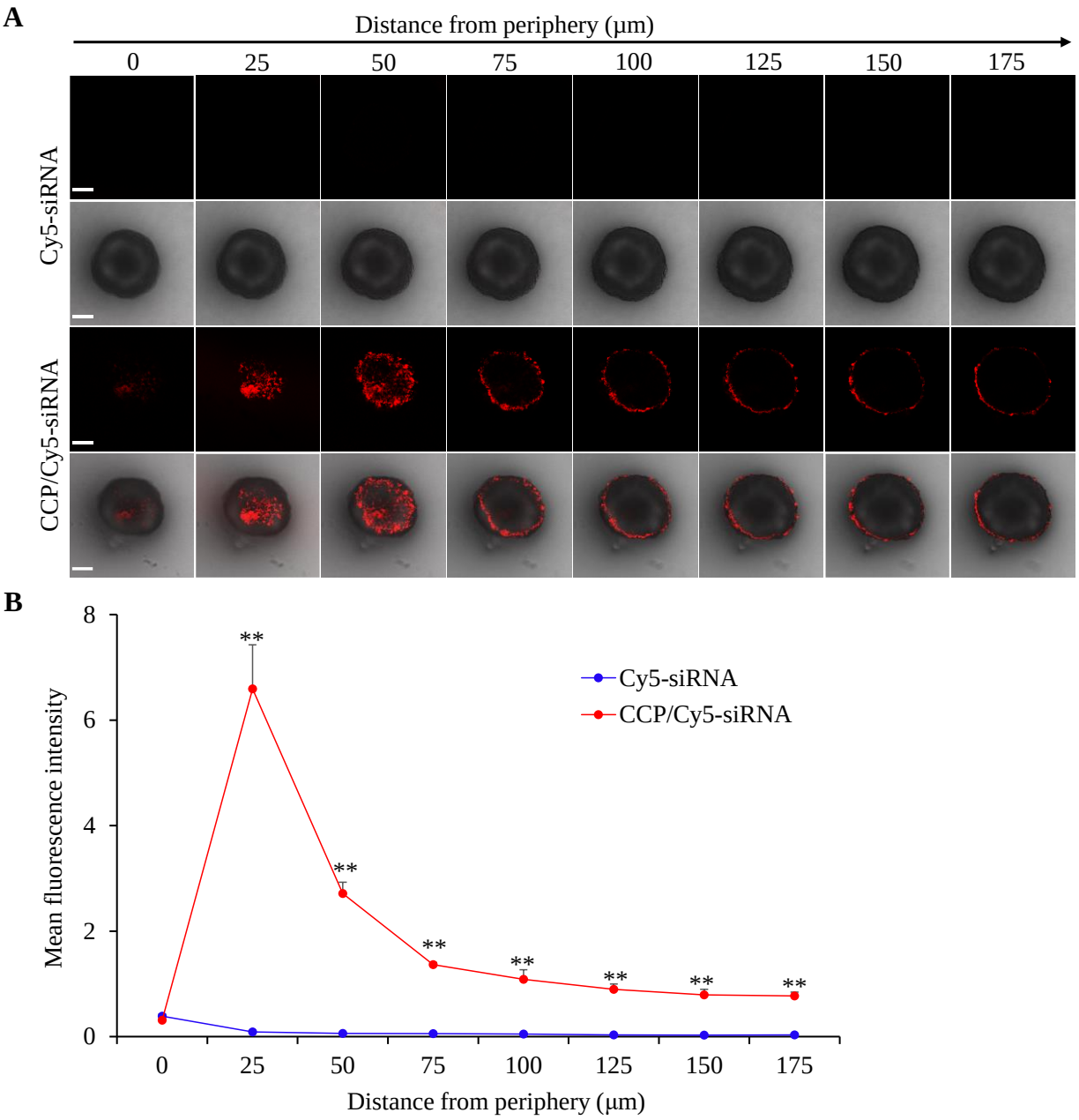

Figure 9. 3D tumor spheroid penetration study. (A) Representative z-stack confocal images of the spheroids, with a z-step of 25 μm, for Cy5-siRNA and CCP/Cy5-siRNA after 4 hours of incubation. (B) Mean fluorescence intensity of Cy5-siRNA in the z-stacked confocal images plotted against the distance from the spheroids' periphery (n = 3). Scale bars, 100 μm. (*p<0.05, **p<0.01)

3.4.9 Cellular uptake study

We next evaluated the cellular uptake of the CCP/siRNA nanocomplex in EMT-6 cells using flow cytometry and fluorescent microscopy. The data from the flow cytometry analysis revealed that the CCP/Cy5-siRNA group displayed much higher cellular uptake compared to the free siRNA treated group after 1, 2, and 4 h transfection (Figures 10A and 10B). Subsequently, we utilized confocal microscopy to investigate the intracellular distribution of the CCP/siRNA nanocomplex in EMT-6 cells. As indicated in Figures 10C and 10D, the results were consistent with those obtained from the flow cytometry analysis. The CCP/siRNA nanocomplex showed significantly higher cellular uptake compared to the control group, suggesting that the cholesterol peptide facilitated the release of siRNA into the cytoplasm through endosome escape.

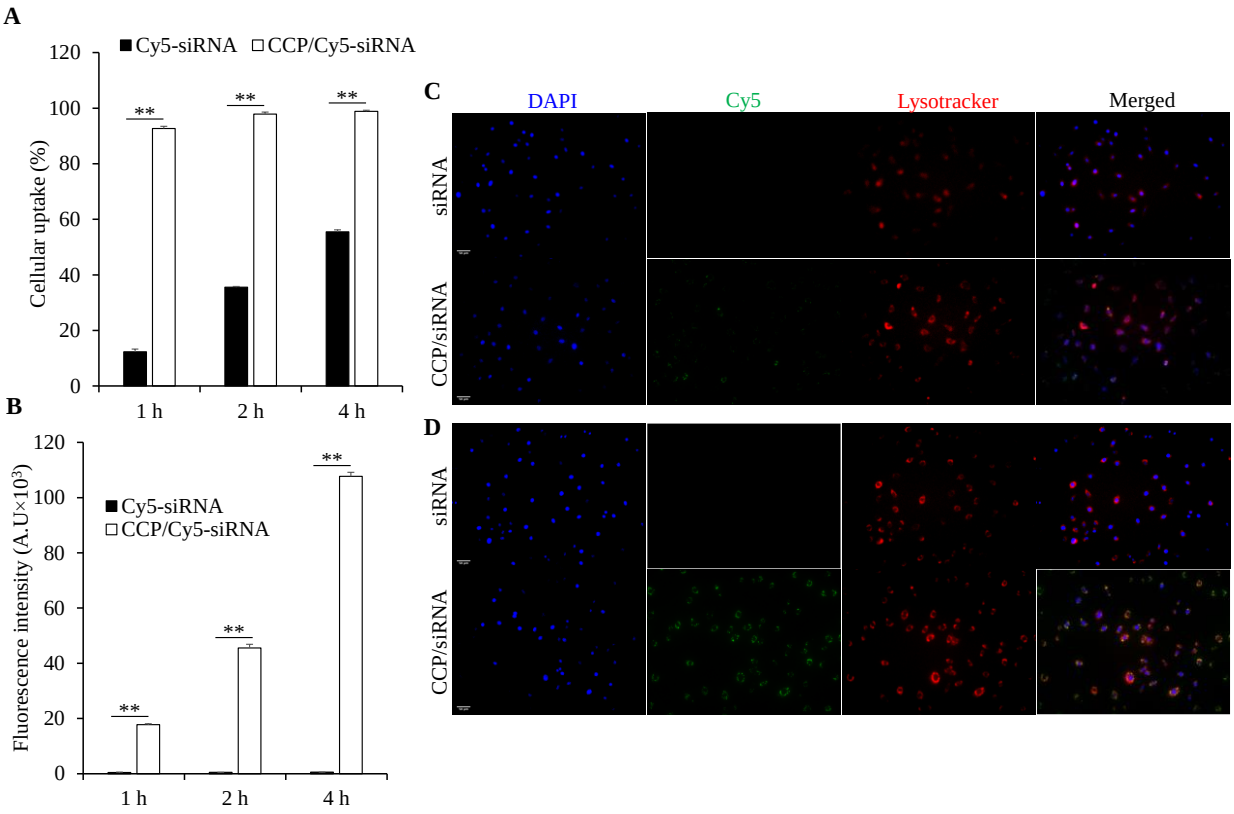

Figure 10. Cellular uptake of the CCP/siRNA nanocomplex in EMT-6 cells. siRNA was labeled with Cy5 for analysis using flow cytometry (A-B) and fluorescent microscopy (C-D). Cellular uptake of Cy5-siRNA in EMT-6 cells was analyzed by flow cytometry after incubation with Cy5-siRNA or CCP/Cy5-siRNA nanocomplex for 1 h, 2 h, and 4 h (A). The fluorescence intensity of EMT-6 cells that take up the siRNA nanocomplexes at 1 h, 2 h, and 4 h (B). Representative fluorescent images of EMT-6 cells after incubation with Cy5-siRNA or CCP/Cy5-siRNA nanocomplex for 2 h (C) and 4 h (D). The scale bar represents 50 μm. All results are presented as the mean ± SD (n=3 independent experiments). (*$p<0.05$, **$p<0.01$)

3.4.10 *In vivo* anti-tumor activity

Anti-tumor activity of IKBKE siRNA was evaluated using an orthotopic TNBC mouse model with EMT-6 tumors. When the tumor sizes reached 50-100 mm^3, the mice were randomly divided into three groups (8 mice each group) and treated with saline, scrambled siRNA, and IKBKE siRNA. The siRNAs were injected peritumorally at a dose of 0.5 mg/kg every three days for a total of five doses as shown in Figure 11A. As illustrated in Figures 11B and 11C, IKBKE siRNA effectively suppressed tumor growth in comparison with the control groups (saline and scrambled siRNA groups). Tumor weights in the IKBKE siRNA treated group were notably smaller than those in other groups, as demonstrated in Figure 11D. We also assessed PD-L1 expression in each collected tumor, and the results indicated an increase in PD-L1 expression after IKBKE siRNA treatment (Figure 11E).

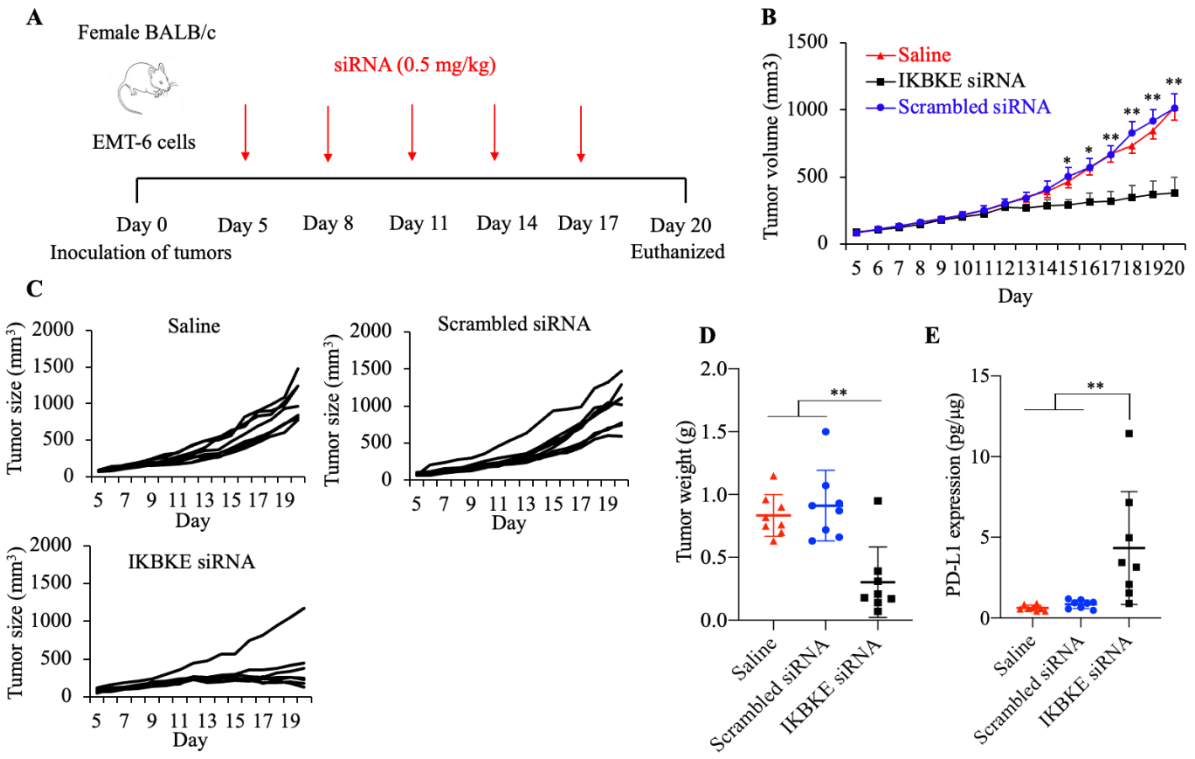

Figure 11. Antitumor activity of the CCP/IKBKE siRNA nanocomplex in an orthotopic syngeneic TNBC mouse model. (A) Schematic diagram of treatment. EMT-6 tumor-bearing BALB/c female mice were peritumorally injected with the scrambled siRNA and IKBKE siRNA at a dose of 0.5 mg/kg every three days for a total of 5 injections. (B) Tumor volume measured over time. Tumor volumes were presented as means ± SEM (n=8). (C) Tumor growth curves of individual mice in each group. (D) Weight of tumors harvested on day 20. (E) The expression of PD-L1 in harvested tumors was measured with Duoset ELISA kits. Tumor weight and protein expression level are presented as mean ± SD (*p<0.05; **p<0.01)

3.4.11 Immunohistochemical (IHC) staining

CD8+ cytotoxic T lymphocytes play critical roles in cancer immunotherapy. CD8+ T cells are the most powerful effectors in antitumor immunity. In some clinical trials, the proliferation of intratumoral CD8+ T cells in tumor specimens from patients has been correlated with the therapeutic outcome of immunotherapy [126]. Many studies have demonstrated the pivotal role of IKBKE in tumorigenesis and metastasis, but few studies have investigated the impact of IKBKE in the tumor microenvironment. We therefore performed immunohistochemical staining for CD8+ T cells in the tumor tissues. As illustrated in Figures 12B and 12C, IKBKE siRNA significantly increased the density of CD8+ T cells in tumor tissues. In addition, we observed higher penetration of CD3+ T cells into the tumor tissue of IKBKE siRNA-treated mice (Figure 12A). By contrast, CD3+ T cells were mainly detected on the periphery of the tumors in saline and scrambled siRNA-treated mice. This data indicates that CCP/IKBKE siRNA nanocomplexes may promote the infiltration or proliferation of T cells.

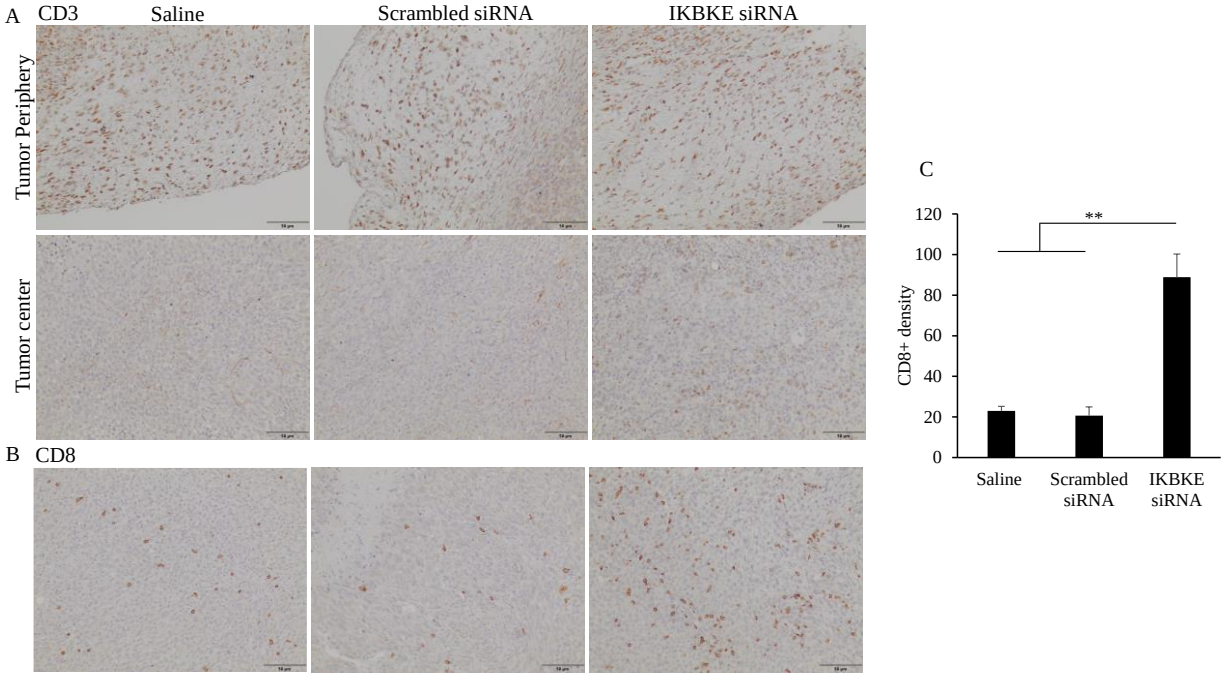

Figure 12. Immunohistochemical staining of tumor specimen. (A) Representative images of tumor sections stained with anti-CD3 antibody. (B) Representative images of tumor sections stained with anti-CD8 antibody. (C) The numbers of CD8+ T cells in each tumor specimen were quantitated after immunohistochemical staining. All data are presented as mean ± SD (*$p<0.05$; **$p<0.01$)

3.5 Discussion and conclusions

TNBC is an aggressive subtype of breast cancer characterized by its high degree of heterogeneity and propensity for metastasis. Compared to other subtypes of breast cancer, TNBC exhibits a high tendency for metastatic spread to distant organs such as the brain, lung, lymph node, and bone. Metastasis is the primary cause of death for majority of TNBC patients, presenting a considerable challenge in the clinical management of this disease [34]. Accumulating evidence has demonstrated the association of IKBKE with tumor metastasis. Numerous studies have revealed that IKBKE plays a role in promoting the migration, invasion, and metastasis of malignant glioma by facilitating the translocation of Snail1 into the nucleus. Knocking down of IKBKE with shRNA destabilizes Snail1 and subsequently inhibits the tumor cell invasion [63, 127]. IKBKE functions as an oncogene in breast cancer and is overexpressed in about 30% of breast cancer cell lines and tumors. Like other canonical members of the IKK family of protein kinases, IKBKE can also activate the NF-kB signaling pathway, which is associated with the cancer stem cells (CSCs) phenotype of breast cancer cells [128]. More recently, evidence has shown that IKBKE promotes tumorigenesis, migration, invasion, and lung metastasis through the phosphorylation and stabilization of the epithelial-mesenchymal transition (EMT) transcription factor Snail. Depleting IKBKE inhibits tumorigenesis and lung metastasis in an *MMTV-PyVMT* mouse model [114]. Therefore, targeting IKBKE may represent a potential strategy to combat breast cancer metastasis. In accordance with these findings, our study demonstrates that silencing IKBKE with siRNA dramatically reduces the proliferation, migration, and invasion of TNBC cells (Figures 1-3).

In our previous studies, we investigated the antitumor activity of IKBKE siRNA in HER-2 positive breast cancer cell lines and a subcutaneous xenograft mouse model involving

MDA-MB-231 cells [15, 16]. In this study, we extended our research to examine the application of mouse IKBKE siRNA in an orthotopic syngeneic mouse model. Syngeneic tumor models are tumors derived from mouse cancer cell lines inoculated into the genetically identical mouse strain. They have fully functional immune systems to enable the study of tumor-immune system interactions in response to treatment [129]. Syngeneic mouse models are immunocompetent and widely used in the evaluation of immunotherapeutic agents. As an effective preclinical immune-oncology model, it has been applied to evaluate the efficacy of novel therapies, study the mechanism of drug action, test the pharmacokinetics and toxicity of treatment [130]. As depicted in Figures 1A and 1B, our custom-designed siRNA specifically silenced IKBKE mRNA expression in mouse breast cancer cells but not the non-malignant human MCF-10A breast cells. This silencing subsequently led to the inhibition of proliferation, migration, and invasion of mouse TNBC EMT-6 cells. Moreover, IKBKE siRNA induced apoptosis in tumor cells and arrested the tumor cycle in S and G2 phases (Figure 4). *In vivo* study demonstrated that peritumoral injection of IKBKE siRNA inhibited tumor growth in EMT-6 bearing syngeneic mouse model, as compared to the groups treated with saline and scrambled siRNA. Taken together, targeting IKBKE with siRNA shows promise as a potential strategy for treating TNBC.

siRNA, as a class of RNA-based therapeutics, represents a highly promising approach for the treatment of various diseases. siRNAs have the capability to selectively knock down the expression of specific genes via RISC-mediated mRNA degradation [117]. However, the application of siRNA as therapeutics is limited by inherent limitations such as their negative charges, large molecular weight, and susceptibility to degradation. Hence, the development of safe and effective delivery systems that facilitate the passage of siRNAs across biological barriers and cell membranes is imperative [116]. In our study, we employed a cholesterol peptide

as a delivery system, which exhibited significant transfection efficiency and increased stability of siRNA, which is consistent with previously reported findings [25]. As shown in Figure 6, the cholesterol peptide/siRNA complex effectively protects siRNA from degradation in mouse serum for up to 16 hours, in contrast to naked siRNA, which was completely degraded within 6 hours. Additionally, we observed increased cellular uptake of cholesterol peptide/siRNA nanocomplex in EMT-6 cells and improved penetration of the siRNA nanocomplex in 3D tumor spheroids (Figures. 9 and 10).

Chemotherapy remains the primary systemic treatment for both early-stage and advanced-stage TNBC due to the absence of targeted treatment options. Unfortunately, there is a higher risk of recurrence in TNBC compared to other breast cancer subtypes, as patients often develop chemoresistance after long-term treatment. This resistance is particularly challenging for metastatic TNBC, accounting for approximately 90% of treatment failures. As a result, there have been very limited therapeutic strategies shown to improve the survival of patients with metastatic TNBC [10]. TNBC is a heterogeneous disease with an unfavorable prognosis, resulting in varied clinical responses among patients. Accumulating evidence indicates that combination therapies, as demonstrated in multiple clinical trials, have achieved superior therapeutic outcomes when compared to single therapies [51, 58]. In our study, we found that IKBKE siRNA effectively inhibited tumor growth in the EMT-6 tumor-bearing orthotopic mouse model. Furthermore, we analyzed the expression of PD-L1 in tumor samples using an ELISA kit and observed a notable upregulation of PD-L1 expression following treatment with IKBKE siRNA (Figure 11E). These findings suggest that combining IKBKE siRNA with immunotherapies, such as PD-L1 immune checkpoint inhibitors, may provide new opportunities for achieving favorable outcomes in the treatment of TNBC.

In summary, our study evaluated the biological activity of the designed IKBKE siRNA and its successful encapsulation and delivery using a cholesterol peptide-based delivery system for TNBC therapy. The CCP/siRNA nanocomplex exhibited high transfection efficiency and potent silencing activity. The silencing of IKBKE with siRNA markedly inhibited tumor cell proliferation, migration, and invasion. The siRNA induced apoptosis in tumor cells and arrested them at the S and G2 phases. CCP/siRNA nanocomplex protected siRNA from degradation and increased cellular uptake in tumor cells. Furthermore, the siRNA nanocomplex exhibited significant inhibition of tumor growth in an orthoptic syngeneic TNBC mouse model. Therefore, the IKBKE siRNA nanocomplex emerges as a promising approach for the treatment of TNBC.

CHAPTER 4

DEVELOPMENT OF CD24 SIRNA FOR TRIPLE-NEGATIVE BREAST CANCER TREATMENT

4.1 Introduction

Breast cancer is the most diagnosed cancer in women. It has high heterogeneity and is broadly classified into four subtypes by the differential expression of receptor markers [2]. Triple-negative breast cancer (TNBC) refers to the breast cancer phenotype which are negative for estrogen receptor (ER), progesterone receptor (PR), and human epidermal receptor 2 (HER2) [45]. TNBC is diagnosed in 10-20% of all breast cancer cases and is characterized by high proliferative rate, early metastasis and recurrence, and poor prognosis [5]. Majority of TNBC is basal-like breast cancer and tends to present in younger women. Compared with other subtypes, about 45% of patients with advanced TNBC will develop distant metastasis and the overall five-year survival rate is around 12%. TNBC treatment is still challenging due to the aggressive and heterogeneous features. There are few treatment approaches developed for TNBC because patients with TNBC are insensitive to available hormonal or HER2 targeted drugs due to the absence of related markers. Even though TNBC is chemo-sensitive, however, the tumors are prone to develop early relapse and resistance [10, 48]. Recent advances have been made in the treatment of programmed death ligand-1 (PD-L1) positive TNBC patients. However, only a fraction of patients show a positive response to PD-L1/PD-1 immune checkpoint inhibitors, and those who initially respond to the treatment but often acquire resistance to these therapies over time [131]. Therefore, the development of new treatment strategies is urgently demanded for TNBC.

CD24 is a heavily glycosylated glycosylphosphatidylinositol (GPI)-anchored surface protein that is typically expressed in hematopoietic cells and some non-hematopoietic cells [74].

Accumulating evidence indicates that CD24 is overexpressed in a variety of cancers, including breast, ovarian, prostate, glioma, lung, and colorectal cancers [17, 18]. CD24 serves as a signaling molecule by binding to various binding partners, such as P-selectin, Siglecs, and the neural adhesion molecule L1CAM [132, 133]. CD24 plays a significant role in tumorigenesis and metastasis of multiple types of cancer [66-69]. Moreover, several studies have suggested CD24 exhibits cytoplasmic accumulation, and intracellular CD24 plays a critical role in tumor progression. One study has shown that intracellular CD24 promotes the growth of prostate tumor cells, and the use of shRNA to silence CD24 reduces tumor growth while preventing the functional inactivation of p53 [70]. In another study, Zhang et al. reported that CD24 is co-expressed with mutant p53 in metastatic prostate tumors. Silencing CD24 enhances the restoration of mutant p53 in human prostate cancer cells and subsequently inhibits both tumor growth and metastasis [71]. More recently, a report has shown that despite the absence of surface CD24, some cancer cells still maintain their aggressiveness, and the presence of nuclear CD24 is positively linked to reduced patient survival [72]. Notably, CD24 expression has been associated with poor prognosis. Evidence reveals that CD24 expression is significantly higher in TNBC in comparison with ER+PR+ breast cancer and healthy breast cells. In addition, CD24 overexpression is associated with poor prognosis in TNBC [19, 20]. Moreover, there is an observed association between CD24 expression and resistance to chemotherapy and targeted therapies in breast cancer and other types of cancer [18, 21]. These data reveal that CD24 is overexpressed in various types of tumors, suggesting it may hold promise as a potential target for cancer therapy.

Small interfering RNAs (siRNAs) with lengths of 21-23 nucleotides downregulate specific genes by binding to their complementary mRNA and triggering RISC-mediated

mRNA degradation [134]. siRNAs show high specificity and potency in inhibiting the target genes of interest. Compared to other antisense therapeutics such as shRNA, siRNA has a smaller size and acts in the cytosol without interaction with chromosomal DNA [116]. Unlike monoclonal antibodies mainly targeting cell surface receptors, siRNA can knock down the expression of all genes encoding surface and intracellular proteins [135]. These data indicate siRNA represents an attractive strategy for treatment of diseases including cancer. However, there are several challenges that need to be overcome such as poor stability, low cellular uptake, and endosomal escape. To widen the application of siRNA as a therapeutic agent, a variety of carriers have been developed for efficient siRNA delivery such as polymers, micelles, liposomes, and nanoparticles [118]. In earlier studies, we reported a cholesteryl peptide-modified delivery system that can efficiently deliver siRNAs by forming micelle-like structures to exert biological activities in animals with negligible cytotoxicity [16, 25, 119]. Here, we exploited the capability of the cholesterol peptide in CD24 siRNA delivery. In this study, we designed four CD24 siRNAs and determined the silencing capacity and biological activities with different methods. Also, we evaluated the correlation of CD24 siRNA with doxorubicin resistance and phagocytosis of tumor cells mediated by macrophages.

4.2 Materials and methods

4.2.1 Materials

Lipofectamine RNAiMAX reagent was purchased from Invitrogen (Carlsbad, CA). CellTiter-Glo Luminescent Cell Viability Assay kit was purchased from Promega (Madison, WI). An Alexa Fluor® 488 annexin V/Dead cell apoptosis kit with Alexa® Fluor 488 annexin V and PI was ordered from Thermo Fisher Scientific (Pittsburgh, PA). Propidium iodide (PI)/RNase was ordered from R&D Systems (Cat# 4817-60-04, Minneapolis, MN); iTaq™ Universal SYBR® Green One-Step Kit was obtained from Bio-Rad (Hercules, CA).

Doxorubicin was ordered from LC Laboratories (Cat# D-4000, Woburn, MA). Cholesterol-Val-Cit-HHHKKHHHKK was ordered from United BioSystems Inc. (Herndon, VA).

4.2.2 Cell lines and cell culture

MDA-MB-231 cell line was isolated at MD Anderson from a pleural effusion of a patient with invasive ductal carcinoma. MDA-MB-231 cells is a basal-like TNBC cell line with mesenchymal phenotype and high invasiveness. MDA-MB-468 cell line was isolated from a pleural effusion of a 51-year-old female human in 1977. MDA-MB-468 cells present basal-like tumors of TNBC and show high expression of Ki67.[136] MDA-MB-231, MDA-MB-468, and MCF-10A cell lines were purchased from the American Type Culture Collection (ATCC). MDA-MB-231 and MDA-MB-468 cells were cultured in Dulbecco's modified Eagle's medium (DMEM) supplied with 10% FBS, penicillin (100 U/ml), and streptomycin (100 μg/ml). MCF-10A cells were cultured in DMEM/F12 with additives obtained from Lonza as a kit (1×MEGM SingleQuots Supplement Pack CC-4136). To make a complete growth medium, cholera toxin (100 ng/ml) and horse serum (5%) were added. All cells were incubated at 37 ℃ in a humidified atmosphere with 5% CO_2.

4.2.3 siRNA design and synthesis

siRNAs targeting human CD24 mRNA (NM_013230.3) were designed using siRNA Design Tool (Eurofins Genomics) and siRNA Wizard Software (InvivoGen). Four siRNAs targeting different regions of human CD24 mRNA were designed and purchased from Ambion. The sequences of these siRNAs are listed in Table 1.

4.2.4 RNA extraction and quantitative RT-PCR

The total RNA was extracted with the TRIzol reagent according to the manufacturer's protocol. mRNA levels were evaluated by real-time RT-PCR using the Universal SYBR Green

One-Step reaction. The primers used human CD24 mRNA are 5'-CTCCTACCCACGCAGATTTATTC-3' (forward) and 5'-AGAGTGAGACCACGAAGAGAC-3' (reverse). The 18s ribosomal RNA was employed as a control, and its forward and reverse primers were 5'-GTCTGTGATGCCCTTAGATG-3' and 5'- AGCTTATGACCCGCACTTAC-3', respectively.

4.2.5 Silencing activity assay

Cells were transfected using a method described in our previous studies [25]. Briefly, 5×10^4 MDA-MB-468 or MDA-MB-231 cells were seeded in 12-well plates and incubated overnight at 37°C. The CD24 siRNAs were condensed with Lipofectamine RNAiMAX reagent and then transfected into the cells at final siRNA concentrations of 25 nM and 50 nM for 24 hours. A scrambled siRNA was used as a negative control. Following transfection, total RNA was extracted using TRIzol Reagent (Cat# 15596018, Invitrogen). The mRNA levels were assessed by RT-qPCR using Universal SYBR Green One-Step reaction and quantified using the comparative threshold (Ct) method with 18s as the reference.

4.2.6 Western blotting

For the western blotting assay, 1×10^5 MDA-MB-468 or MDA-MB-231 cells were seeded in 6-well plates and cultured overnight. Subsequently, the cells were transfected with CD24 siRNA or scrambled siRNA using Lipofectamine RNAiMAX for 48 h. After transfection, cells were lysed using RIPA buffer (Cat# 89901, Thermo Fisher Scientific), and total proteins were collected for sodium dodecyl-sulfate polyacrylamide gel electrophoresis (SDS-PAGE). The proteins from the gel were then transferred onto a PVDF membrane. The PVDF membrane was subsequently blocked with 5% non-fat milk in TBST and probed with the primary antibody (Human CD24 antibody, AF5247, R&D Systems), followed by incubation with an HRP-

conjugated secondary antibody as previously described [25]. β-actin was used as an internal control. Each western blot was conducted independently in triplicate.

4.2.7 Migration and invasion studies

MDA-MB-468 or MDA-MB-231 cells were transfected with CD24 siRNAs using Lipofectamine RNAiMAX reagent. After a 48-hour incubation, the transfected cells were detached and resuspended in serum-free DMEM. For the migration assay, 1×10^5 cells in serum-free medium were seeded in transwell chambers. For the invasion assay, the transwell chambers were coated with 50 μg of Matrigel. 2×10^5 of the MDA-MB-231 cells or 1×10^5 MDA-MB-468 cells in serum-free medium were seeded in the transwell chambers, which were then placed into a 24-well plate, and the bottom of the chambers was immersed in DMEM medium with 10% FBS. After 24 hours, the migrated and invaded cells were fixed with 10% paraformaldehyde and stained with 0.05% crystal violet. The numbers of migrated and invaded cells were quantified using Image J software.

4.2.8 Cell proliferation study

A total of 5,000 MDA-MB-468, MDA-MB-231, or MCF-10A cells were seeded in 96-well plates and incubated overnight at 37°C. CD24 siRNAs were condensed with Lipofectamine RNAiMAX reagent and incubated with the cells at a final siRNA concentration of 50 nM for 6 hours in Opti-medium. After incubation, the Opti-medium was replaced with fresh growth medium specific to each cell line. The cells were then further incubated at 37°C for 2, 3, and 4 days, followed by the addition of 100 μl of CellTiter-Glo buffer (Promega, Madison, WI). The luminescence was subsequently measured using the SpectraMax iD5 Multi-Mode Microplate Reader (Molecular Devices, San Jose, CA).

4.2.9 Apoptosis study

1×10^5 of MDA-MB-468 and MDA-MB-231 cells were seeded in 6-well plates and incubated overnight at 37°C. Then cells were transfected with the CD24 siRNA/Lipofectamine RNAiMAX for 48 hours. After incubation, the cells were trypsinized and stained with Alexa Fluor 488 Annexin V and PI by following the manufacturer's protocol and analyzed via FACScalibur flow cytometry (BD Biosciences, Franklin Lakes, NJ).

4.2.10 Cell cycle study

A total of 1×10^5 MDA-MB-231 or MDA-MB-468 cells were seeded in 6-well plates, incubated overnight, and transfected with siRNA for 24 h. For cell cycle analysis, the cells were detached with EDTA-trypsin, washed twice with cold phosphate buffered saline (PBS), and fixed with ice-cold 70% ethanol at 4°C for a minimum of 4 hours. After fixation, the cells were washed with cold PBS and incubated with Propidium iodide/RNase solution (Cat#4817-60-04, R&D SYSTEMS) for 30 minutes at room temperature. The percentage of cells in the G1, S, and G2 phases was determined using FACScalibur flow cytometry (BD Biosciences, Franklin Lakes, NJ).

4.2.11 Association of CD24 expression and doxorubicin resistance in MDA-MB-231 cells

To investigate the impact of doxorubicin treatment on CD24 expression, we performed RT-PCR and immunostaining assays to assess the levels of CD24 expression after the treatment. For the RT-PCR, total RNA was extracted with TRIzol Reagent after 48-hour treatment with concentrations of 0.2 μM and 0.6 μM doxorubicin, and the mRNA levels were quantified. In the immunostaining assay, 6×10^4 MDA-MB-231 cells were seeded into a 4-well chamber and incubated overnight at 37°C. The cells were treated with doxorubicin at concentrations of 0.2 μM and 0.6 μM for 48 hours, and cells cultured in drug-free medium were used as control.

Following incubation, the cells were fixed with 4% formalin at room temperature for 20 min and then permeabilized with 0.1% Triton X-100 for another 20 min. Subsequently, the cells were stained with a primary anti-CD24 antibody (Cat# ab202073, Abcam) for 20 min at room temperature, followed by incubation with DAPI and a secondary antibody (Goat anti-rabbit IgG H&L (Alexa Fluor 488), Cat# ab150077, Abcam) for an additional 20 min at room temperature. CD24 protein expression was assessed using a Leica SP8 Stellaris Confocal Microscope (Leica Biosystems, Wetzlar, Germany).

To assess the sensitivity of MDA-MB-231 cells to doxorubicin following repeated treatments, we determined cell viability using the CellTiter-Glo reagent. Briefly, 2×10^5 MDA-MB-231 cells were seeded in 6-well plates and incubated overnight at 37°C. Subsequently, the cells were treated with doxorubicin at 0.6 μM for 48 hours, while cells cultured in a drug-free medium were used as the control. After 48 h incubation, the cells were collected and seeded into white 96-well plates and incubated overnight at 37°C. The cells were then treated with various concentrations of doxorubicin for an additional 24 hours, and their viability was measured using the CellTiter-Glo reagent. The IC_{50} of doxorubicin was further determined to evaluate whether CD24 silencing with siRNA sensitizes the MDA-MB-231 cells to doxorubicin. In this case, MDA-MB-231 cells were seeded in 6-well plates and transfected with either CD24 siRNA or scrambled siRNA for 48 hours. The cells were then collected and seeded in white 96-well plates and incubated overnight at 37°C. The culture medium was then discarded, and fresh DMEM medium containing varying concentrations of doxorubicin was added into each well. The cells were incubated for 24 hours at 37°C, and their viability was assessed using the CellTiter-Glo reagent.

4.2.12 *In vitro* phagocytosis assay

Human normal peripheral blood mononuclear cells (PBMCs, Cat# SER-PBMC-200) were ordered from Zen-Bio and phagocytosis was evaluated using PBMC-derived macrophages. Briefly, fresh PBMCs were washed twice with PBS. After resuspension, monocytes were isolated using a human pan monocyte isolation kit (BioLegend) according to the manufacturer's protocol. PBMC-derived macrophages were then cultured and differentiated for 7 days in RPMI 1640 medium supplemented with recombinant human M-CSF (20 ng/ml). After 5 days, recombinant human IL-4 (20 ng/ml) was added to the medium to promote the differentiation of M2 macrophages for another two days. Macrophages were collected on day 7 using TrypLE and used for the phagocytosis assay.

Macrophages and siRNA-transfected tumor cells (MDA-MB-231 and MDA-MB-468 cells) were labeled with cell proliferation dye eFluor 670 and CFSE, respectively, according to the manufacturer's protocol. A total of 5×10^4 eFluor 670-labeled macrophages were seeded to a 96-well clear flat bottom plate and allowed to adhere for 12 hours. Once the macrophages had adhered, 1×10^5 CSFE-labeled tumor cells were added to the wells containing the macrophages and they were co-cultured for 2 hours in a serum-free medium. After incubation, the cells were washed 5 times with PBS to remove non-phagocytotic tumor cells. Phagocytosis was examined using fluorescent microscopy.

4.3 Statistical analysis

The data were presented as the mean ± SD. Statistical analysis was performed using a one-way analysis of variance (ANOVA) with Turkey's post hoc test. A p-value less than 0.05 is considered statically significant.

4.4 Results

4.4.1 Silencing activity of pre-designed CD24 siRNAs

We designed four siRNAs targeting different regions of human CD24 mRNA, as listed in Table 1. The silencing effect of these designed siRNAs was evaluated in MDA-MB-231 and MDA-MB-468 cells at concentrations of 25 nM and 50 nM, using Lipofectamine RNAiMAX. RT-PCR was performed to assess whether the pre-designed siRNAs could effectively knock down CD24 gene expression. As illustrated in Figure 13A, in contrast to the scrambled siRNA (NC group), at least 80% of the mRNA expression was silenced in MDA-MB-468 cells at both 25 nM and 50 nM. For MDA-MB-231 cells (Figure 13B), all four siRNAs silenced approximately 75% of CD24 mRNA expression at 50 nM. However, among the four siRNAs, only CD24 siRNA (Sequence #1) displayed the most significant suppression of CD24 expression (about 65%), while the other three siRNAs achieved less than 50% silencing at 25 nM. These results indicate that CD24 siRNA (Sequence #1) exhibited the most effective silencing effect in both MDA-MB-231 and MDA-MB-468 cells.

We, therefore, evaluated the CD24 protein expression in both MDA-MB-231 and MDA-MB-468 cells following transfection with CD24 siRNA (Sequence #1). As shown in Figures 13C and 13D, there was a notably higher CD24 expression level in MDA-MB-468 cells compared to MDA-MB-231 cells. Importantly, CD24 siRNA (Sequence #1) significantly downregulated CD24 protein expression in both breast cancer cell lines. These findings indicate that the pre-designed siRNA (Sequence #1) effectively reduces CD24 expression at both mRNA and protein levels. Thus, we selected the CD24 siRNA (Sequence #1) for subsequent experiments, referring to it as CD24 siRNA without specific notification.

Additionally, CD24 siRNA successfully silenced mRNA expression in non-malignant MCF-10A human mammary epithelial cells (Figure 14A).

Table 1. Sense strand sequences of CD24 siRNAs

Number	Sequence
CD24-1	5’-CTTCCAGGTGTTACTGTAAtt-3’
CD24-2	5’-GCATTGACCACGACTAATTtt-3’
CD24-3	5’-TTGCATTGACCACGACTAAtt-3’
CD24-4	5’-GGCATTTCCTATCACCTGTTTtt-3’

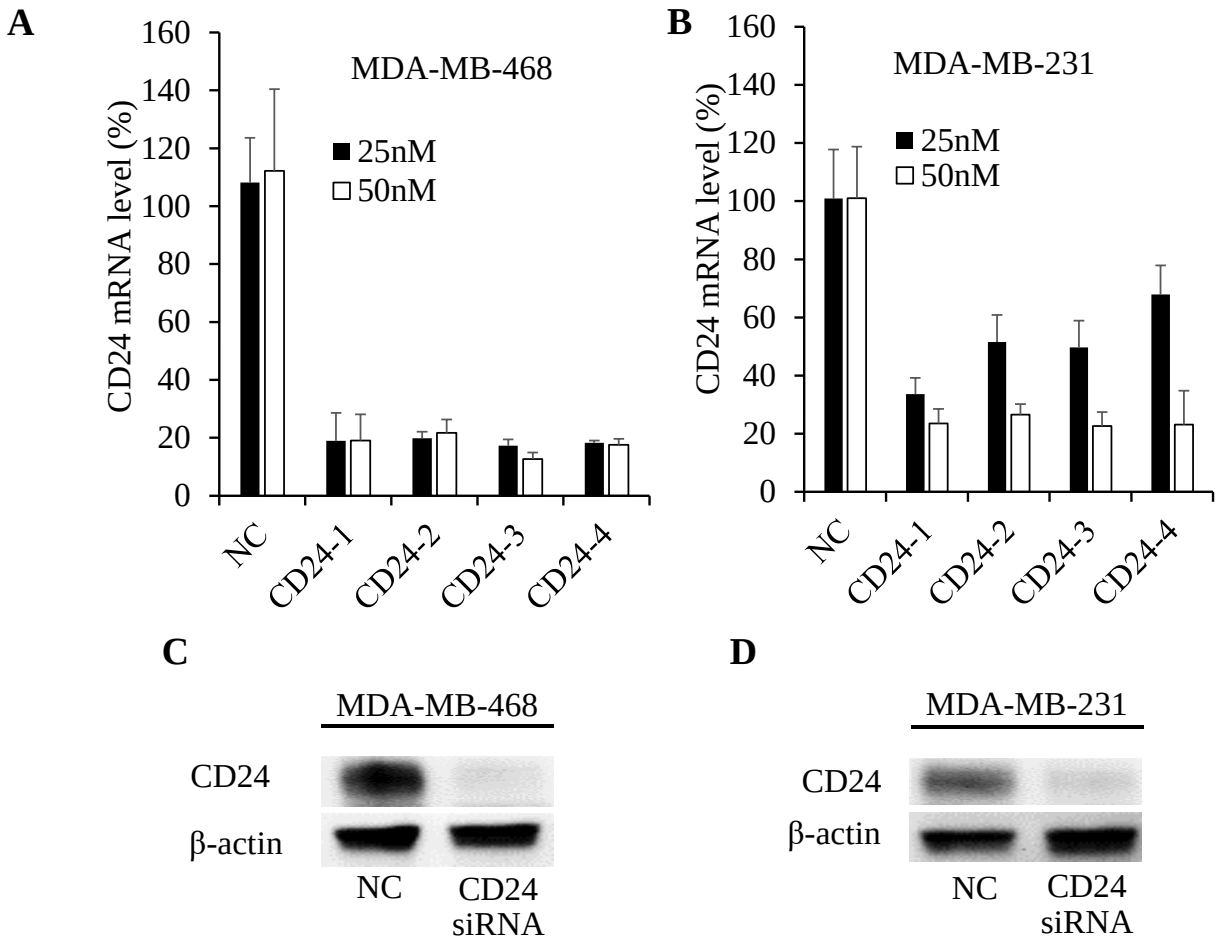

Figure 13. Silencing activities of predesigned CD24 siRNAs in MDA-MB-468 and MDA-MB-231 cells. (A-B) Silencing effect of the CD24 siRNAs at the mRNA level in MDA-MB-468 and MDA-MB-231 cells at concentrations of 25 nM and 50 nM. (C-D) Silencing effect of the CD24 siRNA at the protein level in MDA-MB-468 and MDA-MB-231 cells.

4.4.2 Silencing of CD24 inhibits the proliferation of TNBC cells

Previous studies have revealed that CD24 expression is associated with tumor cell proliferation and that the knockdown of CD24 inhibits cell growth in hormone-receptor-positive breast cancer cells (MCF-7) and gastric cancer AGS cells [137, 138]. In this study, we aimed to determine whether silencing CD24 would also inhibit cell proliferation of TNBC cells (MDA-MB-231 and MDA-MB-468). We treated the breast cancer cells with CD24 siRNA and measured cell proliferation on days 2, 3, and 4 post-transfection. As shown in Figure 14C, MDA-MB-468 cells treated with CD24 siRNA demonstrated a significantly lower proliferation rate when compared to cells treated with scrambled siRNA at different time points (about 56% on day 3 and 72% on day 4 post-transfection, respectively). Similar results were also observed in MDA-MB-231 cells, as shown in Figure 14D. Importantly, while CD24 siRNA effectively downregulated mRNA expression, it did not impact the proliferation of non-malignant MCF-10A human mammary epithelial cells (Figures 14A and 14B). These results confirm that suppression of CD24 expression inhibits the proliferation of TNBC cells. This discovery revealed that CD24 is not only overexpressed but also plays a role in promoting the proliferation of TNBC cells.

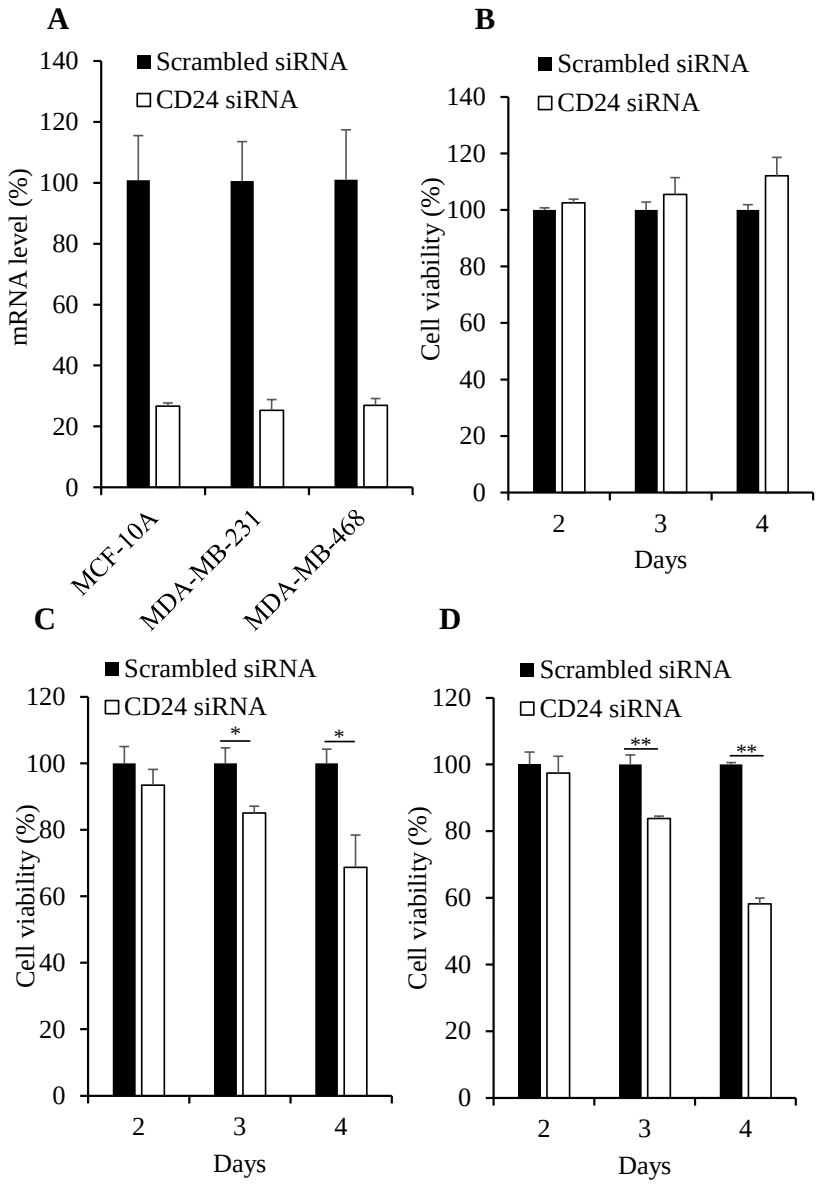

Figure 14. Silencing of CD24 inhibits tumor cell proliferation but not the non-malignant MCF-10A breast cells. (A) mRNA expression level in indicated cells after transfection. Viability of MCF-10A (B), MDA-MB-468 (C), and MDA-MB-231 (D) treated with siRNA for 2, 3, and 4 days. All results are presented as the mean ± SD (n=3). (*$p<0.05$; **$p<0.01$)

4.4.3 Silencing of CD24 inhibits the migration and invasion of TNBC cells

To assess whether silencing CD24 has an impact on the cell migration and invasion capabilities of MDA-MB-231 and MDA-MB-468 cells, we conducted transwell chamber assays. The results presented in Figure 15 reveal that CD24 siRNA significantly reduced the number of migrated and invaded cells. As shown in Figures 15A, 15C, and 15D, approximately 30% of CD24 siRNA-transfected MDA-MB-468 cells were able to pass through the transwell membrane in migration and invasion assays, in contrast to cells treated with scrambled siRNA. In line with these findings in MDA-MB-468 cells, MDA-MB-231 cells treated with siRNA exhibited a significant reduction in cell migration and invasion by 55% and 70%, respectively, when compared to cells treated with scrambled siRNA (Figures 15B and 15E-F). These findings strongly indicate that the suppression of CD24 expression in TNBC cells can effectively inhibit their migration and invasion abilities.

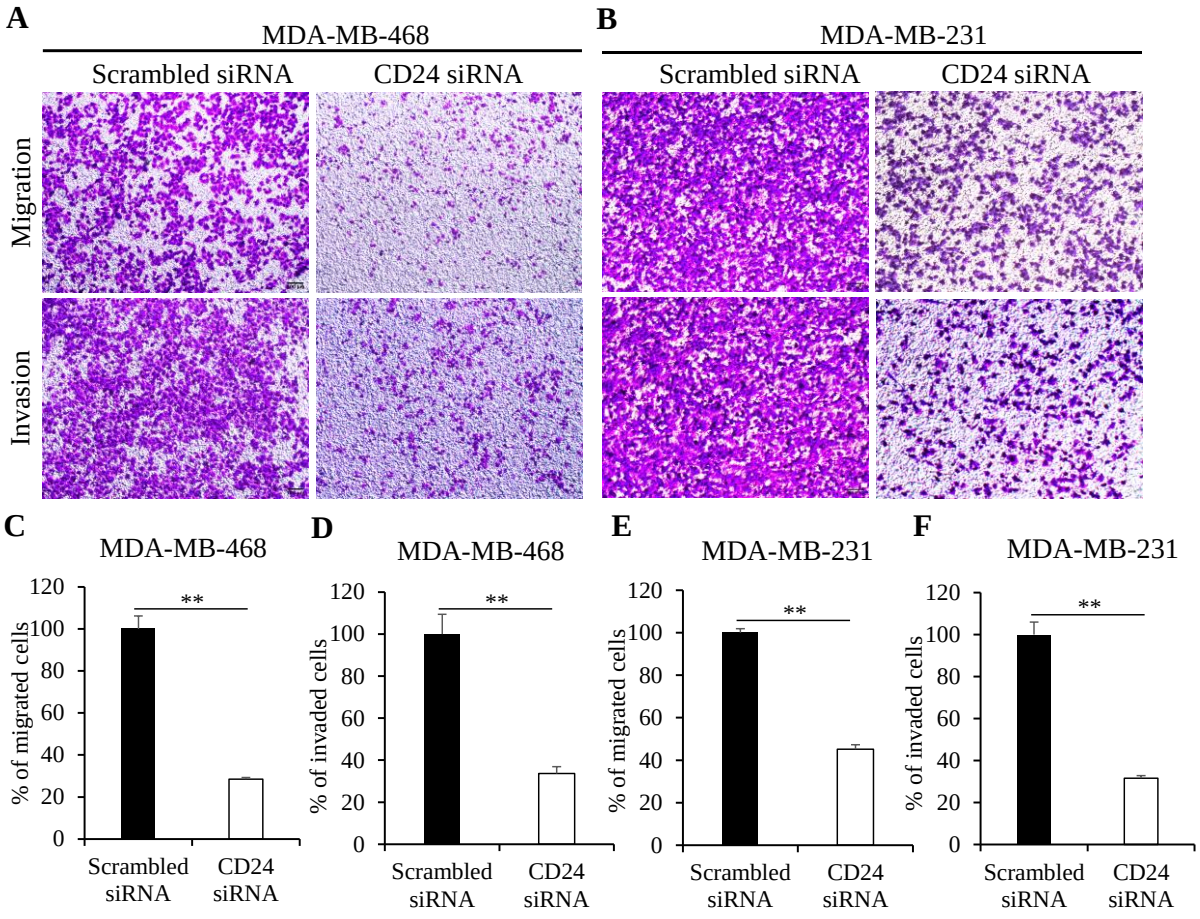

Figure 15. Silencing of CD24 inhibits the migration and invasion of MDA-MB-231 and MDA-MB-468 cells. (A-B) Representative pictures of migrated and invaded MDA-MB-468 and MDA-MB-231 cells after transfection with the scrambled or CD24 siRNA for 24 h. Quantitative analysis of migrated and invaded MDA-MB-468 (C-D) and MDA-MB-231 (E-F) cells. Quantitative analysis was performed by counting the number of migrated or invaded cells at the bottom of the membrane in six random microscope fields from three independent samples. All results are presented as the mean ± SD (n=3). (*p<0.05; **p<0.01)

4.4.4 Silencing of CD24 promotes apoptosis of TNBC cells

We also evaluated the apoptosis of MDA-MB-231 and MDA-MB-468 cells using flow cytometry 48 hours after siRNA transfection. As depicted in Figure 16A and 16B, the results demonstrated that the percentage of early apoptotic MDA-MB-468 cells, indicated in quadrant one (Q1), increased from 1.6% in the scrambled siRNA-treated group to 4.9% in the CD24 siRNA-treated group. As expected, similar results were observed in MDA-MB-231 cells, where the silencing of CD24 significantly induced cell apoptosis in comparison to cells treated with scrambled siRNA (Figure 16C). These findings reveal that CD24 siRNA acts as an inducer of apoptosis in both MDA-MB-231 and MDA-MB-468 cells.

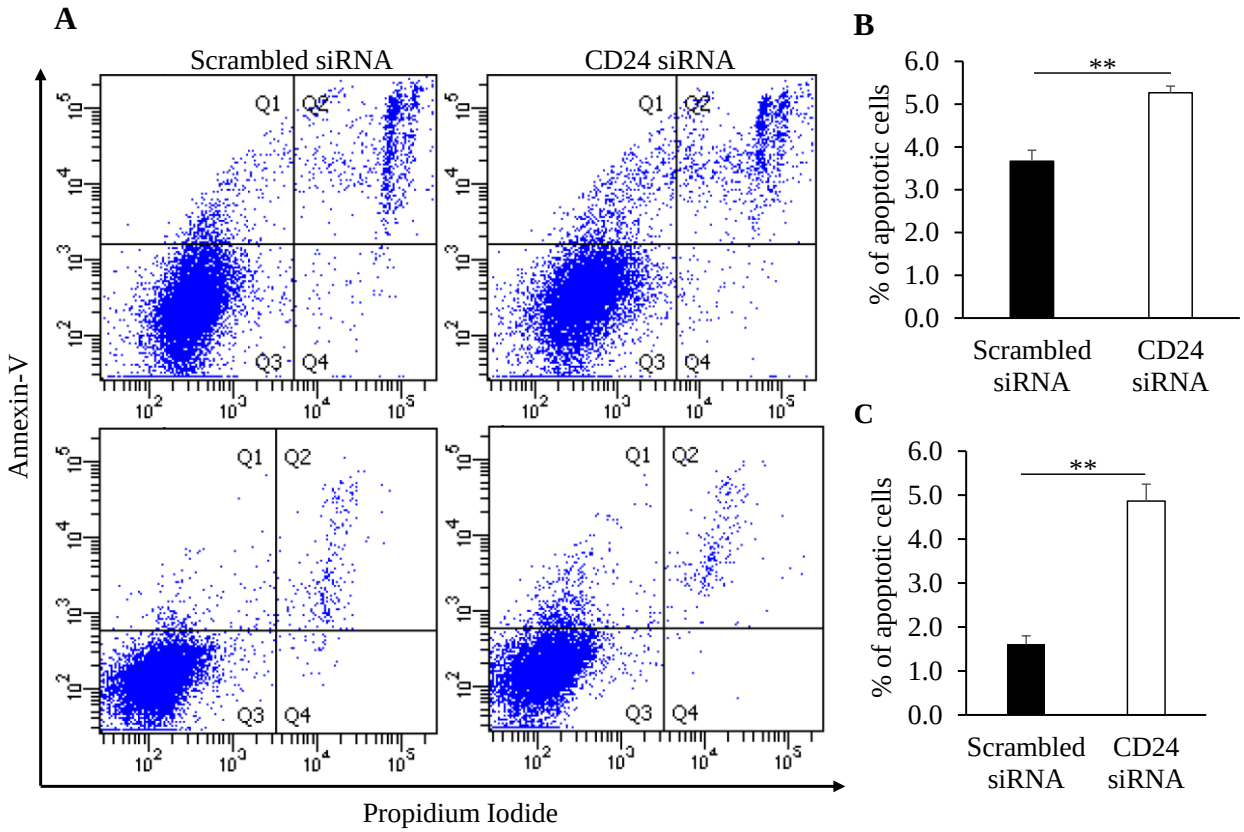

Figure 16. CD24 siRNA induces tumor cell apoptosis. (A) Representative images of MDA-MB-468 cells (top row) and MDA-MB-231 cells (bottom row) in flow cytometry. (B-C) Quantitative analysis of the percentage of apoptotic cells in MDA-MB-468 cells (B) and MDA-MB-231 cells (C). Apoptosis in MDA-MB-231 and MDA-MB-468 cells was determined by flow cytometry using FITC-Annexin-V and propidium iodide (PI) staining at 48 hours after siRNA transfection. All results are presented as the mean ± SD (n=3). (*$p<0.05$; **$p<0.01$)

4.4.5 Silencing of CD24 regulates cell cycle distribution of TNBC cells

To investigate the mechanism underlying the inhibitory effect of CD24 siRNA on the proliferation of TNBC cells, we examined the cell cycle distribution in siRNA-transfected MDA-MB-231 and MDA-MB-468 cells using flow cytometry. As illustrated in Figure 17A-B, a significant increase in the S phase was observed in CD24 siRNA-treated MDA-MB-468 cells compared to the control group. Additionally, there was a decrease in the proportion of cells in the G1 and G2 phases in CD24 siRNA-transfected cells (54.8% in the G1 phase and 2.7% in the G2 phase) in comparison to cells treated with scrambled siRNA (70.0% and 7.8% in G1 and G2 phases, respectively). For MDA-MB-231 cells, those treated with CD24 siRNA displayed an increase in the G1 phase and a decrease in the S phase compared to cells treated with scrambled siRNA transfected cells (Figure 17C-D). These data indicate that CD24 siRNA can induce apoptosis and inhibit cell proliferation in both MDA-MB-468 and MDA-MB-231 cells.

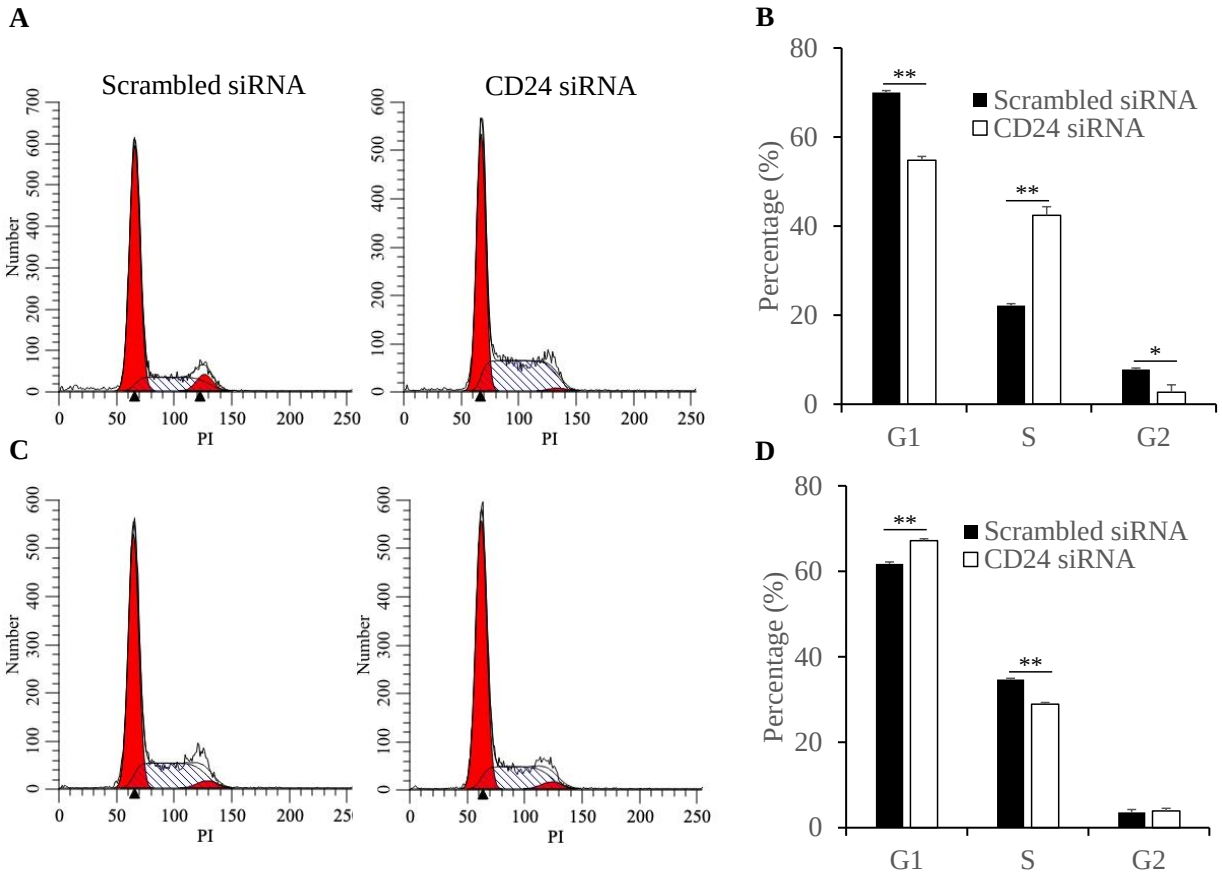

Figure 17. Silencing of CD24 by siRNAs regulates the cell cycle distribution of MDA-MB-468 and MDA-MB-231 cells. (A-B) Representative images and quantitative analysis of cell cycle in MDA-MB-468 cells at 48 hours after siRNA transfection. (C-D) Representative images and quantitative analysis of cell cycle in MDA-MB-231 cells at 48 hours after siRNA transfection. The cell cycle of MDA-MB-231 and MDA-MB-468 cells was determined by flow cytometry using propidium iodide (PI) staining 48 hours after siRNA transfection. All results are presented as the mean ± SD (n=3). (*p<0.05; **p<0.01)

4.4.6 Silencing of CD24 sensitizes MDA-MB-231 cells to doxorubicin

Recently, emerging evidence has suggested that doxorubicin resistance can develop in TNBC cells, including MDA-MB-231 cells [139, 140]. In this study, we conducted various experiments to examine the association between CD24 expression and doxorubicin resistance. When subjected to doxorubicin treatment, the cells underwent morphological changes, transitioning from the spindle-shaped MDA-MB-231 cells to round-shaped giant cells (Figure 18A). Treatment with doxorubicin at concentrations of 0.2 μM and 0.6 μM led to an increase in both CD24 mRNA and protein levels, as indicated in Figures 18B and 18C. As shown in Figure 18C, there was a notable rise in CD24 protein expression within the cytoplasm following treatment at both concentrations. The sensitivity of MDA-MB-231 cells to doxorubicin was evaluated through repeated treatments with doxorubicin. As shown in Figure 19A, cells subjected to repeated treatment at a high concentration displayed higher viability compared to cells treated only once, suggesting that cells may develop resistance after repeated exposure to doxorubicin over an extended period. The IC_{50} of doxorubicin in siRNA-transfected MDA-MB-231 cells were determined using the CellTiter-Glo assay. CD24 siRNA sensitized MDA-MB-231 cells to doxorubicin, as indicated by a reduced IC_{50} value, decreasing from 2 μM to 1 μM (Figure 19B).

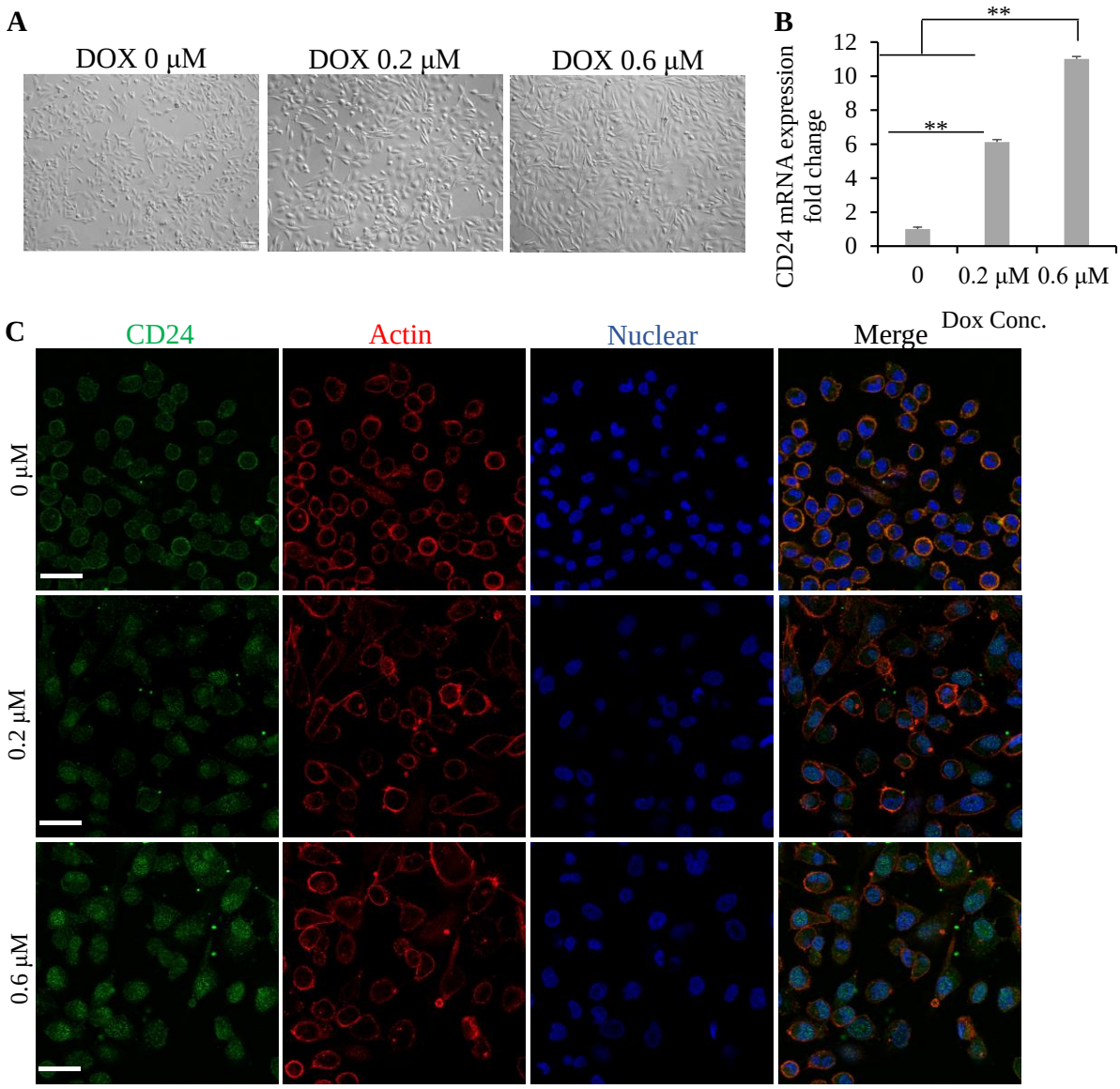

Figure 18. Treatment with doxorubicin upregulates both CD24 mRNA and protein levels in MDA-MB-231 cells. (A) Morphology of MDA-MB-231 cells after being treated with different concentrations of doxorubicin. (B) CD24 mRNA expression was evaluated by RT-PCR at 48 hours after doxorubicin treatment. (C) CD24 protein expression was determined by confocal microscopy after being treated with doxorubicin for 48 hours. Scale bar represents 100 µm. (*$p<0.05$; **$p<0.01$)

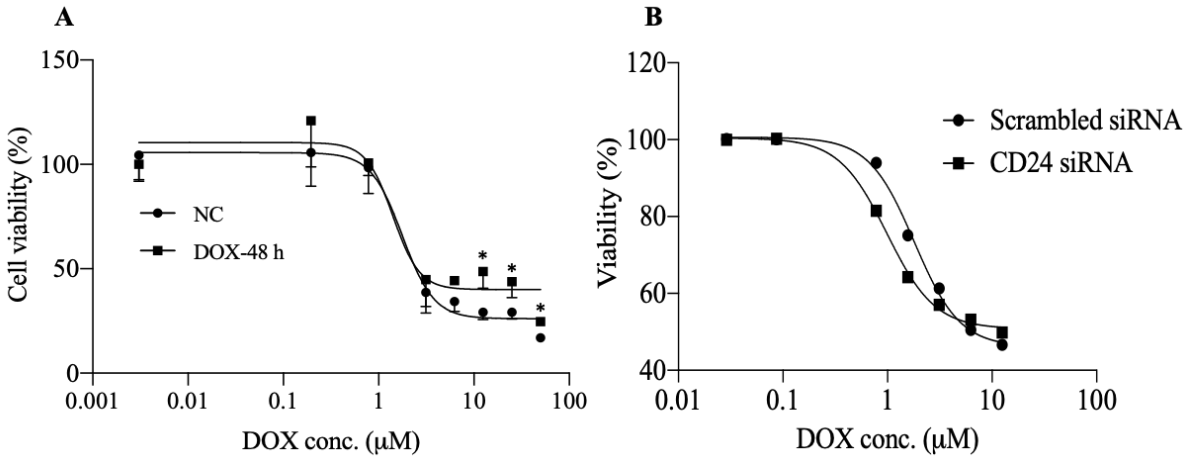

Figure 19. CD24 silencing with siRNA sensitizes MDA-MB-231 cells to doxorubicin. (A) Variability of MDA-MB-231 cells after repeated treatment with doxorubicin. (B) IC_{50} of doxorubicin in siRNA-transfected MDA-MB-231 cells. (*p<0.05; **p<0.01)

4.4.7 Monocytes-derived macrophages-mediated phagocytosis

Tumor-associated macrophages (TAMs) are a major component of the tumor microenvironment (TME) and are often correlated with tumor progression and therapy resistance [141, 142]. High infiltration of TAM has been associated with poor prognosis and reduced patient survival in several different types of cancer, including human breast cancer and gastric cancer. Multiple strategies have been developed to target TAMs, and several clinical trials have assessed their efficacy in a variety of cancers [143-145]. In a recent study, CD24 has been described as a novel target for cancer immunotherapy. CD24 expressed on tumor cells acts as a "don't eat me" to inhibit macrophage-mediated phagocytosis of tumor cells by binding to siglec-10 on innate immune cells, such as TAMs. The loss of CD24 by either deletion of the CD24 gene or blocking it with a monoclonal antibody has been demonstrated to disrupt the interaction of CD24/Siglec-10 and increase macrophage-mediated phagocytosis [20]. Therefore, we conducted the phagocytosis assay by the co-culture of either scrambled or CD24 siRNA transfected tumor cells with macrophages to evaluate macrophage-mediated phagocytosis of tumor cells. In this preliminary study, as illustrated in Figure 20, we observed higher numbers of phagocytotic tumor cells in CD24 siRNA-treated groups. The results can be further confirmed by flow cytometry-based assay.

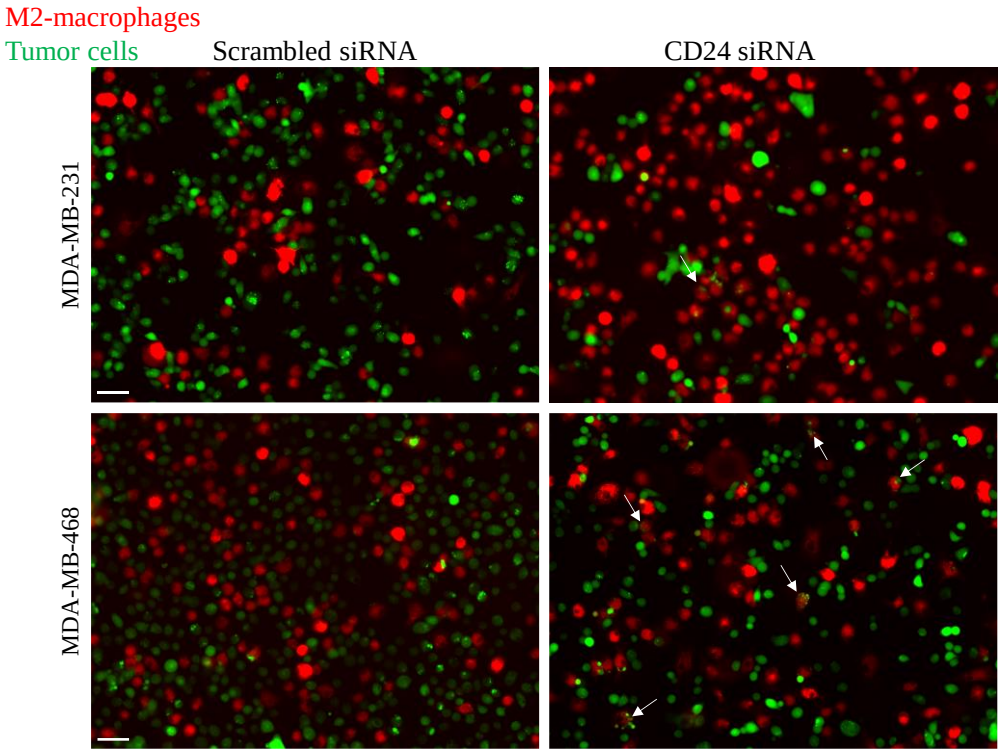

Figure 20. Silencing CD24 increases cancer cell phagocytosis by macrophages. Representative images of phagocytosis. PBMC-derived macrophages were labeled with cell proliferation dye eFluor 670 (red color) and tumor cells (MDA-MB-231 and MDA-MB-468) were labeled with CFSE (green color). Scale bar represents 50 μm.

4.5 Discussion

TNBC is the most aggressive subtype of breast cancer with a poor prognosis. Current therapeutic options often fall short in terms of effectiveness, Necessitating the exploration of novel treatment strategies. There is a growing body of evidence indicating that CD24 plays a critical role in tumorigenesis of various cancers including breast cancer [18]. Hence, targeting CD24 emerges as a promising therapeutic approach for TNBC. In our study, we designed CD24 siRNA and evaluated its silencing effect in TNBC cell lines. As depicted in Figure 13, the designed siRNA successfully silenced CD24 at both mRNA and protein levels. Subsequently, this siRNA inhibited the proliferation, migration, and invasion of TNBC cells, as shown in Figures 14 and 15.

Chemotherapy stands as the primary systemic treatment for TNBC patients due to the absence of targeted receptor markers. However, chemotherapy remains challenging, mainly because most patients experience relapse after treatment, largely attributed to the development of drug resistance [9]. Doxorubicin is among the frequently employed chemotherapeutic agents for various cancers, exerting its effect through DNA intercalation, inhibition of topoisomerase II, and the generation of free radicals. It is a well-known phenomenon that cancer cells often acquire drug resistance after long-term exposure to doxorubicin [140, 146]. In our study, as illustrated in Figure 19A, we observed that at high concentrations, cells subjected to repeat doxorubicin treatment displayed higher cell viability compared to the control group following a 48-hour culture period. Silencing CD24 with siRNA sensitized tumor cells to doxorubicin, resulting in a lower IC_{50} value compared to cells treated with scrambled siRNA. Furthermore, we noted a significant upregulation in CD24 mRNA levels after doxorubicin treatment (Figure

18B). These findings suggest that the upregulation of CD24 may represent a potential mechanism contributing to doxorubicin resistance.

The overexpression of CD24 has been associated with resistance to both chemotherapy and targeted therapies [18]. Moreover, CD24 is involved in antitumor immunity. With the tumor microenvironment, tumor-associated macrophages (TAMs) constitute a significant component and engage in communication with tumor cells, immune cells, and stroma cells. TAMs play a role in tumor progression, metastasis, angiogenesis, and in conferring resistance to various cancer therapies, including immunotherapies [141, 142]. Studies have demonstrated that a high infiltration of TAMs is a negative prognostic factor in breast cancer. Multiple strategies have been developed to target TAMs, and several clinical trials have assessed their efficacy in a variety of cancers [143-145]. A very recent study has provided insight into how CD24 on tumor cells acts as a "don't eat me" signal by interacting with siglec-10 on innate immune cells, such as TAMs. The interaction between CD24 and siglec-10 disrupts macrophages-mediated phagocytosis of tumor cells. Disrupting the CD24-Siglec-10 axis by either deletion the CD24 gene or blocking it with a monoclonal antibody can restore the phagocytotic capability of macrophages [20]. In our study, CD24 siRNA improved the phagocytosis of TNBC cells by macrophages when compared to cells treated with scrambled siRNA (Figure 20). Furthermore, the relationship between CD24 and the therapeutic effectiveness of immunotherapies, such as PD-1/PD-L1 immune checkpoint inhibitors, has been explored. This makes CD24 a promising target for combination therapies aimed at improving cancer treatment. CD24 has been associated with the efficacy of PD-1/PD-L1 inhibitors. In a cohort of NSCLC patients with CD24-positive expression, shorter progression-free survival was observed when PD-L1 expression was low (TPS<50) [147]. Given this evidence, therapeutic targeting of CD24 presents

a potential option to improve the outcomes of TNBC treatment or synergize with tumor immunotherapy.

The surface expression of $CD44^{+}/CD24^{-/low}$ has long been considered a marker for cancer stem cells (CSC) in breast cancer. However, the association of the $CD44^{+}/CD24^{-/low}$ phenotype with clinical outcomes in breast cancer remains controversial [74]. Moreover, the stability of these markers and how their expression changes during metastasis have not been extensively studied. Several studies have reported a significant increase in CD24 expression in distant metastatic sites, such as the lung and liver, in comparison to primary tumors [148, 149]. CSCs display high levels of heterogeneity, suggesting that relying solely on a single CSC marker may not be reliable or sufficient for characterizing the stem-like properties of cancer cells. Studies have demonstrated that high CD24 expression in various human cancers contributes to tumor progression and metastasis [138, 150, 151]. It is worth noting that CD24 not only exists on the cell membrane but also resides in the cytosol or the nucleus [72]. Some aggressive cancer cells exhibit little to no surface CD24 expression, suggesting that the intracellular fraction of CD24 may also play a significant role in tumor growth and metastasis. Therefore, downregulation of CD24 expression is a more effective approach than blocking CD24 on the cell surface using antibodies. For example, silencing of CD24 using short hairpin RNA (shRNA) has been shown to reduce the growth, progression, and metastasis of cancer cells [70, 72]. Taken together, targeting CD24 with siRNA may offer advantages over surface antibody blockade and holds promise for patients with advanced or metastatic cancers. Moreover, the accumulated data strongly suggest that CD24 could serve as a viable therapeutic target for TNBC and potentially for other cancers characterized by CD24 overexpression.

In summary, we observed that silencing the CD24 gene using siRNA has a significant inhibitory effect on the proliferation, migration, and invasion of TNBC cells. Moreover, CD24 siRNA induced apoptosis in these tumor cells. Notably, silencing CD24 also significantly enhanced macrophage-mediated phagocytosis of TNBC cells. Our findings strongly suggest that targeting CD24 with siRNA holds promise as a potential therapeutic strategy for TNBC.

CHAPTER 5

DISCOVERY OF A NOVEL HUMAN DOMAIN ANTIBODY TARGETING PD-L1 FOR CANCER IMMUNOTHERAPY

5.1 Introduction

Immunotherapy is a cancer therapeutic strategy to boost immune responses to eliminate tumor cells. Studies have reported promising results of immunotherapy in a variety of tumors.[79, 152] A breakthrough in cancer immunotherapy is the discovery of inhibitory checkpoint receptors, which act as suppressors of the immune system. Immunotherapies using checkpoint inhibitors targeting these receptors have shown enormous success in the treatment of a diversity of cancers.[153, 154] Among all inhibitory checkpoints, PD-1/PD-L1 is one of the most widely studied immune checkpoint receptors in cancer immunotherapy. Programmed cell death 1 (PD-1), characterized as a negative regulator of immune responses, is induced on activated T cells, but can also induced on non-T cell subsets, including B cells, natural killer cells, and dendritic cells [82]. Engagement of PD-1 with its ligand PD-L1 promotes tumor immune evasion by inhibiting T cell functions [81]. Recent evidence demonstrated that in addition to PD-1, PD-L1 interacts with CD80 expressed on activated T cells and APCs to deliver inhibitory signals[8]. Therefore, PD-1/PD-L1 is emerging as a promising target for cancer treatment. Blockade of PD-1/PD-L1 using monoclonal antibodies has exhibited encouraging therapeutic outcomes in a variety of human malignancies.[82, 83] Currently, there are six monoclonal antibodies targeting PD-1 or PD-L1 approved by the U.S. Food and Drug Administration (FDA) [155]. Despite the success of sdAb in clinical trials and other applications, it is worth mentioning that sdAb has several inherent disadvantages that need to be considered such as poor tumor penetration, immunogenicity, high production cost, and minimal flexibility in structural modification.

A single-domain antibody (sdAb), also known as VHH or nanobody, is an antibody fragment composed of a single variable domain of heavy-chain antibodies (HCAbs) found in the Camelid family [156]. sdAb is the smallest antibody fragment (15 kDa) that maintains a similar antigen-binding affinity as an intact antibody. Since their discovery in 1993, sdAbs have attracted great attention as potential therapeutic and imaging agents, in particular for cancers [157]. Compared to intact antibodies, sdAbs have numerous advantages including small size, good stability, ease of production, low immunogenicity, enhanced tissue penetration, and ease of fusion with other proteins [26, 158]. In general, sdAbs can quickly and homogenously distribute through tumors compared to antibodies. However, sdAbs also show rapid renal clearance because of their small size. This could be a disadvantage for sdAb's therapeutic applications but is a major advantage for using sdAbs as imaging probes or theranostic agents [157, 159]. Another disadvantage of sdAbs is their monovalency which leads to relatively lower affinity and blocking efficiency compared to antibody-based checkpoint inhibitors. This limitation can be addressed by constructing a bivalent or trivalent form of sdAbs [160]. sdAbs can be discovered through animal immunization or various display libraries, such as phage display, yeast display, bacterial display, and ribosome display [95, 161, 162]. Several antibody fragments targeting PD-L1 were recently discovered using phage libraries from camel or alpaca [97, 163]. However, animal-derived antibody fragments may elicit unwanted immune responses, which limit their therapeutic applications. As a result, there is tremendous interest in developing human sdAbs, also called domain antibodies (dAbs), for therapeutic applications. dAbs can be produced by transgenic mice or phagemid libraries. Compared to natural camelid sdAbs, dAbs are more likely to aggregate due to exposure to hydrophobic heavy chain residues that are normally protected by light chain binding [164, 165].

In the current study, we discovered anti-human PD-L1 dAbs using a synthetic human domain antibody phagemid library. The CLV3 dAb exhibits high binding affinity and specificity to human PD-L1. It blocks the PD-1/PD-L1 interaction and inhibits tumor growth in mice implanted with CT26 tumor cells.

5.2 Methods and materials

5.2.1 Cell culture

DU145, CT26, and MCF-7 cell lines were purchased from the American Type Culture Collection (Manassas, VA). Peripheral blood mononuclear cells (PBMCs) were purchased from iXCells Biotechnologies (San Diego, CA). DU145 cells were cultured in DMEM medium with 10% Fetal Bovine Serum (FBS), 100 units/mL penicillin, and 100 mg/mL streptomycin. CT26 cells were cultured in RPMI 1640 medium with 10% FBS, 100 units/mL penicillin, and 100 mg/mL streptomycin. MCF-7 cells were cultured in DMEM medium with 10% FBS, 100 units/mL penicillin, 100 mg/mL streptomycin, and 1% insulin.

5.2.2 Expression and purification of human domain antibody

The gene encoding CLV3 dAb was cloned into the vector pET-22b (+), which was then transformed to *E. coli* BL21 (DE3) to express CLV3. The transformed *E. coli* BL21 cells were cultured at 37℃ in lysogeny broth (LB) medium with ampicillin until the OD_{600} reached 0.6-0.8. The dAb expression was induced at 16℃ overnight in LB medium with the addition of 1 mM IPTG. After overnight incubation, the cell culture was harvested and centrifuged, the cell pellet was collected and resuspended in lysis buffer (20 mM Tris-base, 500 mM NaCl, pH 8.50) after centrifugation. Protein was released after the lysis of bacteria using sonication. After lysis of the bacteria, CLV3 was purified by immobilized metal affinity chromatography using Ni-NTA agarose column (cat# P188221, Fisher Scientific) and eluted by elution buffer (20 mM

Tris-base, 250 mM NaCl, 400 mM imidazole, pH 8.50) according to the manufacturer's procedure. The eluted CLV3 was dialyzed in a lysis buffer containing 5% glycerol or concentrated by Sartorius Vivaspin™ Turbo Centrifugal Concentrators. The purity of the CLV3 protein was assessed by sodium dodecyl sulfate-polyacrylamide gel electrophoresis (SDS-PAGE) with Coomassie blue staining.

5.2.3 Determination of CLV3 dAb aggregation by size exclusion chromatography

To avoid the potential aggregations of the CLV3, 5% glycerol was added to CLV3 dAb solutions (20 mM Tris-base, 500 mM NaCl, pH 8.5). To check potential aggregations, 500 µl of expressed CLV3 in Tris buffer (20 mM Tris-base, 500 mM NaCl, pH 8.5) was injected onto a 24 mL Superdex 75 (SD75) size exclusion chromatography column (GE Healthcare) and eluted in the same buffer.

5.2.4 Surface plasmon resonance (SPR)

Binding affinities of the CLV3 dAb to human PD-L1 ECD and mouse PD-L1 ECD were assessed by SPR (BI4500, Biosensing Instrument) at room temperature. PD-L1 ECD proteins were diluted in 10 mM sodium acetate buffer (pH 5.0) and covalently immobilized to a CM5 sensor chip (Biosensing Instrument) using the Amine Coupling Kit (GE Healthcare). A second channel without protein immobilization was used as a reference. Measurements were performed at a flow rate of 60 µL/min in HBS-P+ buffer (GE Healthcare). Various concentrations of dAbs (10, 25, 50, 100, 250, 500, and 2000 nM) were prepared and employed to calculate the equilibrium dissociation constant (K_D). To evaluate non-specific binding, 125 µg/mL BSA was coated on a CM5 chip after the CM5 chip regenerated with 10 mM NaOH, and binding affinity of the CLV3 dAb to BSA was determined using the same procedure. The data acquired was analyzed using Bi data analysis software.

5.2.5 Binding specificity to tumor cells overexpressing PD-L1

The binding specificity of CLV3 dAb to human PD-L1 was evaluated in PD-L1-positive DU145 cells and PD-L1-deficient MCF-7 cells as described before. Cancer cells were detached by enzyme-free dissociation solution (Gibco, Cat No. 13150016) and suspended at 1×10^6 cells/mL in PBS. Suspended cells were incubated with various concentrations of Cy5-labeled dAbs for 1 h at 37℃ with gentle rotation. After washing, the cells were analyzed by flow cytometry.

5.2.6 Cell apoptosis and cytokine release of co-cultured PBMCs and DU145 cells

Cell apoptosis of human PBMCs was evaluated as previously reported. Briefly, fresh human PBMCs (1.5×10^5 cells/well) were cultured alone or co-cultured with DU145 cells (7.5×10^5 cells/well) in the presence of CLV3 dAb (5 μM) or anti-PD-L1 antibody (1 μM) in 6-well plates at 37℃ for 24 h. After incubation, PBMCs were collected and stained with APC Mouse Anti-Human CD3 antibody (cat# 555342, BD Biosciences, San Jose, CA) to gate T lymphocytes. Apoptosis of CD3-positive T lymphocytes was analyzed using the Alexa Fluor® 488 annexin V/Dead Cell Apoptosis kit (cat# A10788, Fisher Scientific) as per the company's protocol. The supernatant was also harvested for the determination of cytokines including IL-6, IL-10, TNF-α, and IFN-γ using the Bio-Plex Pro assay (Bio-Rad Laboratories, Hercules, CA).

5.2.7 3D tumor spheroids penetration

Penetration of dAbs in 3D tumor spheroids was evaluated as we reported before [120]. Tumor spheroids of CT26 cells were formed using the Cultrex 10×Spheroid Formation ECM (Trivigen, Gaithersburg, MD) according to the manufacturer's protocol. Briefly, 3,000 CT26 cells in a mixture of medium and ECM were seeded in U-bottom 96-well plates. After

centrifugation, the plate was placed at 37°C and incubated for 4 days to form tumor spheroids. CLV3 dAb and anti-PD-L1 antibody were labeled with Cy5 using a Cy5 labeling kit (cat# ab188288, Abcam) according to the manufacturer's protocol. The tumor spheroids were incubated with 500 nM of Cy5-labeled CLV3 dAb and anti-PD-L1 antibody at 37°C for 6 h. After washing, the spheroids were fixed with formalin, and penetration of the dAb or antibody was assessed using confocal microscopy.

5.2.8 Determination of endotoxin in CLV3 dAb by the limulus amebocyte lysate (LAL) test

Bacterial endotoxins, found in the outer membrane of gram-negative bacteria are members of a class of phospholipids called lipopolysaccharides (LPS). The repeated administration of LPS or bacterial endotoxins to experimental animals results in a progressive diminution of some of the biological effects, especially fever. Recombinant proteins expressed in *E. coli* may be contaminated with endotoxin. We, therefore, measured endotoxin in CLV dAb using the ToxinSensor Chromogenic LAL Endotoxin Assay Kit (GenScript, Piscataway, NJ) according to the manufacturer's protocol. The LAL is one of the methods approved by the FDA used for endotoxin testing in recommended proteins. This test is used to detect or quantify endotoxins from Gram-negative bacteria using amoebocyte lysate from the horseshoe crab.

5.3 Statistical analysis

Data are presented as the mean ± standard deviation (SD). The difference between any two groups is determined by one-way analysis of variance (ANOVA) with Tukey's *post hoc* test. A p value less than 0.05 is considered statically significant.

5.4 Results

5.4.1 Expression and purification of the CLV3 dAb

After four rounds of biopanning against human PD-L1 ECD, 45 phage colonies were selected and 9 different nanobody sequences were discovered. Among them, the CLV3 dAb (amino acid sequence shown in Figure 21A) exhibited the highest blocking activity as it blocked 74% of the human PD-1/PD-L1 interaction. Therefore, CLV3 was selected as the best candidate for the following studies due to its high affinity and blocking efficiency.

Both the isopropyl β-D-1-thiogalactopyranoside (IPTG) induced and uninduced bacterial cultures were collected and analyzed using SDS-PAGE to determine the expression of CLV3 dAb. As illustrated in Figure 21 B, a clear band (~14 kD) which is indicated by a white arrow) below 15 kD (indicated as a black arrow) was observed in the induced culture but not in the uninduced culture. To maximize the dAb protein extraction, we next tested the residual CLV3 protein in different fractions during cell lysis and purification. Negligible dAb was remaining in all fractions after purification (Figure 21 C). We next purified the protein with Ni-NTA affinity chromatography since the dAb is a His-tagged protein. As shown in Figure 21D, the CLV3 protein was eluted, and the majority of the protein was recovered in fractions 3-5 with relatively high purity. These data indicate that CLV3 dAb can be expressed in a soluble form under IPTG induction and high-purity protein can be achieved using Ni-NTA affinity chromatography.

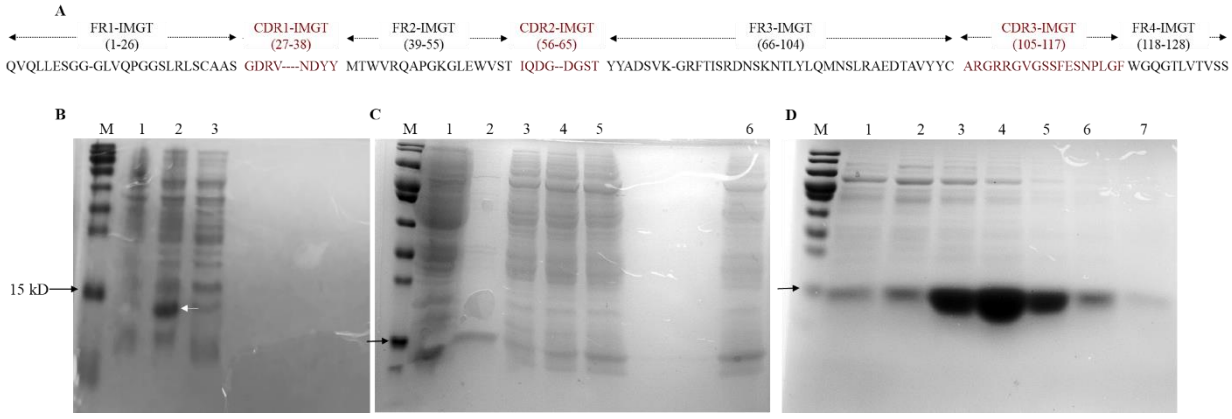

Figure 21. Nanobody expression and purification. (A) The amino acid sequence of the CLV3 dAb. (B) SDS-PAGE of BL21 (DE3)) E coli cell lysate before and after IPTG induction. Protein expression before (lane 1) and after IPTG induction (lane 2), and in flow through was detected (lane 3). (C-D) Purification of CLV3 protein was evaluated using SDS-PAGE. (C) Proteins in the cell lysate after induction (lane 1), flow-through (lane 2), lysis buffer (lane 3), washing buffer (lane 4-5), resin (lane 6), and (D) elution fractions (lane 1-7) were detected.

5.4.2 Determination of aggregation in CLV3 dAb with size-exclusion chromatography (SEC)

Compared to natural camelid sdAbs, dAbs are more likely to aggregate due to exposure of hydrophobic heavy chain residues that are normally protected by light chain binding. We, therefore, used size-exclusion chromatography to monitor potential aggregate in the protein. As illustrated in Figure 22A, the major elution peak was at 12.9 mL, consistent with a small dAb monomer. We refer to this peak as P. Two minor peaks at 8.0 mL, 11.5 mL and a slightly increased baseline between these two peaks were also observed, likely due to aggregation and higher molecular weight impurities. We estimated the percentage monomer dAb versus the aggregates and impurities using the area underneath the major peak (P) and the area under the aggregates and impurities (A). The percentage of monomer is calculated using $P/(A+P) \times 100\%$, which gives 75%. This value suggests that while some aggregation is present, under our experimental condition, majority of the protein is a monomer. We used A280 absorbance for the semi-quantitation of the monomer purity. It is worth mentioning that high molecular weight impurities (not aggregation of the dAb) likely have much high extinction coefficient than the dAb monomer. Therefore, we believe that the purity of the sAb monomer is very likely higher than 75%. Proteins in the elution fractions (Lane 1-24) were evaluated using SDS-PAGE (Figure 22B), no significant aggregation was observed in all elution fractions. These data revealed that CLV3 dAb is stable as a monomer in the buffer.

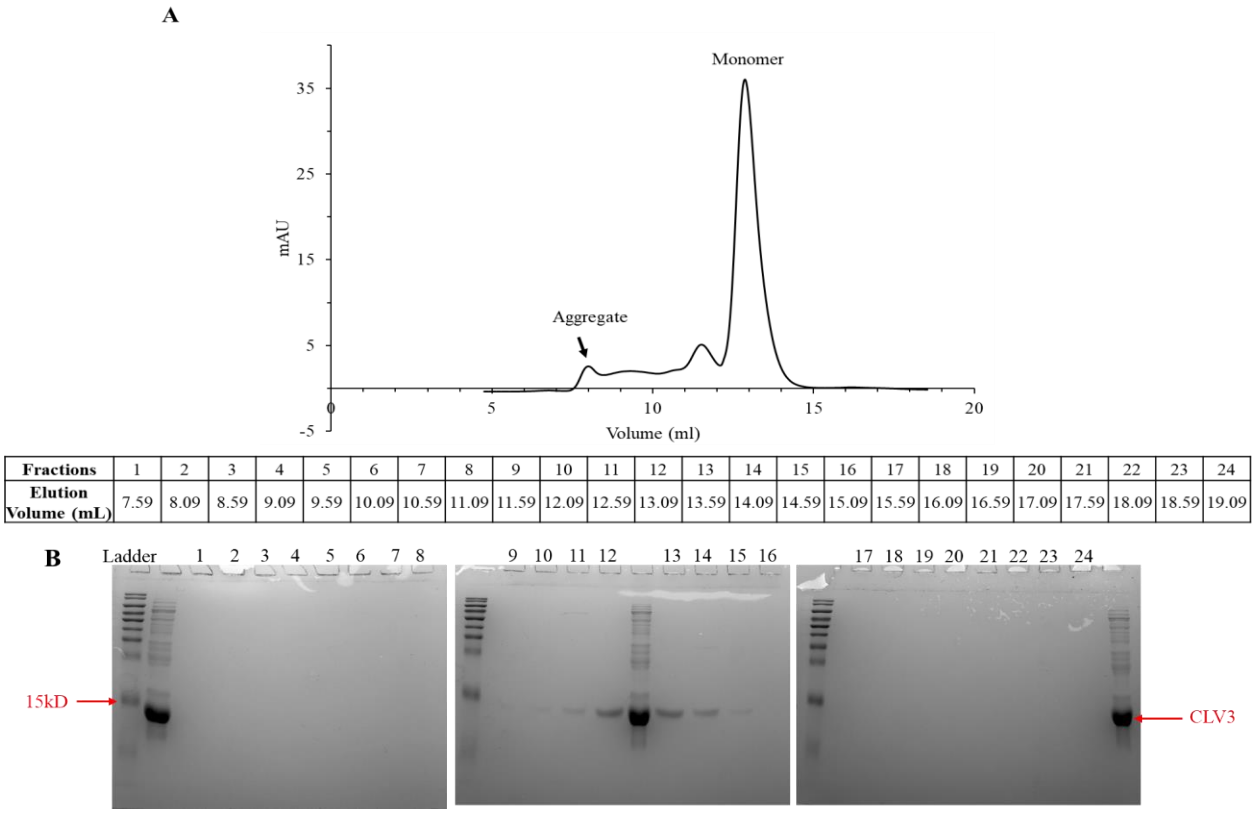

Fractions	1	2	3	4	5	6	7	8	9	10	11	12	13	14	15	16	17	18	19	20	21	22	23	24
Elution Volume (mL)	7.59	8.09	8.59	9.09	9.59	10.09	10.59	11.09	11.59	12.09	12.59	13.09	13.59	14.09	14.59	15.09	15.59	16.09	16.59	17.09	17.59	18.09	18.59	19.09

Figure 22. Elution profile of the CLV3 dAb on a SD75 size exclusion column. (A) Protein 280 nm absorbance is plotted as a function of the elution volume. (B) Proteins in the elution fractions (Lane 1-24) were evaluated using SDS-PAGE.

5.4.3 Binding affinity and specificity of the CLV3 dAb to human and mouse PD-L1

We investigated binding affinities of the CLV3 dAb to human PD-L1 ECD and mouse PD-L1 ECD using SPR. As illustrated in Figure 23, CLV3 shows concentration-dependent binding to both human PD-L1 and mouse PD-L1. The K_d values of CLV3 to human PD-L1 and mouse PD-L1 are 137.5 and 266.8 nM, respectively. By contrast, the SPR responses of BSA to CLV3 are negligible even at high concentration of CLV3, suggesting a minimum binding between CLV3 and BSA.

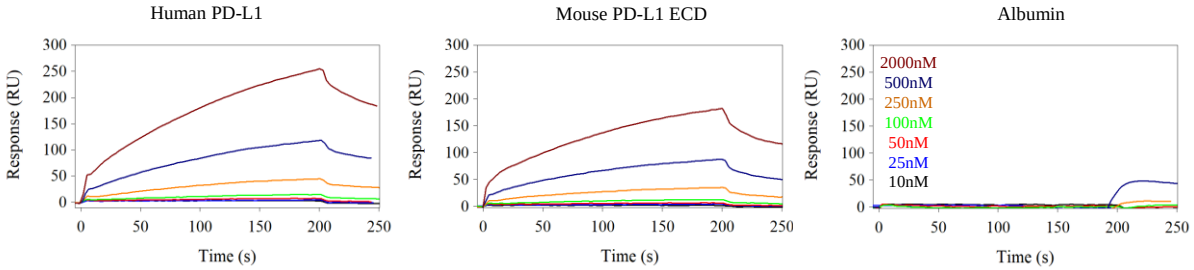

Figure 23. Surface Plasmon Resonance (SPR). Representative SPR sensorgrams of the CLV3 dAb to immobilized human PD-L1 ECD protein, mouse PD-L1 ECD protein, and albumin. The experiment was performed in three replicates.

5.4.4 Binding affinity and specificity of the CLV3 dAb to PD-L1 expressed tumor cells

Binding specificity is a critical consideration in the design of protein-protein interaction blockers which need to bind to their desired protein targets but interact minimally with other molecules. Therefore, we next determined the binding affinity of CLV3 dAb to PD-L1 expressed tumor cells. The specificity of CLV3 to PD-L1 was evaluated in PD-L1-positive DU145 tumor cells and PD-L1 deficient MCF-7 tumor cells (Figure 24). CLV3 showed higher binding affinity to DU145 cells than to MCF-7 cells, suggesting a higher affinity of CLV3 to PD-L1 on tumor cells.

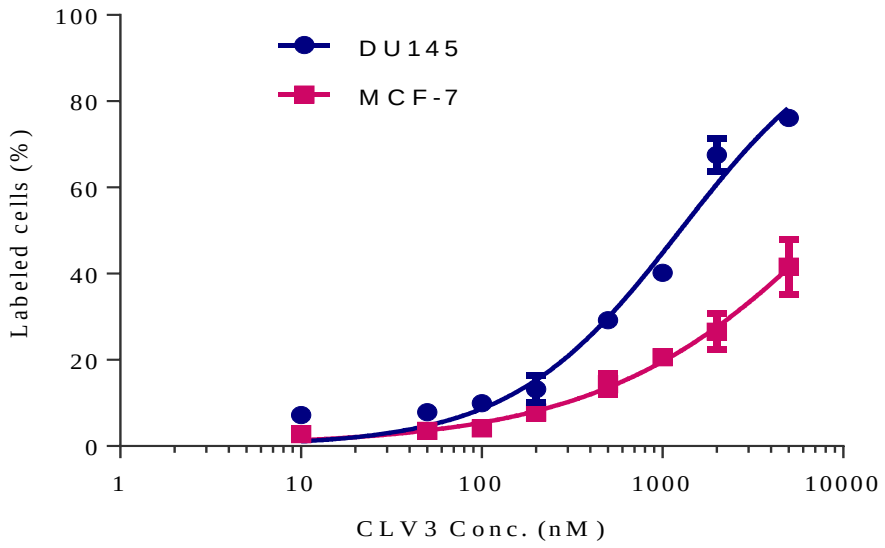

Figure 24. Binding Specificity to Tumor Cells Overexpressing PD-L1. Binding profile of CLV3 to PD-L1-positive DU145 tumor cells and PD-L1-deficient MCF-7 tumor cells.

5.4.5 The CLV3 dAb reduces T-cell apoptosis induced by cancer cells

PD-L1 on the tumor cell surface interacts with PD-1 on immune cells leading to the dysfunction of T cells, including T cell exhaustion, anergy, and apoptosis.[166] We investigated whether CLV3 inhibits the apoptosis of human PBMCs co-cultured with DU145 cancer cells. As shown in Figures 25A, and 25B, the percentage of apoptotic PBMCs increased from 3.7% to 15.4% after co-culture with DU145 cells. The addition of CLV3 dAb or anti-PD-L1 antibody to the co-culture cells significantly reduced apoptosis of PBMCs to 10.6% and 11.25%, respectively. This is in agreement with a previous report, in which tumor-associated PD-L1 induced the apoptosis of cytotoxic T lymphocytes.[167] The authors co-cultured T cells with melanoma cells and found that the tumor cells promoted T cell apoptosis, but apoptosis was not observed in PD-L1 knockout melanoma cells. Moreover, the apoptosis of T cells was significantly reduced after an anti-PD-1 antibody was added to the co-cultured cells.[167]

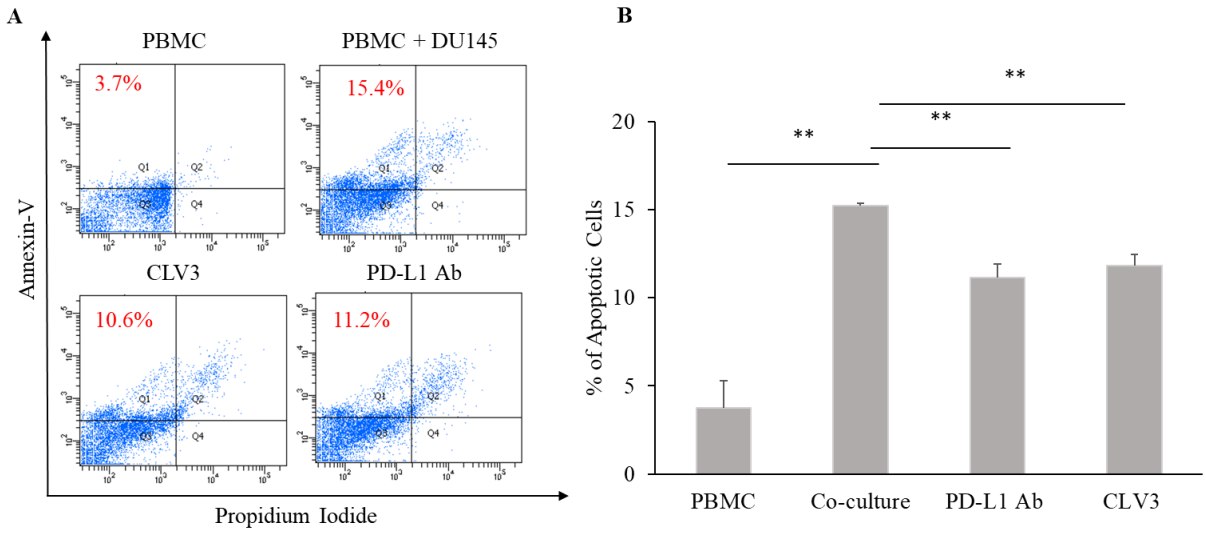

Figure 25. Coculture of human PBMCs and DU145 tumor cells in the presence of the CLV3 dAb. Human PBMCs were cultured alone or co-cultured with DU145 tumor cells in the absence or presence of the CLV3 dAb or anti-PD-L1 antibody for 24 hours. Apoptosis of CD3-positive T cells was evaluated by flow cytometry using the Alexa Fluor® 488 annexin V/Dead Cell Apoptosis kit. Percentage of apoptotic CD3-positive T cells. Results are represented as the mean ± SD (n=3). (**p<0.01).

5.4.6 Analysis of cytokine release

The supernatant extracted from 24 h co-cultures of PBMC with DU145 cells was assayed for IL-6, IL-10, IFN-γ, and TNF-a. IL-10 is an inflammatory cytokine that suppresses anti-tumor immune responses by inducing T cell anergy and inhibiting T cell proliferation. As shown in Figure 26A, the production of IL-10 is significantly increased in the co-culture of DU145 and PBMC in comparison to PBMC alone. Notably, with the addition of CLV3, the IL-10 level significantly decreased compared to coculture. Furthermore, it is important to notice that the IL-10 level did not change much with the treatment of the PD-L1 antibody. TNF-a and IL-6 are multifunctional cytokines involved in chronic inflammation and contribute to the progression of cancer. PBMC co-cultured with tumor cells produced a high amount of IL-6 and TNF-a than PBMC alone. In comparison, IL-6 and TNF-a secretions are slightly reduced in the presence of CLV3 (Figures 26B, C). IFN-γ, a cytotoxic T cell-related cytokine, plays an important role in the activation of various cell types such as natural killer cells and T cells. On the other hand, it also inhibits the growth of malignant cells by inducing apoptosis. As shown in Figure 26D, co-culture with DU145 significantly decreased the ability of PBMC to express IFN-γ, whereas with the addition of CLV3, there was a dramatic increase in the production of IFN-γ.

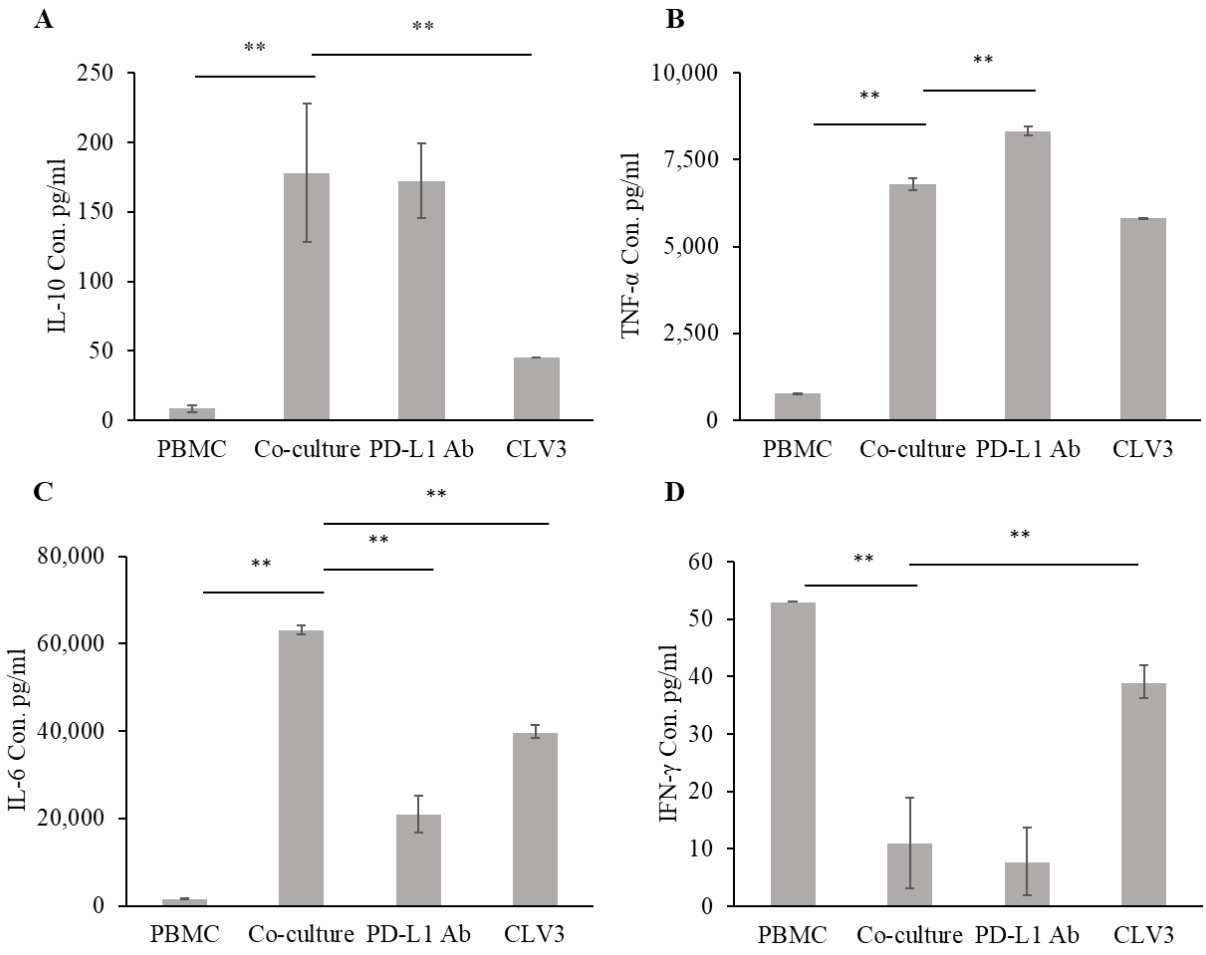

Figure 26. Coculture of human PBMCs and DU145 tumor cells in the presence of the CLV3 dAb. Human PBMCs were cultured alone or co-cultured with DU145 tumor cells in the absence or presence of the CLV3 dAb or anti-PD-L1 antibody for 24 hours. The production of IL-10, TNF-α, IL-6, and IFN-γ by PBMCs. Results are represented as the mean ± SD (n=3). (**p<0.01).

5.4.7 Tumor penetration of the CLV3 dAb and anti-PD-L1 antibody

Tumor extracellular matrix is a major barrier that limits the penetration of antitumor drugs into the tumor microenvironment. 3D tumor spheroid is a useful model to evaluate drug penetration *in vitro*. In this study, a 3D tumor spheroid model of CT26 cells was established to evaluate the penetration of Cy5-labeled CLV3 dAb and anti-PD-L1 antibody. After 6 h incubation, tumor penetration of both CLV3 dAb and anti-PD-L1 antibody was determined by confocal microscopy. As illustrated in Figures 27A, and 27B, after incubation with tumor spheroids for 6 h, lower-molecular weight CLV3 dAb showed a much deeper tumor penetration than antibody. Analysis of mean fluorescence intensity showed that the Cy5-labeled CLV3 dAb was detected as deep as approximately 150 μm from the periphery of the spheroids. By contrast, the Cy5-labeled antibody had much lower fluorescence intensity compared with the anti-PD-L1 antibody and was only detected on the periphery of the spheroids, suggesting very limited tumor penetration.

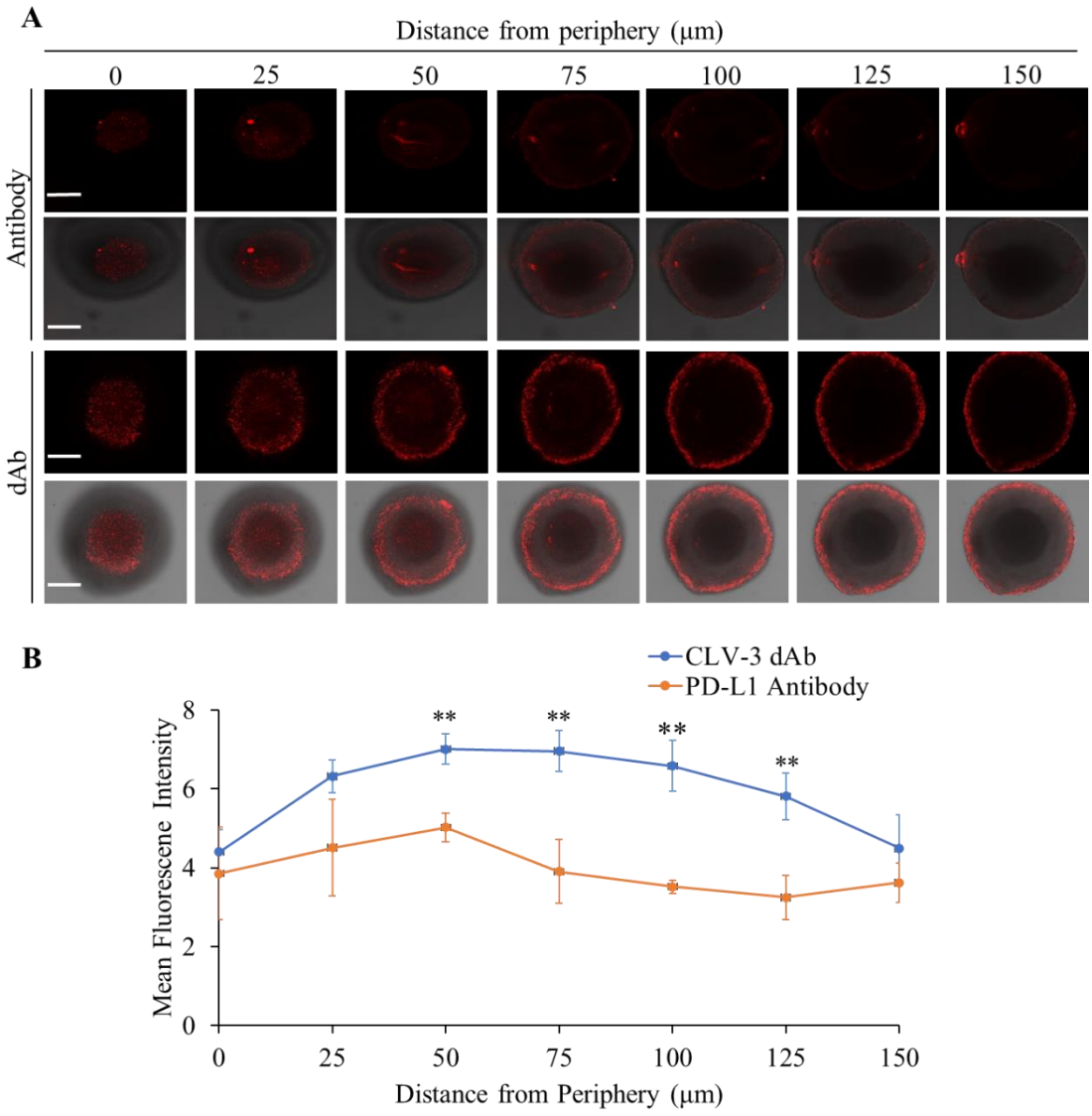

Figure 27. Penetration of CLV3 dAb and anti-PD-L1 antibody in 3D tumor spheroids. (A) Representative z-stacked confocal images of the spheroids with a z-step of 25 μm after 6 h incubation with Cy5-labeled CLV3 dAb or anti-PD-L1 antibody. The scale bar represents 200 μm. (B) Mean fluorescence intensity of the z-stacked images vs. the distance from the periphery of the spheroids. Results are represented as the mean ±SD (n=3 independent spheroids, **p<0.01).

5.4.8 Endotoxin measurement in the CLV3 dAb

Endotoxin detection is critical quality control to ensure the expressed protein is free of endotoxin contaminations. Bacterial Endotoxins Test is a test to detect or quantify bacterial endotoxins of gram-negative bacterial origin using an amoebocyte lysate prepared from blood corpuscle extracts of horseshoe crab. We measured endotoxin in the CLV3 dAb because recombinant proteins expressed in E. coli may be contaminated with endotoxin, which may affect *in vivo* activity studies. The bacterial endotoxin in the CLV3 dAb protein was measured by a chromogenic LAL endotoxin assay kit (Cat. No. L00350) supplied by GenScript, and the detection procedure followed the manufacturer's protocol. According to US Pharmacopeia, the threshold pyrogenic human dose is 5 EU/kg. The maximum injection dose of CLV3 used in our animal study was 10 mg/kg, so the endotoxin limit is 0.5 EU/mg. According to the user manual of the kit, the test is considered valid when the following three conditions are met (as shown in Fig. 28B). Based on the calculations, the endotoxin level in the CLV3 dAb was found 0.087 EU/mg, which equals to 0.87 EU/kg for mice in the animal study with a dose of 10 mg/kg. All three criteria listed are met. Therefore, the endotoxin level tested in the CLV3 dAb is valid and much lower than the threshold pyrogen dose.

A

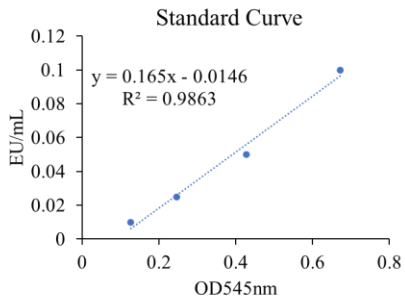

B

Results of the test	Calculations
Endotoxin acceptable level according to US Pharmacopeia	5 EU/kg
Injection dose of CLV3 in the animal study	10 mg/kg
Endotoxin limit=5 EU/kg/(10 mg/kg)	0.5 EU/mg
Endotoxin level in sample	0.087EU/mg
The test is considered valid when the following conditions are met:	
(1) R^2>0.980	R^2=0.9863
(2) Negative control does not exceed the limit of the blank value	OD_{545nm}=0.134<0.261 (blank)
(3) Recovery of added endotoxin at 0.05 EU/ml is within 50-200%	186%

Figure 28. The bacterial endotoxin in the CLV3 dAb protein was measured by a chromogenic LAL endotoxin assay kit. (A) Standard curve for the quantification of endotoxin in chromogenic assay. (B) Calculation of endotoxin concentration in CLV3 dAb.

5.5 Discussion and conclusions

PD-L1 is one of the best described inhibitory immune checkpoints which can mediate cancer cells immune escape by ligation with its receptor PD-1. Thus, several immune checkpoint inhibitors have been developed to block the interaction of PD-1/PD-L1 and successfully applied to the treatment of various cancers in patients. Currently, the FDA has approved three anti-PD-1 (Nivolumab, Pembrolizumab, and Cemiplimab) antibodies and three anti-PD-L1 (Atezolimumab, Durvalumab, and Avelumab) antibodies.[84, 85] The antibodies block the PD-1/PDL1 interaction and subsequently restore the immune cell killing ability.[86, 153]. Compared to traditional intact antibody, sdAb, the smallest naturally occurring antibody fragment in Camelid family, retains a comparable blocking ability as whole antibodies.[160] sdAbs have numerous advantages, including small size, low immunogenicity, and easy production. In addition, sdAbs are also featured with relative short retention time in the circulation. However, although the circulation half-life of dAbs is just about 30 min to 2 h, researchers discovered that dAbs could bind to target proteins (i.e., CD47) after 24 hours.[168, 169] sdAb can also carry payloads (e.g., radioisotopes and cytokines) to the tumor and reduce the systemic exposure because of their rapid systemic clearance but sustained half-life in target tissues. In addition, the production of sdAb is much easier than monoclonal antibody. sdAb can be easily expressed in bacteria with a high yield, which makes the sdAb a good candidate for the scaling up production.[95] Thus, sdAb represents a new type of checkpoint inhibitors for cancer immunotherapy. For example, promising results from one phase III clinical trial of a sdAb (Caplicizumab) targeting acquired thrombotic thrombocytopenic purpura (aTTP) were reported in 2017 [98], and it was approved by the FDA in 2019 as the first nanobody-based drug.

Despite the success of sdAb in clinical trials and other applications, it is worth mentioning that sdAb has several inherent disadvantages that need to be considered during the drug development of sdAbs. In general, sdAbs show rapid renal clearance because of their small size. This is a disadvantage for sdAb's therapeutic applications but is a major advantage for using sdAbs as imaging probes or theranostic agents.[156, 157, 159] Another disadvantage of sdAbs is their monovalency which reduces their affinity and blocking efficiency compared to antibodies. This limitation can be addressed by constructing a bivalent or trivalent form of sdAbs. For example, the bivalent and trivalent formats of a sdAb are 313- and 135-fold more potent, respectively, than the monovalent format.[160] In this study, we discovered different dAbs which efficiently blocked the interaction between PD-L1 expressed on tumor cells and PD-1 on immune cells. Among all these dAbs, CLV3 exhibited the highest binding affinity to PD-L1 and the most potent ability to block the PD-1/PD-L1 interaction. We evaluated the *in vitro* and *in vivo* activity of CLV3 dAb. The CLV3 efficiently blocked PD-1/PD-L1 interaction by binding to PD-L1 with high affinity and specificity. As we expected, the CLV3 dAb exhibited a better tumor penetration in comparison with the anti-PD-L1 antibody. CLV3 successfully inhibited tumor growth and increased the survival rate of tumor-bearing mice compared to the control group. Therefore, our data suggest that CLV3 dAb is a promising immune checkpoint inhibitor for cancer immunotherapy. Due to the smaller size in comparison with monoclonal antibodies, a bivalent or trivalent form can be constructed from the CLV3 dAb to further increase the activity. Moreover, the CLV3 can be linked to other immune checkpoints to construct bispecific inhibitors which can simultaneously target two different tumor-associated antigens.

In conclusion, we discovered several anti-human PD-L1 dAbs using biopanning. Particularly, the CLV3 dAb specifically binds to PD-L1 with high affinity and blocks the PD-1/PD-L1 interaction on tumor cells. The CLV3 displays better tumor penetration compared to the anti-PD-L1 antibody. The CLV3 reduces the apoptosis of PBMCs and increases the IFN-γ release. Therefore, our data suggest that CLV3 dAb is a promising immune checkpoint inhibitor for cancer immunotherapy. Due to the smaller size in comparison with monoclonal antibodies, a bivalent or trivalent form can be constructed from the CLV3 dAb to further increase the activity. Moreover, the CLV3 can be linked to other immune checkpoints to construct bispecific inhibitors which can simultaneously target two different tumor-associated antigens.

Chapter 5 has been published in Frontiers in Immunology (Volume 13, page 1-11, April 2022).[170]

CHAPTER 6

SUMMARY AND CONCLUSIONS

Triple-negative breast cancer (TNBC) is a refractory subtype of breast cancer in the absence of ER, PR, and HER2. Compared with other breast cancer subtypes, TNBC shows a high proliferation rate and a high risk developing metastasis. Therefore, there is a high demand to develop novel therapeutics for TNBC patients. Small interfering RNAs (siRNAs) have the capability to downregulate specific genes via RISC-mediated mRNA degradation [115]. It represents a promising therapeutic tool as it can silence aberrant genes that are essential for the progression of diseases such as cancer [115]. Metastasis is the primary cause of death for the majority of TNBC patients, presenting a considerable challenge in the clinical management of this disease [34]. Accumulating evidence has demonstrated the association of IKBKE with tumor metastasis. Taken together, these studies suggest that IKBKE plays a pivotal role in tumorigenesis and metastasis, and the suppression of IKBKE expression may provide a novel approach to the treatment of TNBC. In this dissertation, we demonstrated that targeting IKBKE with siRNA significantly inhibited the proliferation, migration, and invasion of TNBC cells. Silencing of IKBKE induced cancer cell apoptosis and arrested the cell cycle at the S and G2 phases. The cholesterol peptide/siRNA nanocomplexes (CCP/siRNA nanocomplexes) increased the tumor penetration and cellular uptake of siRNA. The CCP/siRNA nanocomplexes showed low cytotoxicity and disrupted the endosomal membrane to mediate endosomal escape for intracellular siRNA delivery. Moreover, the CCP/siRNA nanocomplex significantly inhibited tumor growth in an orthotopic TNBC mouse model. Overall, this siRNA nanocomplex provides a promising therapy for TNBC.

CD24 is a heavily glycosylated protein linked to the cell membrane via a glycosylphosphatidylinositol (GPI) anchor. CD24 is typically expressed in hematopoietic cells but is also overexpressed in numerous human cancers including breast cancer [74]. Many studies have demonstrated that CD24 plays a significant role in tumor development and progression [66-69]. Moreover, CD24 exhibits a functionally intracellular location of CD24 which can promote tumor progression. [70]. These data reveal that targeting CD24 with siRNA may be a reasonable approach for cancer therapy compared to surface blocking with antibodies. In this study, we showed that the pre-designed CD24 small interfering RNA (siRNA) displayed potent silencing activity in TNBC cells, leading to the efficient inhibition of TNBC cell proliferation, migration, and invasion. CD24 silencing induced apoptosis and cell cycle arrest in tumor cells. Additionally, silencing CD24 enhanced the sensitivity of MDA-MB-231 cells to doxorubicin and increased the phagocytosis of tumor cells by macrophages. In conclusion, targeting CD24 with siRNAs holds promise as a therapeutic strategy for TNBC and other cancers characterized by CD24 overexpression.

Immunotherapy is a treatment that uses patients' immune systems to fight cancers. Studies have reported favorable outcomes of immunotherapy in a variety of tumors especially using checkpoint inhibitors targeting the inhibitory receptors which have shown enormous success in the treatment of a diversity of cancers[79, 152-154]. Programmed cell death ligand 1 (PD-L1) is overexpressed in many human cancer types and is considered a negative factor of the immune response. PD-L1 binds to its receptor PD-1 resulting in tumor immune evasion by inhibiting T cell functions, including T cell activation, proliferation, cytokine secretion, and inducing apoptosis [81]. Therefore, the blockade of PD-1/PD-L1 is emerging as an immunotherapeutic approach for cancer treatment. Monoclonal antibody-based immune

checkpoint inhibitors have exhibited encouraging therapeutic outcomes in a variety of human malignancies.[82, 83] In this study, for the first time, we discovered anti-human PD-L1 human domain antibodies (dAbs) by using a human domain antibody phage library to block PD-1/PD-L1 interaction. Among all 7 different human domain antibody candidates, the CLV3 dAb demonstrated the best binding and blocking affinity to PD-L1 protein and PD-L1 overexpressed cancer cell line. The CLV3 dAb also reversed T-cell apoptosis in the co-culture of PBMC with DU145 tumor cells and exhibited better tumor penetrations compared to the anti-PD-L1 monoclonal antibody. Moreover, the CLV3 dAb significantly inhibited tumor growth in mice implanted with CT26 colon carcinoma cells. These results suggest that CLV3 dAb can be potentially used as an anti-PD-L1 inhibitor for cancer immunotherapy.

Metastasis is a major challenge in TNBC treatment and IKBKE is associated with breast tumor metastasis. In future studies, we will evaluate whether IKBKE siRNA can reduce *in vivo* metastasis of TNBC with different mouse models (e.g., orthotopic and tail vein injection mouse models) and the combination of IKBKE siRNA with immunotherapy. In addition, we will develop delivery systems to increase the stability and tumor accumulation of CD24 siRNA and evaluate the synergistic antitumor activity of CD24 siRNA with doxorubicin in the tumor model.

REFERENCES

1. Siegel, R. L.; Miller, K. D.; Wagle, N. S.; Jemal, A., Cancer statistics, 2023. *CA Cancer J Clin* **2023,** *73* (1), 17-48.

2. Yersal, O.; Barutca, S., Biological subtypes of breast cancer: Prognostic and therapeutic implications. *World J Clin Oncol* **2014,** *5* (3), 412-24.

3. Mohammed, A. A., The clinical behavior of different molecular subtypes of breast cancer. *Cancer Treat Res Commun* **2021,** *29*, 100469.

4. Al-Mahmood, S.; Sapiezynski, J.; Garbuzenko, O. B.; Minko, T., Metastatic and triple-negative breast cancer: challenges and treatment options. *Drug Deliv Transl Res* **2018,** *8* (5), 1483-1507.

5. Yin, L.; Duan, J. J.; Bian, X. W.; Yu, S. C., Triple-negative breast cancer molecular subtyping and treatment progress. *Breast Cancer Res* **2020,** *22* (1), 61.

6. Esfahani, K.; Roudaia, L.; Buhlaiga, N.; Del Rincon, S. V.; Papneja, N.; Miller, W. H., Jr., A review of cancer immunotherapy: from the past, to the present, to the future. *Curr Oncol* **2020,** *27* (Suppl 2), S87-S97.

7. Gong, J.; Chehrazi-Raffle, A.; Reddi, S.; Salgia, R., Development of PD-1 and PD-L1 inhibitors as a form of cancer immunotherapy: a comprehensive review of registration trials and future considerations. *J Immunother Cancer* **2018,** *6* (1), 8.

8. Zou, W.; Wolchok, J. D.; Chen, L., PD-L1 (B7-H1) and PD-1 pathway blockade for cancer therapy: Mechanisms, response biomarkers, and combinations. *Sci Transl Med* **2016,** *8* (328), 328rv4.

9. Nedeljkovic, M.; Damjanovic, A., Mechanisms of Chemotherapy Resistance in Triple-Negative Breast Cancer-How We Can Rise to the Challenge. *Cells* **2019,** *8* (9).

10. Zagami, P.; Carey, L. A., Triple negative breast cancer: Pitfalls and progress. *NPJ Breast Cancer* **2022,** *8* (1), 95.

11. Yin, M.; Wang, X.; Lu, J., Advances in IKBKE as a potential target for cancer therapy. *Cancer Med* **2020,** *9* (1), 247-258.

12. Bainbridge, A.; Walker, S.; Smith, J.; Patterson, K.; Dutt, A.; Ng, Y. M.; Thomas, H. D.; Wilson, L.; McCullough, B.; Jones, D.; Maan, A.; Banks, P.; McCracken, S. R.; Gaughan, L.; Robson, C. N.; Coffey, K., IKBKE activity enhances AR levels in advanced prostate cancer via modulation of the Hippo pathway. *Nucleic Acids Res* **2020,** *48* (10), 5366-5382.

13. House, C. D.; Grajales, V.; Ozaki, M.; Jordan, E.; Wubneh, H.; Kimble, D. C.; James, J. M.; Kim, M. K.; Annunziata, C. M., IKappaKappaepsilon cooperates with either MEK or non-canonical NF-kB driving growth of triple-negative breast cancer cells in different contexts. *BMC Cancer* **2018,** *18* (1), 595.

14. Barbie, T. U.; Alexe, G.; Aref, A. R.; Li, S.; Zhu, Z.; Zhang, X.; Imamura, Y.; Thai, T. C.; Huang, Y.; Bowden, M.; Herndon, J.; Cohoon, T. J.; Fleming, T.; Tamayo, P.; Mesirov, J. P.; Ogino, S.; Wong, K. K.; Ellis, M. J.; Hahn, W. C.; Barbie, D. A.; Gillanders, W. E., Targeting an IKBKE cytokine network impairs triple-negative breast cancer growth. *J Clin Invest* **2014,** *124* (12), 5411-23.

15. Qin, B.; Cheng, K., Silencing of the IKKepsilon gene by siRNA inhibits invasiveness and growth of breast cancer cells. *Breast Cancer Res* **2010,** *12* (5), R74.

16. Zhao, Z.; Li, Y.; Liu, H.; Jain, A.; Patel, P. V.; Cheng, K., Co-delivery of IKBKE siRNA and cabazitaxel by hybrid nanocomplex inhibits invasiveness and growth of triple-negative breast cancer. *Sci Adv* **2020,** *6* (29), eabb0616.

17. Jing, X.; Cui, X.; Liang, H.; Hao, C.; Yang, Z.; Li, X.; Yang, X.; Han, C., CD24 is a Potential Biomarker for Prognosis in Human Breast Carcinoma. *Cell Physiol Biochem* **2018,** *48* (1), 111-119.

18. Panagiotou, E.; Syrigos, N. K.; Charpidou, A.; Kotteas, E.; Vathiotis, I. A., CD24: A Novel Target for Cancer Immunotherapy. *J Pers Med* **2022,** *12* (8).

19. Kwon, M. J.; Han, J.; Seo, J. H.; Song, K.; Jeong, H. M.; Choi, J. S.; Kim, Y. J.; Lee, S. H.; Choi, Y. L.; Shin, Y. K., CD24 Overexpression Is Associated with Poor Prognosis in Luminal A and Triple-Negative Breast Cancer. *PLoS One* **2015,** *10* (10), e0139112.

20. Barkal, A. A.; Brewer, R. E.; Markovic, M.; Kowarsky, M.; Barkal, S. A.; Zaro, B. W.; Krishnan, V.; Hatakeyama, J.; Dorigo, O.; Barkal, L. J.; Weissman, I. L., CD24 signalling through macrophage Siglec-10 is a target for cancer immunotherapy. *Nature* **2019,** *572* (7769), 392-396.

21. Huth, H. W.; Castro-Gomes, T.; de Goes, A. M.; Ropert, C., Translocation of intracellular CD24 constitutes a triggering event for drug resistance in breast cancer. *Sci Rep* **2021,** *11* (1), 17077.

22. Dominska, M.; Dykxhoorn, D. M., Breaking down the barriers: siRNA delivery and endosome escape. *J Cell Sci* **2010,** *123* (Pt 8), 1183-9.

23. Tatiparti, K.; Sau, S.; Kashaw, S. K.; Iyer, A. K., siRNA Delivery Strategies: A Comprehensive Review of Recent Developments. *Nanomaterials (Basel)* **2017,** *7* (4).

24. Singh, A.; Trivedi, P.; Jain, N. K., Advances in siRNA delivery in cancer therapy. *Artif Cells Nanomed Biotechnol* **2018,** *46* (2), 274-283.

25. Li, Y.; Zhao, Z.; Lin, C. Y.; Liu, Y.; Staveley, O. K. F.; Li, G.; Cheng, K., Silencing PCBP2 normalizes desmoplastic stroma and improves the antitumor activity of chemotherapy in pancreatic cancer. *Theranostics* **2021,** *11* (5), 2182-2200.

26. Kijanka, M.; Dorresteijn, B.; Oliveira, S.; van Bergen en Henegouwen, P. M., Nanobody-based cancer therapy of solid tumors. *Nanomedicine (Lond)* **2015,** *10* (1), 161-74.

27. Safarzadeh Kozani, P.; Safarzadeh Kozani, P.; Rahbarizadeh, F., The Potential Applicability of Single-Domain Antibodies (VHH): From Checkpoint Blockade to Infectious Disease Therapy. *Trends Med Sci* **2021,** *1* (2), e114888.

28. Hwang, S. Y.; Park, S.; Kwon, Y., Recent therapeutic trends and promising targets in triple negative breast cancer. *Pharmacol Ther* **2019,** *199*, 30-57.

29. Mehanna, J.; Haddad, F. G.; Eid, R.; Lambertini, M.; Kourie, H. R., Triple-negative breast cancer: current perspective on the evolving therapeutic landscape. *Int J Womens Health* **2019,** *11*, 431-437.

30. O'Reilly, D.; Sendi, M. A.; Kelly, C. M., Overview of recent advances in metastatic triple negative breast cancer. *World J Clin Oncol* **2021,** *12* (3), 164-182.

31. Furlanetto, J.; Loibl, S., Optimal Systemic Treatment for Early Triple-Negative Breast Cancer. *Breast Care (Basel)* **2020,** *15* (3), 217-226.

32. Adel, N. G., Current treatment landscape and emerging therapies for metastatic triple-negative breast cancer. *Am J Manag Care* **2021,** *27* (5 Suppl), S87-S96.

33. Cocco, S.; Piezzo, M.; Calabrese, A.; Cianniello, D.; Caputo, R.; Lauro, V. D.; Fusco, G.; Gioia, G. D.; Licenziato, M.; De Laurentiis, M., Biomarkers in Triple-Negative Breast Cancer: State-of-the-Art and Future Perspectives. *Int J Mol Sci* **2020,** *21* (13).

34. Almansour, N. M., Triple-Negative Breast Cancer: A Brief Review About Epidemiology, Risk Factors, Signaling Pathways, Treatment and Role of Artificial Intelligence. *Front Mol Biosci* **2022,** *9*, 836417.

35. Allison, K. H.; Hammond, M. E. H.; Dowsett, M.; McKernin, S. E.; Carey, L. A.; Fitzgibbons, P. L.; Hayes, D. F.; Lakhani, S. R.; Chavez-MacGregor, M.; Perlmutter, J.; Perou, C. M.; Regan, M. M.; Rimm, D. L.; Symmans, W. F.; Torlakovic, E. E.; Varella, L.; Viale, G.; Weisberg, T. F.; McShane, L. M.; Wolff, A. C., Estrogen and Progesterone Receptor Testing in Breast Cancer: ASCO/CAP Guideline Update. *J Clin Oncol* **2020,** *38* (12), 1346-1366.

36. Wolff, A. C.; Hammond, M. E. H.; Allison, K. H.; Harvey, B. E.; Mangu, P. B.; Bartlett, J. M. S.; Bilous, M.; Ellis, I. O.; Fitzgibbons, P.; Hanna, W.; Jenkins, R. B.; Press, M. F.; Spears, P. A.; Vance, G. H.; Viale, G.; McShane, L. M.; Dowsett, M., Human Epidermal Growth Factor Receptor 2 Testing in Breast Cancer: American Society of Clinical Oncology/College of American Pathologists Clinical Practice Guideline Focused Update. *J Clin Oncol* **2018,** *36* (20), 2105-2122.

37. Obidiro, O.; Battogtokh, G.; Akala, E. O., Triple Negative Breast Cancer Treatment Options and Limitations: Future Outlook. *Pharmaceutics* **2023,** *15* (7).

38. Wahba, H. A.; El-Hadaad, H. A., Current approaches in treatment of triple-negative breast cancer. *Cancer Biol Med* **2015,** *12* (2), 106-16.

39. Gadi, V. K.; Davidson, N. E., Practical Approach to Triple-Negative Breast Cancer. *J Oncol Pract* **2017,** *13* (5), 293-300.

40. Azoury, F.; Misra, S.; Barry, A.; Helou, J., Role of radiation therapy in triple negative breast cancer: current state and future directions—a narrative review. *Precision Cancer Medicine* **2021,** *5*.

41. Yao, Y.; Chu, Y.; Xu, B.; Hu, Q.; Song, Q., Radiotherapy after surgery has significant survival benefits for patients with triple-negative breast cancer. *Cancer Med* **2019,** *8* (2), 554-563.

42. Woo, J.; Moon, B. I.; Kwon, H.; Lim, W., Effect of radiotherapy sequence on long-term outcome in patients with node-positive breast cancer: a retrospective study. *Sci Rep* **2022,** *12* (1), 10729.

43. Nguyen, A. T.; Shiao, S. L.; McArthur, H. L., Advances in Combining Radiation and Immunotherapy in Breast Cancer. *Clin Breast Cancer* **2021,** *21* (2), 143-152.

44. To, N. H.; Nguyen, H. Q.; Thiolat, A.; Liu, B.; Cohen, J.; Radosevic-Robin, N.; Belkacemi, Y.; TransAtlantic Radiation Oncology, N.; Association of, R.; Oncology of the Mediterranean, A., Radiation therapy for triple-negative breast cancer: emerging role of microRNAs as biomarkers and radiosensitivity modifiers. A systematic review. *Breast Cancer Res Treat* **2022,** *193* (2), 265-279.

45. Bou Zerdan, M.; Ghorayeb, T.; Saliba, F.; Allam, S.; Bou Zerdan, M.; Yaghi, M.; Bilani, N.; Jaafar, R.; Nahleh, Z., Triple Negative Breast Cancer: Updates on Classification and Treatment in 2021. *Cancers (Basel)* **2022,** *14* (5).

46. Lee, J., Current Treatment Landscape for Early Triple-Negative Breast Cancer (TNBC). *J Clin Med* **2023,** *12* (4).

47. Won, K. A.; Spruck, C., Triple-negative breast cancer therapy: Current and future perspectives (Review). *Int J Oncol* **2020,** *57* (6), 1245-1261.

48. Yang, R.; Li, Y.; Wang, H.; Qin, T.; Yin, X.; Ma, X., Therapeutic progress and challenges for triple negative breast cancer: targeted therapy and immunotherapy. *Mol Biomed* **2022,** *3* (1), 8.

49. Gooding, A. J.; Schiemann, W. P., Epithelial-Mesenchymal Transition Programs and Cancer Stem Cell Phenotypes: Mediators of Breast Cancer Therapy Resistance. *Mol Cancer Res* **2020,** *18* (9), 1257-1270.

50. Crown, J.; O'Shaughnessy, J.; Gullo, G., Emerging targeted therapies in triple-negative breast cancer. *Ann Oncol* **2012,** *23 Suppl 6*, vi56-65.

51. Li, Y.; Zhang, H.; Merkher, Y.; Chen, L.; Liu, N.; Leonov, S.; Chen, Y., Recent advances in therapeutic strategies for triple-negative breast cancer. *J Hematol Oncol* **2022,** *15* (1), 121.

52. Zhang, J.; Xia, Y.; Zhou, X.; Yu, H.; Tan, Y.; Du, Y.; Zhang, Q.; Wu, Y., Current landscape of personalized clinical treatments for triple-negative breast cancer. *Front Pharmacol* **2022,** *13*, 977660.

53. Kalimutho, M.; Parsons, K.; Mittal, D.; Lopez, J. A.; Srihari, S.; Khanna, K. K., Targeted Therapies for Triple-Negative Breast Cancer: Combating a Stubborn Disease. *Trends Pharmacol Sci* **2015,** *36* (12), 822-846.

54. Hegde, P. S.; Chen, D. S., Top 10 Challenges in Cancer Immunotherapy. *Immunity* **2020,** *52* (1), 17-35.

55. Thomas, R.; Al-Khadairi, G.; Decock, J., Immune Checkpoint Inhibitors in Triple Negative Breast Cancer Treatment: Promising Future Prospects. *Front Oncol* **2020,** *10*, 600573.

56. Keenan, T. E.; Tolaney, S. M., Role of Immunotherapy in Triple-Negative Breast Cancer. *J Natl Compr Canc Netw* **2020,** *18* (4), 479-489.

57. Emens, L. A., Immunotherapy in Triple-Negative Breast Cancer. *Cancer J* **2021,** *27* (1), 59-66.

58. Luo, C.; Wang, P.; He, S.; Zhu, J.; Shi, Y.; Wang, J., Progress and Prospect of Immunotherapy for Triple-Negative Breast Cancer. *Front Oncol* **2022,** *12*, 919072.

59. Bianchini, G.; De Angelis, C.; Licata, L.; Gianni, L., Treatment landscape of triple-negative breast cancer - expanded options, evolving needs. *Nat Rev Clin Oncol* **2022,** *19* (2), 91-113.

60. Liu, Y.; Hu, Y.; Xue, J.; Li, J.; Yi, J.; Bu, J.; Zhang, Z.; Qiu, P.; Gu, X., Advances in immunotherapy for triple-negative breast cancer. *Mol Cancer* **2023,** *22* (1), 145.

61. Verhelst, K.; Verstrepen, L.; Carpentier, I.; Beyaert, R., IkappaB kinase epsilon (IKKepsilon): a therapeutic target in inflammation and cancer. *Biochem Pharmacol* **2013,** *85* (7), 873-80.

62. Tang, X.; Jin, L.; Cao, P.; Cao, K.; Huang, C.; Luo, Y.; Ma, J.; Shen, S.; Tan, M.; Li, X.; Zhou, M., MicroRNA-16 sensitizes breast cancer cells to paclitaxel through suppression of IKBKB expression. *Oncotarget* **2016,** *7* (17), 23668-83.

63. Lu, J.; Yang, Y.; Guo, G.; Liu, Y.; Zhang, Z.; Dong, S.; Nan, Y.; Zhao, Z.; Zhong, Y.; Huang, Q., IKBKE regulates cell proliferation and epithelial-mesenchymal transition of human malignant glioma via the Hippo pathway. *Oncotarget* **2017,** *8* (30), 49502-49514.

64. Durand, J. K.; Zhang, Q.; Baldwin, A. S., Roles for the IKK-Related Kinases TBK1 and IKKepsilon in Cancer. *Cells* **2018,** *7* (9).

65. Qiao, J.; Chen, Y.; Mi, Y.; Jin, H.; Wang, L.; Huang, T.; Li, H.; Song, Y.; Cao, J.; Wu, B.; Wang, Q.; Zou, Z., Macrophages confer resistance to BET inhibition in triple-negative breast cancer by upregulating IKBKE. *Biochem Pharmacol* **2020,** *180*, 114126.

66. Baumann, P.; Cremers, N.; Kroese, F.; Orend, G.; Chiquet-Ehrismann, R.; Uede, T.; Yagita, H.; Sleeman, J. P., CD24 expression causes the acquisition of multiple cellular properties associated with tumor growth and metastasis. *Cancer Res* **2005,** *65* (23), 10783-93.

67. Bretz, N. P.; Salnikov, A. V.; Perne, C.; Keller, S.; Wang, X.; Mierke, C. T.; Fogel, M.; Erbe-Hofmann, N.; Schlange, T.; Moldenhauer, G.; Altevogt, P., CD24 controls Src/STAT3 activity in human tumors. *Cell Mol Life Sci* **2012,** *69* (22), 3863-79.

68. Wang, W.; Wang, X.; Peng, L.; Deng, Q.; Liang, Y.; Qing, H.; Jiang, B., CD24-dependent MAPK pathway activation is required for colorectal cancer cell proliferation. *Cancer Sci* **2010,** *101* (1), 112-9.

69. Smith, S. C.; Oxford, G.; Wu, Z.; Nitz, M. D.; Conaway, M.; Frierson, H. F.; Hampton, G.; Theodorescu, D., The metastasis-associated gene CD24 is regulated by Ral GTPase and is a mediator of cell proliferation and survival in human cancer. *Cancer Res* **2006,** *66* (4), 1917-22.

70. Wang, L.; Liu, R.; Ye, P.; Wong, C.; Chen, G. Y.; Zhou, P.; Sakabe, K.; Zheng, X.; Wu, W.; Zhang, P.; Jiang, T.; Bassetti, M. F.; Jube, S.; Sun, Y.; Zhang, Y.; Zheng, P.; Liu, Y., Intracellular CD24 disrupts the ARF-NPM interaction and enables mutational and viral oncogene-mediated p53 inactivation. *Nat Commun* **2015,** *6*, 5909.

71. Zhang, W.; Yi, B.; Wang, C.; Chen, D.; Bae, S.; Wei, S.; Guo, R. J.; Lu, C.; Nguyen, L. L.; Yang, W. H.; Lillard, J. W.; Zhang, X.; Wang, L.; Liu, R., Silencing of CD24 Enhances the PRIMA-1-Induced Restoration of Mutant p53 in Prostate Cancer Cells. *Clin Cancer Res* **2016,** *22* (10), 2545-54.

72. Duex, J. E.; Owens, C.; Chauca-Diaz, A.; Dancik, G. M.; Vanderlinden, L. A.; Ghosh, D.; Leivo, M. Z.; Hansel, D. E.; Theodorescu, D., Nuclear CD24 Drives Tumor Growth and Is Predictive of Poor Patient Prognosis. *Cancer Res* **2017,** *77* (18), 4858-4867.

73. Ahmed, M. A.; Aleskandarany, M. A.; Rakha, E. A.; Moustafa, R. Z.; Benhasouna, A.; Nolan, C.; Green, A. R.; Ilyas, M.; Ellis, I. O., A CD44(-)/CD24(+) phenotype is a poor prognostic marker in early invasive breast cancer. *Breast Cancer Res Treat* **2012,** *133* (3), 979-95.

74. Zhang, P.; Zheng, P.; Liu, Y., Amplification of the CD24 Gene Is an Independent Predictor for Poor Prognosis of Breast Cancer. *Front Genet* **2019,** *10*, 560.

75. Kim, S. K.; Cho, S. W., The Evasion Mechanisms of Cancer Immunity and Drug Intervention in the Tumor Microenvironment. *Front Pharmacol* **2022,** *13*, 868695.

76. Marshall, J. S.; Warrington, R.; Watson, W.; Kim, H. L., An introduction to immunology and immunopathology. *Allergy Asthma Clin Immunol* **2018,** *14* (Suppl 2), 49.

77. Chen, D. S.; Mellman, I., Oncology meets immunology: the cancer-immunity cycle. *Immunity* **2013,** *39* (1), 1-10.

78. Chen, D. S.; Mellman, I., Elements of cancer immunity and the cancer-immune set point. *Nature* **2017,** *541* (7637), 321-330.

79. Zhang, Y.; Zhang, Z., The history and advances in cancer immunotherapy: understanding the characteristics of tumor-infiltrating immune cells and their therapeutic implications. *Cell Mol Immunol* **2020,** *17* (8), 807-821.

80. Marin-Acevedo, J. A.; Dholaria, B.; Soyano, A. E.; Knutson, K. L.; Chumsri, S.; Lou, Y., Next generation of immune checkpoint therapy in cancer: new developments and challenges. *J Hematol Oncol* **2018,** *11* (1), 39.

81. Han, Y.; Liu, D.; Li, L., PD-1/PD-L1 pathway: current researches in cancer. *Am J Cancer Res* **2020,** *10* (3), 727-742.

82. Jiang, Y.; Chen, M.; Nie, H.; Yuan, Y., PD-1 and PD-L1 in cancer immunotherapy: clinical implications and future considerations. *Hum Vaccin Immunother* **2019,** *15* (5), 1111-1122.

83. Alsaab, H. O.; Sau, S.; Alzhrani, R.; Tatiparti, K.; Bhise, K.; Kashaw, S. K.; Iyer, A. K., PD-1 and PD-L1 Checkpoint Signaling Inhibition for Cancer Immunotherapy: Mechanism, Combinations, and Clinical Outcome. *Front Pharmacol* **2017,** *8*, 561.

84. Robert, C., A decade of immune-checkpoint inhibitors in cancer therapy. *Nat Commun* **2020,** *11* (1), 3801.

85. Shiravand, Y.; Khodadadi, F.; Kashani, S. M. A.; Hosseini-Fard, S. R.; Hosseini, S.; Sadeghirad, H.; Ladwa, R.; O'Byrne, K.; Kulasinghe, A., Immune Checkpoint Inhibitors in Cancer Therapy. *Curr Oncol* **2022,** *29* (5), 3044-3060.

86. Rosenberg, S. A., Cancer immunotherapy comes of age. *Nat Clin Pract Oncol* **2005,** *2* (3), 115.

87. Chen, Y.; Huang, H.; Liu, Y.; Wang, Z.; Wang, L.; Wang, Q.; Zhang, Y.; Wang, H., Engineering a High-Affinity PD-1 Peptide for Optimized Immune Cell-Mediated Tumor Therapy. *Cancer Res Treat* **2022,** *54* (2), 362-374.

88. Liu, J.; Chen, Z.; Li, Y.; Zhao, W.; Wu, J.; Zhang, Z., PD-1/PD-L1 Checkpoint Inhibitors in Tumor Immunotherapy. *Front Pharmacol* **2021,** *12*, 731798.

89. Guzik, K.; Tomala, M.; Muszak, D.; Konieczny, M.; Hec, A.; Blaszkiewicz, U.; Pustula, M.; Butera, R.; Domling, A.; Holak, T. A., Development of the Inhibitors that Target

the PD-1/PD-L1 Interaction-A Brief Look at Progress on Small Molecules, Peptides and Macrocycles. *Molecules* **2019,** *24* (11).

90. Zhai, W.; Zhou, X.; Zhai, M.; Li, W.; Ran, Y.; Sun, Y.; Du, J.; Zhao, W.; Xing, L.; Qi, Y.; Gao, Y., Blocking of the PD-1/PD-L1 interaction by a novel cyclic peptide inhibitor for cancer immunotherapy. *Sci China Life Sci* **2021,** *64* (4), 548-562.

91. Yin, S.; Chen, Z.; Chen, D.; Yan, D., Strategies targeting PD-L1 expression and associated opportunities for cancer combination therapy. *Theranostics* **2023,** *13* (5), 1520-1544.

92. Wang, T.; Cai, S.; Cheng, Y.; Zhang, W.; Wang, M.; Sun, H.; Guo, B.; Li, Z.; Xiao, Y.; Jiang, S., Discovery of Small-Molecule Inhibitors of the PD-1/PD-L1 Axis That Promote PD-L1 Internalization and Degradation. *J Med Chem* **2022,** *65* (5), 3879-3893.

93. Lai, W. Y.; Huang, B. T.; Wang, J. W.; Lin, P. Y.; Yang, P. C., A Novel PD-L1-targeting Antagonistic DNA Aptamer With Antitumor Effects. *Mol Ther Nucleic Acids* **2016,** *5* (12), e397.

94. An, Y.; Li, X.; Yao, F.; Duan, J.; Yang, X. D., Novel Complex of PD-L1 Aptamer and Albumin Enhances Antitumor Efficacy In Vivo. *Molecules* **2022,** *27* (5).

95. Muyldermans, S., Nanobodies: natural single-domain antibodies. *Annu Rev Biochem* **2013,** *82*, 775-97.

96. Harmsen, M. M.; De Haard, H. J., Properties, production, and applications of camelid single-domain antibody fragments. *Appl Microbiol Biotechnol* **2007,** *77* (1), 13-22.

97. Zhang, F.; Wei, H.; Wang, X.; Bai, Y.; Wang, P.; Wu, J.; Jiang, X.; Wang, Y.; Cai, H.; Xu, T.; Zhou, A., Structural basis of a novel PD-L1 nanobody for immune checkpoint blockade. *Cell Discov* **2017,** *3*, 17004.

98. Sheridan, C., Ablynx's nanobody fragments go places antibodies cannot. *Nat Biotechnol* **2017,** *35* (12), 1115-1117.

99. Johnson, C. B.; Win, S. Y., Combination therapy with PD-1/PD-L1 blockade: An overview of ongoing clinical trials. *Oncoimmunology* **2018,** *7* (4), e1408744.

100. Yi, M.; Zheng, X.; Niu, M.; Zhu, S.; Ge, H.; Wu, K., Combination strategies with PD-1/PD-L1 blockade: current advances and future directions. *Mol Cancer* **2022,** *21* (1), 28.

101. Page, D. B.; Bear, H.; Prabhakaran, S.; Gatti-Mays, M. E.; Thomas, A.; Cobain, E.; McArthur, H.; Balko, J. M.; Gameiro, S. R.; Nanda, R.; Gulley, J. L.; Kalinsky, K.; White, J.; Litton, J.; Chmura, S. J.; Polley, M. Y.; Vincent, B.; Cescon, D. W.; Disis, M. L.; Sparano, J. A.; Mittendorf, E. A.; Adams, S., Two may be better than one: PD-1/PD-L1 blockade combination approaches in metastatic breast cancer. *NPJ Breast Cancer* **2019,** *5*, 34.

102. Sato, H.; Okonogi, N.; Nakano, T., Rationale of combination of anti-PD-1/PD-L1 antibody therapy and radiotherapy for cancer treatment. *Int J Clin Oncol* **2020,** *25* (5), 801-809.

103. Gong, J.; Le, T. Q.; Massarelli, E.; Hendifar, A. E.; Tuli, R., Radiation therapy and PD-1/PD-L1 blockade: the clinical development of an evolving anticancer combination. *J Immunother Cancer* **2018,** *6* (1), 46.

104. Zhang, J. Y.; Yan, Y. Y.; Li, J. J.; Adhikari, R.; Fu, L. W., PD-1/PD-L1 Based Combinational Cancer Therapy: Icing on the Cake. *Front Pharmacol* **2020,** *11*, 722.

105. Kong, X.; Lu, P.; Liu, C.; Guo, Y.; Yang, Y.; Peng, Y.; Wang, F.; Bo, Z.; Dou, X.; Shi, H.; Meng, J., A combination of PD-1/PD-L1 inhibitors: The prospect of overcoming the weakness of tumor immunotherapy (Review). *Mol Med Rep* **2021,** *23* (5).

106. Lan, Y.; Zhang, D.; Xu, C.; Hance, K. W.; Marelli, B.; Qi, J.; Yu, H.; Qin, G.; Sircar, A.; Hernandez, V. M.; Jenkins, M. H.; Fontana, R. E.; Deshpande, A.; Locke, G.; Sabzevari, H.; Radvanyi, L.; Lo, K. M., Enhanced preclinical antitumor activity of M7824, a bifunctional fusion protein simultaneously targeting PD-L1 and TGF-beta. *Sci Transl Med* **2018,** *10* (424).

107. Strauss, J.; Heery, C. R.; Schlom, J.; Madan, R. A.; Cao, L.; Kang, Z.; Lamping, E.; Marte, J. L.; Donahue, R. N.; Grenga, I.; Cordes, L.; Christensen, O.; Mahnke, L.; Helwig, C.; Gulley, J. L., Phase I Trial of M7824 (MSB0011359C), a Bifunctional Fusion Protein Targeting PD-L1 and TGFbeta, in Advanced Solid Tumors. *Clin Cancer Res* **2018,** *24* (6), 1287-1295.

108. Kim, C. G.; Sang, Y. B.; Lee, J. H.; Chon, H. J., Combining Cancer Vaccines with Immunotherapy: Establishing a New Immunological Approach. *Int J Mol Sci* **2021,** *22* (15).

109. Soares, K. C.; Rucki, A. A.; Wu, A. A.; Olino, K.; Xiao, Q.; Chai, Y.; Wamwea, A.; Bigelow, E.; Lutz, E.; Liu, L.; Yao, S.; Anders, R. A.; Laheru, D.; Wolfgang, C. L.; Edil, B. H.; Schulick, R. D.; Jaffee, E. M.; Zheng, L., PD-1/PD-L1 blockade together with vaccine therapy facilitates effector T-cell infiltration into pancreatic tumors. *J Immunother* **2015,** *38* (1), 1-11.

110. Duraiswamy, J.; Kaluza, K. M.; Freeman, G. J.; Coukos, G., Dual blockade of PD-1 and CTLA-4 combined with tumor vaccine effectively restores T-cell rejection function in tumors. *Cancer Res* **2013,** *73* (12), 3591-603.

111. Li Yi, G. G., Jiabo Li, Xiaoguang Fan, Tao Li, Luqing Tong, Peidong Liu, Xuya Wang, Feng Yuan, Shengping Yu, Qiang Huang, and Xuejun Yang, IKBKE, a prognostic factor preferentially expressed in mesenchymal glioblastoma, modulates tumoral

immunosuppression through the STAT3/PD - L1 pathway. *Clinical and Translational Medicine* **2020,** *10* (3), 1-18.

112. Guo, J. P.; Shu, S. K.; He, L.; Lee, Y. C.; Kruk, P. A.; Grenman, S.; Nicosia, S. V.; Mor, G.; Schell, M. J.; Coppola, D.; Cheng, J. Q., Deregulation of IKBKE is associated with tumor progression, poor prognosis, and cisplatin resistance in ovarian cancer. *Am J Pathol* **2009,** *175* (1), 324-33.

113. Boehm, J. S.; Zhao, J. J.; Yao, J.; Kim, S. Y.; Firestein, R.; Dunn, I. F.; Sjostrom, S. K.; Garraway, L. A.; Weremowicz, S.; Richardson, A. L.; Greulich, H.; Stewart, C. J.; Mulvey, L. A.; Shen, R. R.; Ambrogio, L.; Hirozane-Kishikawa, T.; Hill, D. E.; Vidal, M.; Meyerson, M.; Grenier, J. K.; Hinkle, G.; Root, D. E.; Roberts, T. M.; Lander, E. S.; Polyak, K.; Hahn, W. C., Integrative genomic approaches identify IKBKE as a breast cancer oncogene. *Cell* **2007,** *129* (6), 1065-79.

114. Xie, W.; Jiang, Q.; Wu, X.; Wang, L.; Gao, B.; Sun, Z.; Zhang, X.; Bu, L.; Lin, Y.; Huang, Q.; Li, J.; Guo, J., IKBKE phosphorylates and stabilizes Snail to promote breast cancer invasion and metastasis. *Cell Death Differ* **2022,** *29* (8), 1528-1540.

115. Whitehead, K. A.; Langer, R.; Anderson, D. G., Knocking down barriers: advances in siRNA delivery. *Nat Rev Drug Discov* **2009,** *8* (2), 129-38.

116. Wang, J.; Lu, Z.; Wientjes, M. G.; Au, J. L., Delivery of siRNA therapeutics: barriers and carriers. *AAPS J* **2010,** *12* (4), 492-503.

117. Paunovska, K.; Loughrey, D.; Dahlman, J. E., Drug delivery systems for RNA therapeutics. *Nat Rev Genet* **2022,** *23* (5), 265-280.

118. Gao, K.; Huang, L., Nonviral methods for siRNA delivery. *Mol Pharm* **2009,** *6* (3), 651-8.

119. Qin, B.; Chen, Z.; Jin, W.; Cheng, K., Development of cholesteryl peptide micelles for siRNA delivery. *Journal of controlled release : official journal of the Controlled Release Society* **2013,** *172* (1), 159-168.

120. Liu, H.; Zhao, Z.; Zhang, L.; Li, Y.; Jain, A.; Barve, A.; Jin, W.; Liu, Y.; Fetse, J.; Cheng, K., Discovery of low-molecular weight anti-PD-L1 peptides for cancer immunotherapy. *J Immunother Cancer* **2019,** *7* (1), 270.

121. Evans, B. C.; Nelson, C. E.; Yu, S. S.; Beavers, K. R.; Kim, A. J.; Li, H.; Nelson, H. M.; Giorgio, T. D.; Duvall, C. L., Ex vivo red blood cell hemolysis assay for the evaluation of pH-responsive endosomolytic agents for cytosolic delivery of biomacromolecular drugs. *J Vis Exp* **2013,** (73), e50166.

122. Lin, C. Y.; Mamani, U. F.; Guo, Y.; Liu, Y.; Cheng, K., Peptide-Based siRNA Nanocomplexes Targeting Hepatic Stellate Cells. *Biomolecules* **2023,** *13* (3).

123. Khononov, I.; Jacob, E.; Fremder, E.; Dahan, N.; Harel, M.; Raviv, Z.; Krastev, B.; Shaked, Y., Host response to immune checkpoint inhibitors contributes to tumor aggressiveness. *J Immunother Cancer* **2021,** *9* (3).

124. White, E.; Lattime, E. C.; Guo, J. Y., Autophagy Regulates Stress Responses, Metabolism, and Anticancer Immunity. *Trends Cancer* **2021,** *7* (8), 778-789.

125. Yun, C. W.; Lee, S. H., The Roles of Autophagy in Cancer. *Int J Mol Sci* **2018,** *19* (11).

126. Tumeh, P. C.; Harview, C. L.; Yearley, J. H.; Shintaku, I. P.; Taylor, E. J.; Robert, L.; Chmielowski, B.; Spasic, M.; Henry, G.; Ciobanu, V.; West, A. N.; Carmona, M.; Kivork, C.; Seja, E.; Cherry, G.; Gutierrez, A. J.; Grogan, T. R.; Mateus, C.; Tomasic, G.; Glaspy, J. A.; Emerson, R. O.; Robins, H.; Pierce, R. H.; Elashoff, D. A.; Robert, C.; Ribas,

A., PD-1 blockade induces responses by inhibiting adaptive immune resistance. *Nature* **2014,** *515* (7528), 568-71.

127. Liu, Y.; Guo, G.; Lu, Y.; Chen, X.; Zhu, L.; Zhao, L.; Li, C.; Zhang, Z.; Jin, X.; Dong, J.; Yang, X.; Huang, Q., Silencing IKBKE inhibits the migration and invasion of glioblastoma by promoting Snail1 degradation. *Clin Transl Oncol* **2022,** *24* (5), 816-828.

128. Orlova, Z.; Pruefer, F.; Castro-Oropeza, R.; Ordaz-Ramos, A.; Zampedri, C.; Maldonado, V.; Vazquez-Santillan, K.; Melendez-Zajgla, J., IKKepsilon regulates the breast cancer stem cell phenotype. *Biochim Biophys Acta Mol Cell Res* **2019,** *1866* (4), 598-611.

129. Zeng, Z.; Wong, C. J.; Yang, L.; Ouardaoui, N.; Li, D.; Zhang, W.; Gu, S.; Zhang, Y.; Liu, Y.; Wang, X.; Fu, J.; Zhou, L.; Zhang, B.; Kim, S.; Yates, K. B.; Brown, M.; Freeman, G. J.; Uppaluri, R.; Manguso, R.; Liu, X. S., TISMO: syngeneic mouse tumor database to model tumor immunity and immunotherapy response. *Nucleic Acids Res* **2022,** *50* (D1), D1391-D1397.

130. Ireson, C. R.; Alavijeh, M. S.; Palmer, A. M.; Fowler, E. R.; Jones, H. J., The role of mouse tumour models in the discovery and development of anticancer drugs. *Br J Cancer* **2019,** *121* (2), 101-108.

131. Xupeng Bai, J. N., Julia Beretov, Peter Graham, Yong Li, Immunotherapy for triple-negative breast cancer: A molecular insight into the microenvironment, treatment, and resistance. *Journal of the National Cancer Center* **2021,** *1* (3), 75-87.

132. Altevogt, P.; Sammar, M.; Huser, L.; Kristiansen, G., Novel insights into the function of CD24: A driving force in cancer. *Int J Cancer* **2021,** *148* (3), 546-559.

133. Wu, H.; Liu, J.; Wang, Z.; Yuan, W.; Chen, L., Prospects of antibodies targeting CD47 or CD24 in the treatment of glioblastoma. *CNS Neurosci Ther* **2021,** *27* (10), 1105-1117.

134. Lam, J. K.; Chow, M. Y.; Zhang, Y.; Leung, S. W., siRNA Versus miRNA as Therapeutics for Gene Silencing. *Mol Ther Nucleic Acids* **2015,** *4* (9), e252.

135. Vicentini, F. T.; Borgheti-Cardoso, L. N.; Depieri, L. V.; de Macedo Mano, D.; Abelha, T. F.; Petrilli, R.; Bentley, M. V., Delivery systems and local administration routes for therapeutic siRNA. *Pharm Res* **2013,** *30* (4), 915-31.

136. Holliday, D. L.; Speirs, V., Choosing the right cell line for breast cancer research. *Breast Cancer Res* **2011,** *13* (4), 215.

137. Jiao, X. L.; Zhao, C.; Niu, M.; Chen, D., Downregulation of CD24 inhibits invasive growth, facilitates apoptosis and enhances chemosensitivity in gastric cancer AGS cells. *Eur Rev Med Pharmacol Sci* **2013,** *17* (13), 1709-15.

138. Ma, Z. L.; Chen, Y. P.; Song, J. L.; Wang, Y. Q., Knockdown of CD24 inhibits proliferation, invasion and sensitizes breast cancer MCF-7 cells to tamoxifen in vitro. *Eur Rev Med Pharmacol Sci* **2015,** *19* (13), 2394-9.

139. Alkaraki, A.; Alshaer, W.; Wehaibi, S.; Gharaibeh, L.; Abuarqoub, D.; Alqudah, D. A.; Al-Azzawi, H.; Zureigat, H.; Souleiman, M.; Awidi, A., Enhancing chemosensitivity of wild-type and drug-resistant MDA-MB-231 triple-negative breast cancer cell line to doxorubicin by silencing of STAT 3, Notch-1, and beta-catenin genes. *Breast Cancer* **2020,** *27* (5), 989-998.

140. Paramanantham, A.; Jung, E. J.; Kim, H. J.; Jeong, B. K.; Jung, J. M.; Kim, G. S.; Chan, H. S.; Lee, W. S., Doxorubicin-Resistant TNBC Cells Exhibit Rapid Growth with Cancer Stem Cell-like Properties and EMT Phenotype, Which Can Be Transferred to Parental Cells through Autocrine Signaling. *Int J Mol Sci* **2021,** *22* (22).

141. Salemme, V.; Centonze, G.; Cavallo, F.; Defilippi, P.; Conti, L., The Crosstalk Between Tumor Cells and the Immune Microenvironment in Breast Cancer: Implications for Immunotherapy. *Front Oncol* **2021,** *11*, 610303.

142. Lopez-Yrigoyen, M.; Cassetta, L.; Pollard, J. W., Macrophage targeting in cancer. *Ann N Y Acad Sci* **2021,** *1499* (1), 18-41.

143. Mantovani, A.; Allavena, P.; Marchesi, F.; Garlanda, C., Macrophages as tools and targets in cancer therapy. *Nat Rev Drug Discov* **2022,** *21* (11), 799-820.

144. Xiang, X.; Wang, J.; Lu, D.; Xu, X., Targeting tumor-associated macrophages to synergize tumor immunotherapy. *Signal Transduct Target Ther* **2021,** *6* (1), 75.

145. Williams, C. B.; Yeh, E. S.; Soloff, A. C., Tumor-associated macrophages: unwitting accomplices in breast cancer malignancy. *NPJ Breast Cancer* **2016,** *2*, 15025-.

146. Thorn, C. F.; Oshiro, C.; Marsh, S.; Hernandez-Boussard, T.; McLeod, H.; Klein, T. E.; Altman, R. B., Doxorubicin pathways: pharmacodynamics and adverse effects. *Pharmacogenet Genomics* **2011,** *21* (7), 440-6.

147. Ozawa, Y.; Harutani, Y.; Oyanagi, J.; Akamatsu, H.; Murakami, E.; Shibaki, R.; Hayata, A.; Sugimoto, T.; Tanaka, M.; Takakura, T.; Furuta, K.; Okuda, Y.; Sato, K.; Teraoka, S.; Ueda, H.; Tokudome, N.; Kitamura, Y.; Fukuoka, J.; Nakanishi, M.; Koh, Y.; Yamamoto, N., CD24, not CD47, negatively impacts upon response to PD-1/L1 inhibitors in non-small-cell lung cancer with PD-L1 tumor proportion score < 50. *Cancer Sci* **2021,** *112* (1), 72-80.

148. Shipitsin, M.; Campbell, L. L.; Argani, P.; Weremowicz, S.; Bloushtain-Qimron, N.; Yao, J.; Nikolskaya, T.; Serebryiskaya, T.; Beroukhim, R.; Hu, M.; Halushka, M. K.; Sukumar, S.; Parker, L. M.; Anderson, K. S.; Harris, L. N.; Garber, J. E.; Richardson, A.

L.; Schnitt, S. J.; Nikolsky, Y.; Gelman, R. S.; Polyak, K., Molecular definition of breast tumor heterogeneity. *Cancer Cell* **2007,** *11* (3), 259-73.

149. Liu, W.; Zhang, Y.; Wei, S.; Bae, S.; Yang, W. H.; Smith, G. J.; Mohler, J. L.; Fontham, E. T. H.; Bensen, J. T.; Sonpavde, G. P.; Chen, G. Y.; Liu, R.; Wang, L., A CD24-p53 axis contributes to African American prostate cancer disparities. *Prostate* **2020,** *80* (8), 609-618.

150. Overdevest, J. B.; Thomas, S.; Kristiansen, G.; Hansel, D. E.; Smith, S. C.; Theodorescu, D., CD24 offers a therapeutic target for control of bladder cancer metastasis based on a requirement for lung colonization. *Cancer Res* **2011,** *71* (11), 3802-11.

151. Overdevest, J. B.; Knubel, K. H.; Duex, J. E.; Thomas, S.; Nitz, M. D.; Harding, M. A.; Smith, S. C.; Frierson, H. F.; Conaway, M.; Theodorescu, D., CD24 expression is important in male urothelial tumorigenesis and metastasis in mice and is androgen regulated. *Proceedings of the National Academy of Sciences of the United States of America* **2012,** *109* (51), E3588-96.

152. Kruger, S.; Ilmer, M.; Kobold, S.; Cadilha, B. L.; Endres, S.; Ormanns, S.; Schuebbe, G.; Renz, B. W.; D'Haese, J. G.; Schloesser, H.; Heinemann, V.; Subklewe, M.; Boeck, S.; Werner, J.; von Bergwelt-Baildon, M., Advances in cancer immunotherapy 2019 - latest trends. *J Exp Clin Cancer Res* **2019,** *38* (1), 268.

153. Pardoll, D. M., The blockade of immune checkpoints in cancer immunotherapy. *Nat Rev Cancer* **2012,** *12* (4), 252-64.

154. Naimi, A.; Mohammed, R. N.; Raji, A.; Chupradit, S.; Yumashev, A. V.; Suksatan, W.; Shalaby, M. N.; Thangavelu, L.; Kamrava, S.; Shomali, N.; Sohrabi, A. D.; Adili, A.;

Noroozi-Aghideh, A.; Razeghian, E., Tumor immunotherapies by immune checkpoint inhibitors (ICIs); the pros and cons. *Cell Commun Signal* **2022,** *20* (1), 44.

155. Twomey, J. D.; Zhang, B., Cancer Immunotherapy Update: FDA-Approved Checkpoint Inhibitors and Companion Diagnostics. *AAPS J* **2021,** *23* (2), 39.

156. Debie, P.; Lafont, C.; Defrise, M.; Hansen, I.; van Willigen, D. M.; van Leeuwen, F. W. B.; Gijsbers, R.; D'Huyvetter, M.; Devoogdt, N.; Lahoutte, T.; Mollard, P.; Hernot, S., Size and affinity kinetics of nanobodies influence targeting and penetration of solid tumours. *Journal of controlled release : official journal of the Controlled Release Society* **2020,** *317*, 34-42.

157. Lecocq, Q.; De Vlaeminck, Y.; Hanssens, H.; D'Huyvetter, M.; Raes, G.; Goyvaerts, C.; Keyaerts, M.; Devoogdt, N.; Breckpot, K., Theranostics in immuno-oncology using nanobody derivatives. *Theranostics* **2019,** *9* (25), 7772-7791.

158. De Meyer, T.; Muyldermans, S.; Depicker, A., Nanobody-based products as research and diagnostic tools. *Trends Biotechnol* **2014,** *32* (5), 263-70.

159. Broos, K.; Lecocq, Q.; Raes, G.; Devoogdt, N.; Keyaerts, M.; Breckpot, K., Noninvasive imaging of the PD-1:PD-L1 immune checkpoint: Embracing nuclear medicine for the benefit of personalized immunotherapy. *Theranostics* **2018,** *8* (13), 3559-3570.

160. Awad, R. M.; Lecocq, Q.; Zeven, K.; Ertveldt, T.; De Beck, L.; Ceuppens, H.; Broos, K.; De Vlaeminck, Y.; Goyvaerts, C.; Verdonck, M.; Raes, G.; Van Parys, A.; Cauwels, A.; Keyaerts, M.; Devoogdt, N.; Breckpot, K., Formatting and gene-based delivery of a human PD-L1 single domain antibody for immune checkpoint blockade. *Mol Ther Methods Clin Dev* **2021,** *22*, 172-182.

161. Zolghadr, K.; Mortusewicz, O.; Rothbauer, U.; Kleinhans, R.; Goehler, H.; Wanker, E. E.; Cardoso, M. C.; Leonhardt, H., A fluorescent two-hybrid assay for direct visualization of protein interactions in living cells. *Mol Cell Proteomics* **2008,** *7* (11), 2279-87.

162. Yau, K. Y.; Groves, M. A.; Li, S.; Sheedy, C.; Lee, H.; Tanha, J.; MacKenzie, C. R.; Jermutus, L.; Hall, J. C., Selection of hapten-specific single-domain antibodies from a non-immunized llama ribosome display library. *J Immunol Methods* **2003,** *281* (1-2), 161-75.

163. Broos, K.; Lecocq, Q.; Xavier, C.; Bridoux, J.; Nguyen, T. T.; Corthals, J.; Schoonooghe, S.; Lion, E.; Raes, G.; Keyaerts, M.; Devoogdt, N.; Breckpot, K., Evaluating a Single Domain Antibody Targeting Human PD-L1 as a Nuclear Imaging and Therapeutic Agent. *Cancers (Basel)* **2019,** *11* (6).

164. Clarke, S. C.; Ma, B.; Trinklein, N. D.; Schellenberger, U.; Osborn, M. J.; Ouisse, L. H.; Boudreau, A.; Davison, L. M.; Harris, K. E.; Ugamraj, H. S.; Balasubramani, A.; Dang, K. H.; Jorgensen, B.; Ogana, H. A. N.; Pham, D. T.; Pratap, P. P.; Sankaran, P.; Anegon, I.; van Schooten, W. C.; Bruggemann, M.; Buelow, R.; Force Aldred, S., Multispecific Antibody Development Platform Based on Human Heavy Chain Antibodies. *Front Immunol* **2018,** *9*, 3037.

165. Nilvebrant, J.; Tessier, P. M.; Sidhu, S. S., Engineered Autonomous Human Variable Domains. *Current pharmaceutical design* **2016,** *22* (43), 6527-6537.

166. Wang, J.; Yuan, R.; Song, W.; Sun, J.; Liu, D.; Li, Z., PD-1, PD-L1 (B7-H1) and Tumor-Site Immune Modulation Therapy: The Historical Perspective. *J Hematol Oncol* **2017,** *10* (1), 34.

167. Dong, H.; Strome, S. E.; Salomao, D. R.; Tamura, H.; Hirano, F.; Flies, D. B.; Roche, P. C.; Lu, J.; Zhu, G.; Tamada, K.; Lennon, V. A.; Celis, E.; Chen, L., Tumor-

associated B7-H1 promotes T-cell apoptosis: a potential mechanism of immune evasion. *Nat Med* **2002,** *8* (8), 793-800.

168. Dougan, M.; Ingram, J. R.; Jeong, H. J.; Mosaheb, M. M.; Bruck, P. T.; Ali, L.; Pishesha, N.; Blomberg, O.; Tyler, P. M.; Servos, M. M.; Rashidian, M.; Nguyen, Q. D.; von Andrian, U. H.; Ploegh, H. L.; Dougan, S. K., Targeting Cytokine Therapy to the Pancreatic Tumor Microenvironment Using PD-L1-Specific VHHs. *Cancer Immunol Res* **2018,** *6* (4), 389-401.

169. Gainkam, L. O.; Caveliers, V.; Devoogdt, N.; Vanhove, C.; Xavier, C.; Boerman, O.; Muyldermans, S.; Bossuyt, A.; Lahoutte, T., Localization, mechanism and reduction of renal retention of technetium-99m labeled epidermal growth factor receptor-specific nanobody in mice. *Contrast Media Mol Imaging* **2011,** *6* (2), 85-92.

170. Liu, H.; Liu, Y.; Zhao, Z.; Li, Y.; Mustafa, B.; Chen, Z.; Barve, A.; Jain, A.; Yao, X.; Li, G.; Cheng, K., Discovery of Anti-PD-L1 Human Domain Antibodies for Cancer Immunotherapy. *Front Immunol* **2022,** *13*, 838966.

VITA

Yanli Liu was born on May 14th, 1988, in Shandong Province, China. She received her Bachelor of Science degree in Yantai University in June 2012. Then, she received her Master of Science in Bioengineering from East China University of Science and Technology in June 2015.

She joined the WuXi Biologics which is a Contract Research Organization (CRO) company and worked as a scientist in department of Protein Analytical Sciences from 2015-2018.

She started working at Dr. Kun Cheng's lab as a Graduate Research Assistant and Graduate Teaching Assistant in the division of Pharmacology and Pharmaceutical Sciences in University of Missouri-Kansas City in 2018. Yanli's project is mainly focusing on 1) Development of cholesterol peptide-based delivery system to deliver IKBKE siRNA for triple-negative breast cancer. 2) Discovery of CD24 siRNAs for triple-negative breast cancer. 3) Discovery of anti-PD-L1 human domain antibody for cancer immunotherapy. She participated and published 11 different papers and received awards, including UMKC Women's Graduate Assistance Fund Award (from 2020 to 2023), UMKC School of Graduate Studies Travel Grant (2022,2023), UMKC School of Graduate Studies (SGS) Research Grant (2022), UMKC School of Pharmacy Somerset Scholarship (2021), UMKC School of Pharmacy William D. Mason Memorial Graduate Scholarship. She served as Vice President in Controlled Release Society (CRS) UMKC student chapter (2020-2021). She served as a Secretary in Controlled Release Society (CRS) UMKC student chapter (2019-2022). She also served as Treasurer in UMKC Pharmaceutical Sciences Graduate Students Association (PSGSA) (2020-2021).

PUBLICATIONS

1. **Yanli Liu**, Chien-Yu Lin, Yuhan Guo, Zhen Zhao, Sherin George Shaji, Yongren Li, Reaid Hasan, Kun Cheng. Suppression of IKBKE expression with siRNA for triple-negative breast cancer treatment (in preparation for submission)
2. Bahaa Mustafa, John Fetse, Sashi Kandel, Chien-Yu Lin, Pratik Adhikary, Umar-Farouk Mamani, **Yanli Liu**, Mohammed Nurudeen Ibrahim, Mohammed Alahmari, Kun Cheng. (2023) Discovery of Anti-CD47 Peptides as New Innate Immune Checkpoint Inhibitors.
3. Chien-Yu Lin, Evanthia Omoscharka, **Yanli Liu**, and Kun Cheng. (2023) Establishment of a Rat Model of Alcoholic Liver Fibrosis with Simulated Human Drinking Patterns and Low-Dose Chemical Stimulation. Biomolecules 13 (9), 1293
4. Chien-Yu Lin, Umar-Farouk Mamani, Yuhan Guo, **Yanli Liu**, Kun Cheng. (2023) Peptide-Based siRNA Nanocomplexes to Hepatic Stellate Cells for the Treatment of Liver Fibrosis. Biomolecules 13 (3), 448
5. John Fetse, Zhen Zhao, Hao Liu, Umar-Farouk Mamani, Bahaa Mustafa, Pratik Adhikary, Mohammed Ibrahim, **Yanli Liu**, Pratikkumar Patel, Maryam Nakhjiri, Mohammed Alahmari, Guangfu Li, and Kun Cheng. (2022) Discovery of Cyclic Peptide Inhibitors Targeting PD-L1 for Cancer Immunotherapy. J. Med. Chem. 65 (18), 12002–12013
6. Hao Liu*, **Yanli Liu***, Zhen Zhao, Yuanke Li, Bahaa Mustafa, Zhijin Chen, Ashutosh Barve, Akshay Jain, Xiaolan Yao, Guangfu Li, Kun Cheng. (2022) Discovery of Anti-PD-L1 Human Domain Antibodies for Cancer Immunotherapy. Front Immunol. 13: 838966 **(* co-first authors)**
7. Pratik Adhikary, Sashi Kandel, Umar-Farouk Mamani, Bahaa Mustafa, Siyuan Hao, Jianming Qiu, John Fetse, **Yanli Liu**, Nurudeen Mohammed Ibrahim, Yongren Li, Chien-

Yu Lin, Evanthia Omoscharka, Kun Cheng. (2021) Discovery of Small Anti-ACE2 Peptides to Inhibit SARS-CoV-2 Infectivity. Adv. Therap. 4, 2100087

8. Yuanke Li, Zhen Zhao, Chien-Yu Lin, **Yanli Liu**, Kevin F Staveley-OCarroll, Guangfu Li, Kun Cheng. (2021) Silencing PCBP2 normalizes desmoplastic stroma and improves the antitumor activity of chemotherapy in pancreatic cancer. Theranostics 11(5):2182-2200
9. Jiazhu Xu, Qi Fang, **Yanli Liu**, Yan Zhou, Zhaoyang Ye, Wen-Song Tan. (2020) In Situ Ornamenting of Poly(ε-caprolactone) Electrospun Fibers with Varying Fiber Diameters Using Chondrocyte Extracellular Matrix for Improving Chondrogenesis of Mesenchymal Stem Cells. Colloids and surfaces B: Biointerfaces 197
10. Hao Liu, Zhen Zhao, Li Zhang, Yuanke Li, Akshay Jain, Ashutosh Barve, Wei Jin, **Yanli Liu**, John Fetse & Kun Cheng. (2019) Discovery of low-molecular weight anti-PD-L1 peptides for cancer immunotherapy. Journal for ImmunoTherapy of Cancer 270
11. **Yanli Liu**, Jiazhu Xu, Yan Zhou, Zhaoyang Ye, Wen-Song Tan. (2017) Layer-by-layer assembled polyelectrolytes on honeycomb-like porous poly(ε-caprolactone) films modulate the spatial distribution of mesenchymal stem cells. Materials Science and Engineering C 78: 579–588
12. Lei Xu, Yuxi Wu, **Yanli Liu**, Yan Zhou, Zhaoyang Ye & Wen-song Tan. (2017) Non-contact Coculture Reveals a Comprehensive Response of Chondrocytes Induced by Mesenchymal Stem Cells through Trophic Secretion. Tissue Engineering and Regenerative Medicine 15: 37-48